EPIGENETIC REGULATION OF SKIN DEVELOPMENT AND POSTNATAL HOMEOSTASIS

THE ROLE OF CHROMATIN ARCHITECTURAL PROTEIN CTCF IN THE CONTROL OF KERATINOCYTE DIFFERENTIATION AND EPIDERMAL BARRIER FORMATION

I. Malashchuk

Principal Supervisor: Professor VA Botchkarev

Associate Supervisor: Dr Michael Fessing

Associate Supervisor: Dr Andrei Mardaryev

School of Medical Sciences

University of Bradford

2016

ABSTRACT

Igor Malashchuk

Epigenetic Regulation of Skin Development and Postnatal Homeostasis

The role of chromatin architectural protein Ctcf in the control of Keratinocyte Differentiation and Epidermal Barrier Formation

Keywords: three dimensional genome organisation, skin, Ctcf, microarray, fluorescent in situ hybridization

Epigenetic regulatory mechanisms play important roles in the control of lineage-specific differentiation during development. However, mechanisms that regulate higher-order chromatin remodelling and transcription of keratinocyte-specific genes that are clustered in the genome into three distinct loci (Keratin type I/II loci and Epidermal Differentiation Complex (EDC) during differentiation of the epidermis are poorly understood. By using 3D-Fluorescent In Situ Hybridization (FISH), we determined that in the epidermal keratinocytes, the KtyII and EDC loci are located closely to each other in the nuclear compartment enriched by the nuclear speckles. However, in KtyII locus knockout mice, EDC locus moved away from the KtyII locus flanking regions and nuclear speckles towards the nuclear periphery, which is associated with marked changes in gene expression described previously. Chromatin architectural protein Ctcf has previously been implicated in the control of long-range enhancer-promoter contacts and inter-chromosomal interactions. Ctcf is broadly expressed in the skin including epidermal keratinocytes and hair follicles. Conditional Keratin 14-driven *Ctcf* ablation in mice results in the increase of the epidermal thickness, proliferation, alterations of the epidermal barrier and the development of epidermal pro-inflammatory response. Epidermal barrier defects in *Krt14CreER/Ctcf* fl/fl mice are associated with marked changes in gene expression in the EDC and KtyII loci, which become topologically segregated in the nucleus upon *Ctcf* ablation. Therefore, these data suggest that Ctcf serves as critical determinant regulating higher-order chromatin organization in lineage-specific gene loci in epidermal keratinocytes, which is required for the proper control of gene expression, maintenance of the epidermal barrier and its function.

ACKNOWLEDGEMENTS

I would like to thank my supervisors Professor Vladimir Botchkarev, Dr Andrei Mardaryev and Dr Michael Fessing for their advice, patience and support during the project.

I would, also, like to thank Dr Jana Rudolf for helping with the research and being a role model in the lab. Furthermore, I would like to thank Dr Valentina Rapisarda for teaching me 3D FISH technology.

Special thanks to my family for personal support.

Finally, I would like to thank the University of Bradford, administration staff and everybody at the Centre for Skin Sciences for providing excellent facilities and support structure for post graduate study.

CONTENTS

LIST OF FIGURES

LIST OF TABLES

LIST OF EQUATIONS

ABBREVIATIONS

ΔNp63	p63 isoform lacking terminal transactivation domain
5caC	Carboxylcytosine
5fC	Formylcytosine
5hmC	hydroxy-methylcytosine
5mC	Methylcytosine
APS	Alkaline Phosphatase Staining
BAC	Bacterial Artificial Chromosome
BER	base excision repair
BMP	Bone Morphogenetic Protein
BSA	Bovine serum albumin
C	Cytosine
C/EBP	CCAAT/enhancer-binding protein
DAPI	4,6- Diamidino-2-phenylindole, dihydrochloride
DNMT	DNA methyltransferases
FBS	Fetal Bovine Serum
FGF	fibroblast growth factors
FITC	Fluorescein isothiocyanate
GRHL3	grainyhead-like 3
H&E	Hematoxylin and eosin staining
HAT	histone acetyl trasferase
HDAC	histone deacetylase
KLF4	Kruppel-like factor 4

MAPK	mitogen-activated protein kinase
NF-κB	nuclear factor-κB
NICD	Notch Intracellular Domain
NT	Nick Translation – a technique used in FISH probe preparation
PCR	Polymerase chain reaction
RT	Room temperature
SAM	adenosyl-L-methionine
SSC	Saline-sodium Citrate buffer
TAD	topologically associated domain
TAp63	p63 isoform containing transactivation domain
TDG	thymine DNA glycosylase (TDG)
TET	ten-eleven-translocation

1. INTRODUCTION

Skin has a surface area of around $2m^2$ in an adult human, which makes it the largest organ of the body (Di Meglio et al., 2011). In addition, the skin carries out a number of functions that are vital for the survival of the organism. These functions include providing a physical and biochemical barrier between the internal organs and the outside environment, protection against ultra-violet radiation and microorganisms, thermal and water regulation (Di Meglio et al., 2011). In addition to the skin being sensory perceptive, it is also elastic, stiff and has high tensile strength (Hussain et al., 2013). These biomechanical properties of the skin enable species to interact with the outside world, while at the same time being protected from physical trauma and other environmental stressors.

Due to the skin being such a crucial organ in maintaining the human health and also important for social interactions makes the study of skin development as one of the key areas of biomedical research. One of the best models for studying mechanisms regulating skin development and pathobiology of skin disorders are mice (*Mus musculus*) because of their quick reproductive rate and the established techniques that enable easy generation of genetically-engineered mutants (Peters et al., 2007).

1.1. Molecular mechanisms that control development of the epidermis

The biochemical and biophysical properties of epidermal barrier can be attributed to orchestrated expression of the epidermis-specific groups of genes locates in the Keratin Type I locus (mouse chromosome 11), Keratin Type II locus (mouse chromosome 15) and Epidermal Differentiation Complex (mouse Chromosome 3) (Gdula et al., 2013).

The skin of an adult mouse is established during the different stages of its embryonic development. After gastrulation, the outer ectoderm cells eventually become epidermal progenitor cells. This happens at E9.5 (embryonic day 9.5) when the germinative (basal) layer is established and these cells begin to express Keratin 5 (**Fig. 1.1.a**) (Koster and Roop, 2007). Then by E14.5, the basal cells give rise to temporary cell layer called the periderm and an intermediate layer. Initially, the intermediate layer, which is located between the basal layer and the periderm, are able to proliferate. However, at E15.5 they lose this ability and give rise to the spinous layer. The cells from the spinous layer enter a terminal differentiation program to produce granular layer by E16.5. Finally, the epidermal barrier (conrnified layer) is established by E18.5, which coincides with the loss of the periderm (**Fig. 1.1.a**) (Koster and Roop, 2007).

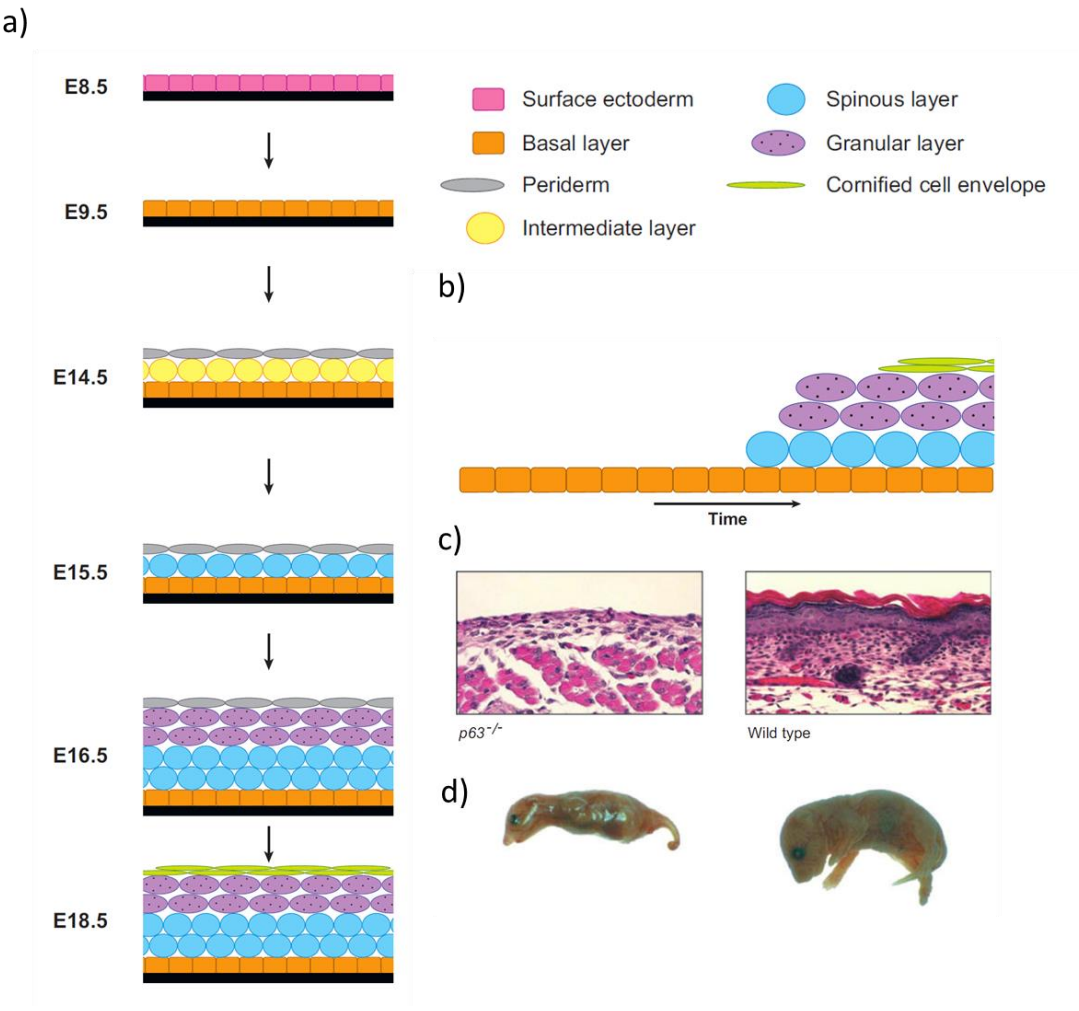

Figure 1.1. Schematic illustration of the development of mouse epidermis. a) Development of the epidermis during embryogenesis from E8.5 to E18.5. b) Development of permanent skin epidermal layers over time. c) Epidermal formation of wild type mice is completed by birth (right), however, *p63-/-* mice (left) are born with a single layer of ectodermal cells and die shortly after birth due to dehydration. d) Images of *p63-/-* and wild-type mice. Modified from (Koster and Roop, 2007).

1.1.1. Molecular mechanisms responsible for establishment and maintenance of the basal epidermal layer

The neuroectoderm is a single layer of cells that is found on the outer embryo after gastrulation. This layer gives rise to the nervous system and the skin epithelium. Wnt signalling pathways is the switch that regulates which fate the cells of the neuroectoderm will take (Fuchs, 2007). In the presence of Wnt signalling the ectoderm takes the epidermal fate because it stops responding to the fibroblast growth factors (FGFs) which in turn prevents downregulation of bone morphogenetic protein (BMPs) signalling (**Fig. 1.2**). When Wnt signalling is absent, the cells from the ectoderm progress to neurogenesis because of their response to the FGFs, which leads to the inhibition of BMP signalling (**Fig. 1.2**).

The main characteristics of basal keratinocytes are the presence of keratins K5 and K14 and ability to proliferate (Byrne et al., 1994). The development of these features in basal cells is linked with the expression of transcription factor p63. Transgenic mice lacking *p63* do not develop the basal layer and do not express K5 or K14 (Mills et al., 1999) and die soon after birth due to dehydration (**Fig. 1.1.c,d**). Different isomers of p63 protein are derived due to the presence of two promoters on the *p63* gene. The p63 isoforms might contain N-terminal transactivation (TA) domain or might not contain this domain (ΔN) (Yang et al., 1998). The first isoform to be expressed in the epidermis is TAp63, which is able to induce the expression of K14 (Koster et al., 2004). Interestingly, the transcription factor (AP-2γ) that is implicated in regulating the expression of K14 (Byrne et al., 1994) is

a direct target of TAp63α. Another isoform is ΔNp63α (without TA), which is expressed in the epidermis after the commitment of epidermal keratinocytes to stratification, can also induce the expression of K14 (Romano et al., 2007). Therefore, ΔNp63α may be involved in maintaining K14 expression in the basal cells postnatally.

Epidermal fate is also associated with the expression of proteins required for cell adhesion, which are components of the desmosomes (Berika and Garrod, 2014). Perp is an adhesion protein essential for epithelial integrity that is expressed in the basal layer and is regulated by p63 (Ihrie et al., 2005).

Also, TAp63 and ΔNp63 isoforms are required to modulate terminal differentiation (Koster et al., 2004; Truong et al., 2006). Troung et el (2006) used primary keratinocytes under-expressing p63 to generate grafts and discovered that these grafts were hypoproliferative. Other data obtained from in vitro experiments indicated that ΔNp63α bind to the promoters of p21 and 14-3-3σ and reduces their expression (Westfall et al., 2003). These genes are upregulated during terminal differentiation. Interestingly, ΔNp63α is also required to regulate a signalling cascade which controls epidermal morphogenesis. Downregulation of p63 prevents K1 expression (Koster et al., 2007). ΔNp63α prevents terminal differentiation of basal cells by inhibiting Notch, it is also involved in a complex cross-talk with other specific aspects of Notch function required in the early stages of differentiation and K1 expression (Nguyen et al., 2006). Furthermore, a cyclin dependent kinase inhibitor p57Kip2 required for terminal differentiation is induced,

while cell-cycle progression genes, such as cyclin B2 and cdc2, are repressed by the ΔNp63α (Beretta et al., 2005; Testoni and Mantovani, 2006). Most likely, the reason why ΔNp63α has two opposing functions can be explained by its different roles fulfilled in the early transit-amplifying and the late-transit amplifying basal keratinocytes (Koster et al., 2007).

1.1.2. Molecular mechanism responsible for the formation of intermediate layer

The formation of the intermediate layer is associated with the changes in the plane of cell division in the basal layer (Koster et al., 2007). At the early stages of skin development (E12.5) the formation of mitotic spindle is symmetric and parallel to the basement membrane (Blanpain and Fuchs, 2009). Between E12.5 to E14.5-E17.5 (i.e., during the stratification process), the number of cell divisions which are asymmetric and perpendicular to the basement membrane rise from 0% to 70% (Blanpain and Fuchs, 2009). In Drosophila, it was discovered that this process is associated with asymmetric distribution of proteins in the cytoplasm of dividing cells (Roegiers and Jan, 2004). One of these proteins is Inscuteable which has a role in asymmetric distribution of cell fate determinants (Roegiers and Jan, 2004). The intermediate layer that expresses K1 and continues to proliferate, even if it is only for a short period of time, indicates that expression of K1 and cell-cycle inhibition are not linked (Koster and Roop, 2007). Down-regulation of ΔNp63α in basal keratinocytes prevents the formation of the intermediate layer and the induction of K1 expression,

implying that this transcription factor is critical for the initiation of epidermal stratification (Koster et al., 2007).

Pathways that function downstream of ΔNp63α and contribute to the intermediate layer formation are Notch signalling and BMPs (**Fig. 1.2**). Other pathways that contribute to the formation of stratified epidermis are mitogen-activated protein kinase (MAPK), nuclear factor-κB (NF-κB), the AP2 family, the CCAAT/enhancer-binding protein (C/EBP) transcriptional regulators, interferon regulatory factor 6 (IRF6), grainyhead-like 3 (GRHL3) and Kruppel-like factor 4 (KLF4) (Blanpain and Fuchs, 2009).

Notch signalling pathway includes interaction of an extracellular ligand interacts with the Notch receptor, resulting in the release of the NICD (Notch Intracellular Domain) and forming of a new complex with proteins MAML (mastermind-like) and RBP-J inducing the expression of the target genes (Artavanis-Tsakonas et al., 1999). One of the targets of Notch signalling is K1, the expression of which is reduced in RBP-J-/- epidermis (Blanpain et al., 2006). However, K1 expression is induced synergistically by both Notch and ΔNp63α.

1.1.3. Molecular mechanism responsible for the formation of the spinous epidermal layer

As indicated by studies of the developing mouse embryo (Koster et al., 2007), there is a switch from a mitotic to a post-mitotic state of cells in the intermediate layer, which is associated with a loss of proliferation and a transition to spinous layer (**Fig. 1.1**). The transcription factor ΔNp63α is also

required for this process: ΔNp63α targets a gene IKKα which regulates epidermal stratification (Koster et al., 2007). Epidermal cells in mice lacking IKKα fail to develop granular and cornified layers and the K1 expressing cells do not lose their mitotic activity (Koster and Roop, 2007). Mouse models with similar phenotype include mice expressing a mutant 14-3-3σ (Li et al., 2005), mice without IRF6 activity (Ingraham et al., 2006), and mice without Ovol1. The reason why the intermediate cells in mice lacking Ovol1 were not able to exit mitotic state was because Ovol1 directly targets c-Myc for transcriptional repression (Nair et al., 2006). Even though the epidermal phenotype of those three mouse models is similar, a direct interaction or relationship between them is yet to be determined.

In the postnatal epidermis, the intermediate cell layer does not exist and the cells in the spinous layer are replenished directly from the basal layer. Notch signalling is a key regulator of the switch between proliferation and terminal differentiation (Koster and Roop, 2007). Notch1 causes growth suppression by inducing the expression of $p21^{WAF1/Cip1}$ (Rangarajan et al., 2001). Interestingly, even though ablation of Notch1 showed hyperproliferation in the basal layer, the spinous layer form normally (Rangarajan et al., 2001). Notch2 was able to compensate for the lack of Notch1. However, dowregulation of all Notch activity by ablating downstream factor RBP-J reduced the expression of spinous-layer specific markers, such as K1 and Involucrin (Blanpain et al., 2006). Hes1 which promotes terminal differentiation is targeted by Notch (Nguyen et al., 2006). Impaired Notch signalling can also result in the development of skin tumours. For example, skin squamous cell carcinomas develop when a

dominant-negative form of MAML1 is overexpressed (Proweller et al., 2006). Also, spontaneous epidermal tumours develop when Notch1 is ablated in postnatal skin (Nicolas et al., 2003).

1.1.4. Molecular mechanism responsible for the spinous – granular layer transition in the epidermis

The process of the spinous to granular layer transition is associated with the down-regulation of K1 and K10 both in vitro and in vivo (Yuspa et al., 1989). One of the key molecules responsible for terminal differentiation of epidermis is the calcium (Ca^{2+}) ion. The extracellular concentration gradient of the Ca^{2+} is a triggers required for the formation of the spinous layer, granular layer and the cornified cell envelope. *In vitro*, if primary mouse keratinocytes (PMKs) are exposed to Ca^{2+}, they initiate the terminal differentiation program which works similar to the terminal differentiation program *in vivo* (Yuspa et al., 1989). Also, in PMKs, Ca^{2+} exposure leads to increase in the levels of diacyl-glycerol and phosphatidylinositol metabolism, which implicates phosphorylation of protein kinase C (PKC) in the differentiation program (Lee and Yuspa, 1991). Specifically, PKCα isoform is the only Ca^{2+} responsive serine/threonine kinase expressed in keratinocytes (Yang et al., 2003). Also, PKC causes down-regulation of K1 and K10 during transition from the spinous to granular cells, and up-regulation of the granular layer-specific markers, which are loricrin, filaggrin and transglutamase (Dlugosz and Yuspa, 1993). Another PKC isoform

PKCη is also expressed in keratinocytes, but is not responsive to Ca^{2+}; however, it can also induce keratinocyte differentiation (Ohba et al., 1998).

Interestingly, several Ca^{2+} binding proteins implicated in the epidermal stratification have been identified. For example, granular cells which lack Ca^{2+} sensing receptor have a reduced expression of loricrin and filaggrin (Komuves et al., 2002). However, if this receptor is overexpressed, the spinous and granular layers are expanded and filaggrin levels are increased (Turksen and Troy, 2003). In addition, the Dxl3 which may promote filaggrin expression is increased (Turksen and Troy, 2003). Interestingly, Dxl3 expression is regulated by p63 and DNA-binding activity of Dxl3 is regulated by PKC (Park et al., 2001).

1.1.5 Molecular mechanisms involved in the control of epidermal barrier formation

Epidermal barrier formation includes the establishment of the cornified cell envelope during the final steps of the epidermal stratification program (**Fig. 1.1**). The transcription factors Klf4 and Grainyhead-like epithelial transactivator (Grhl3/Get1) have been found to play important roles in this process. Firstly, mutants which under-express and over-express Klf4 display either defects in the cornified envelope structure or in accelerated barrier formation, respectively (Jaubert et al., 2003; Segre et al., 1999). Further microarray analysis on Klf4 transgenic skin identified Connexin26 to serve as a target, whose expression is inhibited by Klf4 (Patel et al., 2006). Furthermore, overexpression of Connexin26 resulted in the epidermal

barrier defects (Djalilian et al., 2006). Mice lacking transcription factor Grhl3 also show defects in the barrier formation (Yu et al., 2006). Specifically, the defects were due to down-regulation of the genes involved in the control of lipid metabolism and cell adhesion (Yu et al., 2006). Furthermore, many of the lipid metabolism genes are also implicated in the barrier defects in mice lacking GATA-3 (de Guzman Strong et al., 2006). Keratinocyte specific deletion of Arnt also leads to the defects in the lipid metabolism (Geng et al., 2006). Mice ablated for Grhl3 apart from the defects in lipid metabolism also have abnormal expression of the tight junction genes, which are vital for the cell-cell adhesion and establishment of an effective epidermal barrier (Yu et al., 2006). The importance of the tight junctions is particularly emphasized by the fact that mice deficient in claudin-1 died within 1 day after birth due to dehydration (Furuse et al., 2002). Furthermore, E-cadherins are essential for regulation of the tight junctions, because absence of E-cadherin leads to improper localization of the key tight junctional proteins such as claudins (Tunggal et al., 2005).

Epidermal differentiation complex (EDC) contains the key genes encoding the components of the cornified cell envelope, which are expressed at high levels in the epidermis. The EDC contains genes belonging to S100 gene family, small proline reach protein (SPRR) family, late cornified envelope (LCE) family, as well as Loricrin and Profillagrin (*Flg*) (**Fig.1.10**).

The S100 family has 14 genes in the EDC and 13 are expressed in normal or diseased epidermis (Eckert et al., 2004). Loricrin contributes

about 70% to the mass to the cornified layer (Steinert and Marekov, 1995). Interestingly though, Loricrin knock-out mice are viable and the skin phenotype only last for the first 4-5 days after birth. It is thought that SPRRs, which are co-expressed with Loricrin, are able to compensate Loricrin functions (Koch et al., 2000). SPRRs have three sub families which are SPRR1/2 and 3 and have strong sequence homology with the Loricrin and Involucrin (Gibbs et al., 1993).

The LCE family contains 18 genes that form the central EDC domain. Their structure is quite similar to the SPRR proteins, both have protein crosslinking functions and serve as the cornified envelope precursors (Marshall et al., 2001). Profillagrin contributes to cell compaction by binding to and condensing the keratin cytoskeleton (Sandilands et al., 2009). Loss of Profillagrin results in a poorly formed cornified layer, defects in epidermal barrier formation, and the skin is prone to the water loss (Fallon et al., 2009).

The cornified envelope is composed of the proteins most of which originate from the genes located in the Epidermal Differentiation Complex (EDC, mouse chromosome 3). These genes include loricirin, filaggrins, involucrin, small proline-rich proteins (SPRRs), S100 protein family members, late cornified envelope proteins (LCEs).

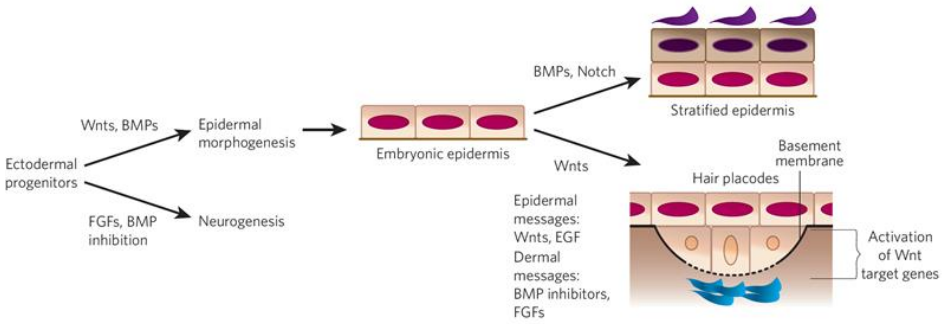

Figure 1.2. Initial signalling steps that determine the specification of embryonic skin. Modified from (Fuchs, 2007).

1.2 Hair follicle is a dynamic mini organ of the skin

Hair is well known for being important for thermoregulation, physical protection, sensory perception and social interactions in mammals. Interestingly, just like the formation of cornified layer of the epidermis, hair shaft production involves terminal differentiation of keratinocytes, except, this process takes place in the hair follicle (HF) rather than the epidermis (**Fig. 1.3**) (Reviewed in Schneider et al.). HF formation is associated with a complex prototypic coordination involving ectoderm-mesoderm during foetal skin development (Reviewed in Fuchs, 2007; Schmidt-Ullrich and Paus, 2005). *De novo* HF formation have also been shown to happen in adult mouse skin (Chuong et al., 2007; Ito et al., 2007). Most importantly, throughout the lifetime of a mammal HFs undergo cycle transformations (Paus and Foitzik, 2004; Stenn and Paus, 2001).

The HF cycle can be characterised by three phases, which are growth (anagen), apoptosis-medicated regression (catagen) and quiescence (telogen) (Fgure 1.4) (Paus and Foitzik, 2004; Stenn and Paus, 2001). Each new cycle is associated with the production of new hair shaft after the old one has been shed (this process is called exogen) (Paus and Foitzik, 2004; Stenn and Paus, 2001). Mouse mutants have been very useful in understanding the molecular mechanisms involved in HF development and cycling (Nakamura et al., 2013).

1.2.1. Structure of the hair follicle

The HF consists of two parts, one of which is a permanent portion of the HF, while the other one undergoes remodelling during HF cycling (Reviewed in Botchkarev and Paus, 2003) (**Fig. 1.3.b**). Cycling portion of the HF contains secondary hair germ that is transformed into the hair bulb during active hair growth phase (anagen) (**Fig. 1.3.b,c**). In turn, the permanent part of the HF contains the infundibulum, the function of which is to provide an opening for the shaft through the skin, as well as sebaceous gland which duct is entered into the lower part of the infundibulum (Reviewed in Schneider et al., 2009).

Below the HF infundibulum is the region called isthmus (**Fig. 1.3.b**) where the sensory nerves form a collar of fibers around the HF and the arrector pili muscle is attached to the connective tissue sheath surrounding the HF epithelium (**Fig. 1.3.a**) (Reviewed in Schneider et al., 2009). The bulge, which marks the end of the permanent region, is located at the bottom of the isthmus and contains HF stem cells that contribute to the regeneration of the cyclic portion of the HF during anagen, as well as to epidermal regeneration during wound healing (**Fig. 1.3.b**) (Reviewed in Schneider et al., 2009). The anagen bulb, which contains the matrix keratinocytes and hair pigmentation machinery, is separated from the bulge by suprabulbar HF epithelium. During anagen, cells of the outer root sheath and melanocyte progenitors originating from the corresponding precursors residing in the secondary hair germ, move downwards and, after reaching the hair bulb, generate hair matrix keratinocytes or pigment-producing melanocytes,

respectively. The hair matrix keratinocytes have a high proliferation capacity and differentiate into the hair shaft and inner root sheath keratinocytes, while their number and proliferative activity determines the size of the bulb and diameter of the hair shaft. Terminal differentiation of the hair matrix keratinocytes results in various types of cells of the hair shaft (medulla, cortex, cuticle) and the inner root sheath (Huxley, Henley and companion layer cells) (**Fig. 1.3.c**) (Reviewed in Schneider et al., 2009). Melanocytes residing in the hair bulb, generate a pigment, which they transport into differentiating hair shaft keratinocytes, thus providing pigmentation for the hairs.

The dermal papilla, a mesenchymal command center of the HF, consists of the densely packed fibroblasts of mesenchymal origin. During anagen, some of these cells proliferate, and secrete growth factors and components of the extracellular matrix, that promote high proliferation rate in hair bulb keratinocytes. Furthermore, HF is enclosed by mesenchymally-derived connective tissue sheath, which cells are also capable of trafficking to the dermal papilla during anagen (**Fig. 1.3.c**) (Reviewed in Fuchs, 2007; Schneider et al., 2009; Stenn and Paus, 2001).

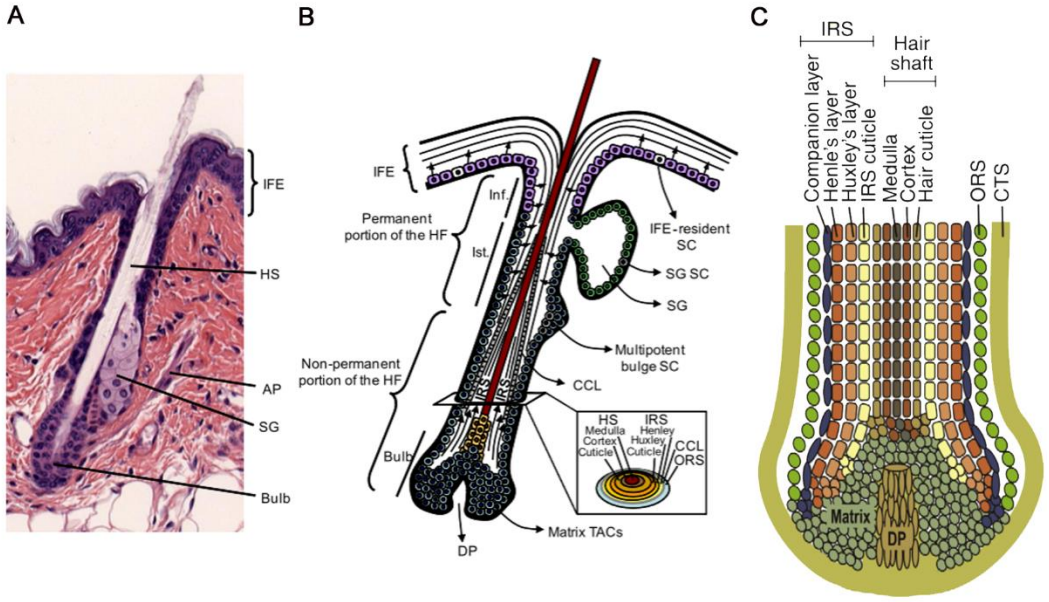

Figure 1.3. Structure of the hair follicle. (**A**) Haematoxylin and eosin staining of mouse back skin hair follicle in telogen phase. (**B**) Schematic representation of the hair follicle and location of the stem cell compartments in the HF and epidermis. (**C**) Schematic drawing illustrating the concentric layers of the outer root sheath (ORS), inner root sheath (IRS) and shaft in the bulb. AP, arrector pili; CCL, companion cell layer; DP, dermal papilla; HF, hair follicle; HS, hair shaft; IFE, interfollicular epidermis; Inf, infundibulum; IRS, inner root sheath; Ist, Isthmus; ORS, outer root sheath, SC, stem cells; SG, sebaceous gland; TACs, transit-amplifying cells; CTS: connective tissue sheath. Modified from (Margadant et al., 2010) (A,B) and (Schneider et al., 2009) (C).

1.2.2. Hair follicle cycling

HF cycling occurs regularly throughout the lifetime of an organism. In *Mus musculus,* HF cycling begins at about 17 days after birth after the first hair has been generated during morphogenesis (**Fig. 1.4**). From approximately day 17 to day 20, the HF undergoes apoptosis-driven involution (catagen) and enters the resting phase (telogen). The HF remains in telogen until the first anagen, which begins at about 3-3.5 weeks after birth (**Fig. 1.4**). It should be noted that the first telogen phase lasts for just a few days, while the second phase lasts up to 3 weeks (Reviewed in Fuchs, 2007; Schneider et al., 2009; Stenn and Paus, 2001).

The catagen phase can be described as a process during which the lower part of the hair follicles regresses by apoptosis of the keratinocytes making up the matrix, inner root sheath and outer root sheath. By the end of catagen, the survived hair bulb keratinocytes form secondary hair germ located just beneath the bulge. The stem cells in the bulge do not undergo apoptosis. In mice, the hair shaft from previous cycle remains in the HF even through new hair shaft comes out through the same hair canal. Shedding of the hair shaft occur through mechanical process, which mechanisms are still poorly understood, during the phase called exogen (Reviewed in Fuchs, 2007; Schneider et al., 2009; Stenn and Paus, 2001).

In mice, HF cycling tends to be synchronised among most HFs. However, as the animals age, the time of the telogen phase expands and HFs become less synchronised. In humans, on the other hand, synchronisation is only observed during morphogenesis and becomes

asynchronous after birth (Reviewed in Paus and Foitzik, 2004; Schneider et al., 2009).

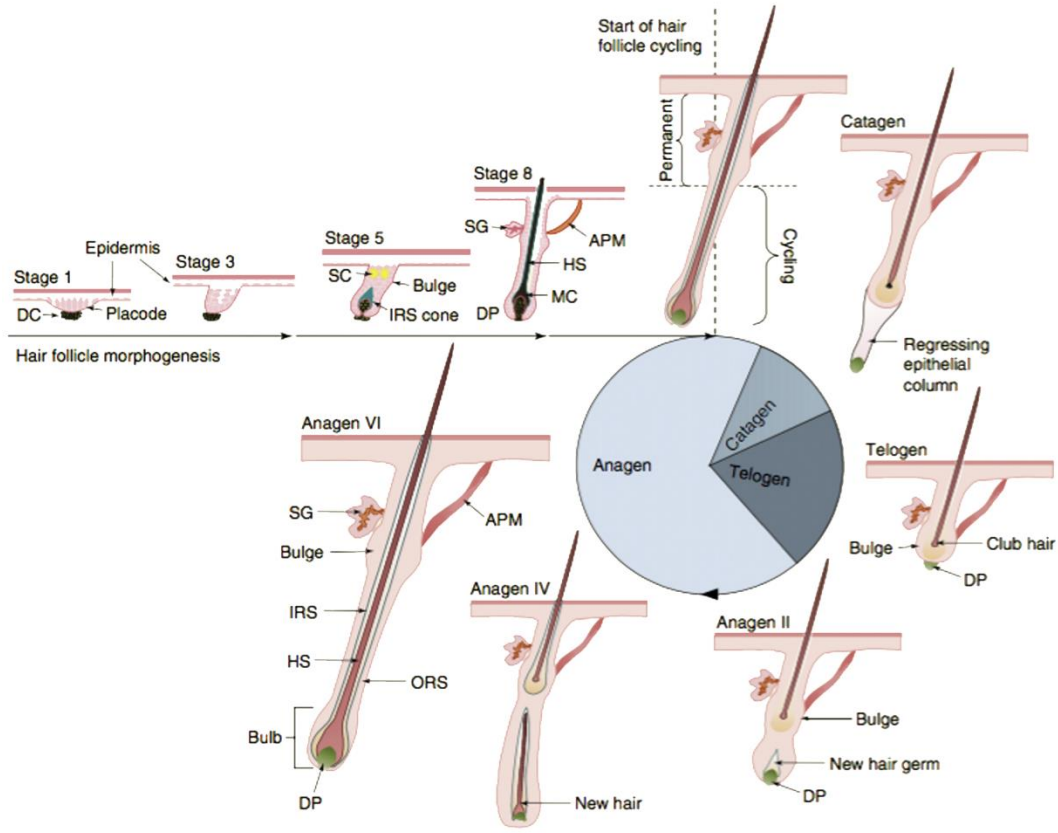

Figure 1.4. Key stages of hair follicle cycle. APM: arrector pili muscle; DC, dermal condensate (green); DP: dermal papilla (green); HS: hair shaft (brown); IRS: inner root sheath (blue); MC: melanocytes; ORS: outer root sheath; SC: sebocytes (yellow); SG: sebaceous gland. Modified from (Schneider et al., 2009).

1.2.3. Molecular mechanisms involved in hair follicle morphogenesis and regeneration

The fundamental requirement for initiation of HF morphogenesis is the signalling exchange between skin epithelium and mesenchyme. The molecules involved in this communication come from at least 5 family members, which include TNF, FGF, TGF-β/BMP, Hedgehog and Wnt families (Reviewed in Fuchs, 2007; Schmidt-Ullrich and Paus, 2005; Schneider et al., 2009).

The process of the HF morphogenesis can be split into three stages which are induction, organogenesis and cytodifferentiation (**Fig. 1.5**) (Reviewed in Rishikaysh et al., 2014). For HF induction, Wnt ligand expression and secretion are required as the first step. Wnts 3/4/6 are essential for HF initiation, while Wnts 2/7b/10a/10b are required for further steps of HF development (Andl et al., 2002; Zhang et al., 2009). The function of Wnt pathway is to stabilise β-catenin signalling in the dermis thereby regulating proliferation and aggregation of dermal fibroblasts (**Fig. 1.5**). Stablization of β-catenin in the dermis is then followed by expression of β-catenin in the epithelium of hair follicle placodes and later in the dermal condensate cells found in the dermal papilla (DasGupta and Fuchs, 1999; Fuchs, 2007; Noramly et al., 1999; Zhang et al., 2009). Lack of dermal β-catenin is associated with reduced β-catenin activity and downregulation of Edar expression in the epidermis as well as with failure of fibrobrast aggregation (Yang et al., 2012). The Wnt/β-catenin control the expression of Eda and its receptor Edar, which are important for activating NF-κB

pathway in the HF epithelial progenitor cells (Durmowicz et al., 2002; Laurikkala et al., 2002; Pummila et al., 2007).

NF-κB signalling pathway, Wnt10a/10b and Wnt inhibitor Dkk4 are very important for further steps of the HF placode development. The expression of Dkk4 is coordinated by NF-κB and LEF/TCF/β-catenin. Eda/Edar signalling directly activates expression of Wnt10b and NF-κB is important for preserving the levels of Wnt10b as well as of Wnt10a (Zhang et al., 2009).

The Wnt/β-catenin and Eda/Edar induce the expression of fibroblast growth factor (FGF) 20 in the early stage HF placode (Huh et al., 2013). FGF20 is responsible for condensation of dermal fibroblasts and dermal papilla formation. The likely candidate receptors that could be involved in FGF recognition include FGFR1 and FGF2B. HF development is retarded following the FGFR2B deletion. During HF initiation, the receptors for keratinocyte growth factor (KGF) and epidermal growth factor (EGF) are downregulated (Chen et al., 2012; Petiot et al., 2003; Richardson et al., 2009).

HF organogenesis begins once keratinocytes gain immense proliferative ability by inhibiting Bone Morphogenetic Protein (BMP) and by overexpressing Sonic hedgehog (Shh) in the HF placode (Reviewed in Fuchs and Horsley, 2008; Millar, 2002)). The dermis produces the inhibitor of BMP called Noggin, which enables Lef1 to induce HF epithelia (Botchkarev et al., 1999). Eda/Edar/Nf-κB activate Shh, which in turns activates the expression of Cyclin D1 (Andl et al., 2002; Laurikkala et al.,

2002). Shh is not required for HF induction but is essential for down-growth of the HF associated with organogenesis (St-Jacques et al., 1998). Shh signalling is active in both the epithelium and dermal condensate. Interestingly, epithelial Shh is required for Noggin expression and sustained expression of Shh is dependent on inhibition of BMP by Noggin (Reviewed in Rishikaysh et al., 2014). Thus, communication between the HF epithelium and the mesenchyme is essential, especially for the maturation and function of the dermal papilla. Other signalling components involved in driving Noggin expression that come from the HF epithelium include laminin-511 and platelet-derived growth factor (PDGF), while the dermal components include β-catenin and PDGFα (Gao et al., 2008; Rishikaysh et al., 2014). When laminin-511 and β-catenin interact, they initiate the formation of primary dermal cilia, which is essential for the subsequent formation of the dermal condensate (Lehman et al., 2009). Activation of PDGFRα by PDGF combined with Shh signalling is required for the secretion of Noggin by the dermal cells. The proliferation of HF epithelium occurs as a result of activation of Ras/MAPK pathway by transcription factor called Snail, which itself is activated by TGF-β2 signalling. Absence of TGF-β2 or Snail stalls HF morphogenesis (Jamora et al., 2005).

Cytodifferentiation is the final stage of HF development which involves the production of all the remaining structural components of the HF (**Fig. 1.5**). The inner root sheath formation is regulated by the transcription factors Gata3 and Cutl (Ellis et al., 2001; Kurek et al., 2007). The hair shaft forms as a result of BMP signalling activity in both epithelium and mesenchyme, while transcription factors Msx2, FoxN1 and Hoxc13 regulate

hair-specific differentiation of hair matrix cells (Godwin and Capecchi, 1998; Johns et al., 2005; Kulessa et al., 2000; Ma et al., 2003; Tkatchenko et al., 2001). FoxN1 has an additional role in controlling the pigment transfer from melanocytes to keratinocytes (Mecklenburg et al., 2001; Weiner et al., 2007). The expression of *FoxN1* gene occurs as a result of cooperation between the Wnt5a and Notch signalling pathway.

BMP6, which reduces cell migration, and Sostdc1 (inhibitor of BMP6) are also important for regulation of hair growth (Clavel et al., 2012). Both genes are transcriptional targets of Sox2. Sox2-mediated up- or down-regulation of the BMP6 and Sostdc1 are important for the control of hair growth (Clavel et al., 2012). BMP and BMPRIA have also been implicated in the HF cytodifferentiation, specifically in the establishment of progenitor cells of the inner root sheath and hair shaft through the cross-talk between HF epithelium and dermal papilla (Botchkarev et al., 1999; Kobielak et al., 2003). The BMPRIA is the only known BMP receptor located in the HF epithelium (Kobielak et al., 2003). Its activation by BMP4 induces terminal differentiation of the inner root sheath progenitor cells through the expression of GATA3 (Xu et al., 1999). Furthermore, hair shaft development, which involves Wnt signalling, is mediated by BMPRIA. In this BMPRIA activity is important for maintaining Lef1 levels and stabilization of β-catenin (Kobielak et al., 2003). Lef-1 also induces the expression of potent hair shaft differentiation factors Dlx3 and Hoxc13 (Hwang et al., 2008). Currently, it is believed that epithelial BMP4 activates a number of transcriptional factors including Msx1, which are able to induce BMP4 expression in the dermis (Saadi et al., 2013).

HF regeneration (telogen to anagen transition) involves the cross-talk between the BMP and Wnt signalling pathways. The communication between the stem cells located in the HF and the dermal papilla is essential at the beginning of this process. TGF-β2 activates Smad2/3 pathway in the stem cells and expression of *Tmeff1* is induced (Oshimori and Fuchs, 2012). Tmeff1 is able to promote telogen to anagen transition by lowering the threshold of BMP (Oshimori and Fuchs, 2012). The first cells to be activated during regeneration are secondary hair germ cells (Greco et al., 2009). The newly formed dermal papilla provides the signals for the undifferentiated bulge stem cells, which are located along the outer root sheath, to proliferate. This cells become transient amplifying matrix cells, which being in contact with dermal papilla differentiate into inner root sheath and hair shaft (Reviewed in Rishikaysh et al., 2014).

The process of anagen-catagen transition involves massive apoptosis in the cycling portion of the hair follicle, which is regulated by a number of pro-apoptotic signalling pathways (TNF, neurotrophin receptor), as well as by FGF receptor signalling (Reviewed in Stenn and Paus, 2001). During catagen, selected epithelial cells in the cycling portion of the HF survive and form the secondary hair germ, while the dermal papilla cells do not undergo apoptosis and form a ball of condensed cells beneath the secondary hair germ. During telogen, the communication between the epithelial and mesenchymal cells of the hair follicle appear to be minimal, while signalling exchange is activated during new hair cycle (Botchkarev and Kishimoto, 2003).

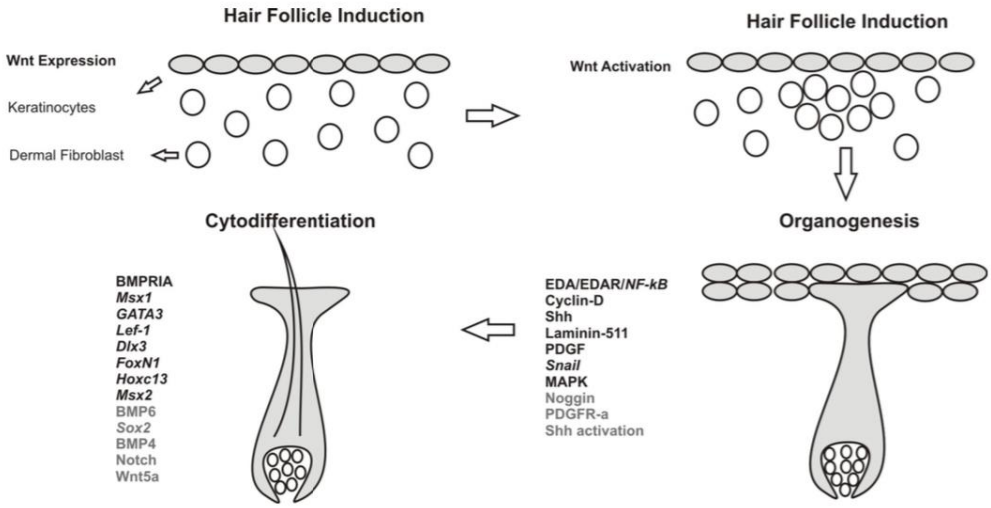

Figure 1.5. Hair follicle morphogenesis. Explained in text (Adapted from Rishikaysh et al., 2014)

1.3. Epigenetic regulatory mechanisms that control development of the epidermis

The term ‘epigenetics’ was first proposed by Conrad Waddington who defined it as “the branch of biology which studies the causal interactions between genes and their products which bring the phenotype into being” (Waddington, 1968). Initially, this was a broad terminology which included all molecular pathways that regulate the expression of the genotype into a particular phenotype (Dupont et al., 2009). However, after tremendous amount of progress in epigenetic research it now has a narrower definition which is “the study of changes in gene function that are mitotically and/or meiotically heritable and that do not entail a change in the DNA sequence” (Wu and Morris, 2001).

It is fascinating that all the cells of an organism have identical DNA content but the observed phenotypes of the different tissues and organs are completely different. These differences are due to different gene expression programs that are established in tissue-specific progenitor cells and their differentiating daughter cells (Fessing, 2014). DNA-binding transcription factors, which are able to induce or repress gene expression by recognising the specific sequence of DNA bases in the promoter regions, can contribute towards determining the pattern of gene expression (Bird, 2002). However, during development, the transcription potentials of the genome can be restricted in a manner that cannot only be explained by DNA transcription factors themselves (Bird, 2002).

During terminal keratinocyte differentiation in the epidermis, nucleus shows dramatic changes in the morphology and transit from an active state seen in the basal, spinous and granular layers to inactive state becoming a part of the keratinized cornified layer and epidermal barrier (Botchkarev et al., 2012). There are a number of epigenetic mechanisms that can affect the development of an animal and are able to fulfil the criterion of heritability. Epigenetic mechanisms most often associated with regulating gene expression programs are DNA modifications via DNA methylation and hydroxy-methylation, post-translational histone modifications, Polycomb-dependent gene silencing, higher order chromatin remodelling and three-dimensional (3D) genome organisation (Ho and Crabtree, 2010). Their mechanisms of action and roles in epidermal development are explained in more details below.

1.3.1. DNA methylation and hydroxy-methylation

DNA methylation and hydroxy-methylation are part of DNA modification processes that control gene expression. DNA methylation is carried out by DNA methyltransferases (DNMTs), which are capable of transferring a methyl group from a methyl donor, S-adenosyl-L-methionine (SAM), to the 5-position of cytosine in CpG dinucleotide, thereby producing methylcytosine (5mCpG) (Jin and Robertson, 2013). Hydroxy-methylation is carried out by ten-eleven-translocation (TETs) enzymes, which work by oxidising the 5 position of methylcytosine, thereby producing hydroxymethylcytosine (5hmCpG) (Branco et al., 2012). The role of hydroxy-methylation is not fully understood, however, it is believed that

5hmC is an intermediate mark which results in the loss of 5mC and/or it might be an epigenetic mark that recruits unique chromatin or transcription modifying enzymes (Branco et al., 2012).

DNA methyltransferases (DNMTs)

The family of DNMTs includes four members which are DNMT1, DNMT3A, DNMT3B and DNMT3L. The enzymatic activity of DNMT3L is absent, however, it does stimulate catalytic activity in culture by physically associating with DNMT3A and DNMT3B and is required for embryonic survival past E8.5 (Gopalakrishnan et al., 2008; Kareta et al., 2006). DNMT1 is crucial for maintaining DNA methylation in daughter cells after replication (Lei et al., 1996; Li et al., 1992), while DNMT3A and DNMT3B are essential for *de novo* DNA methylation (Okano et al., 1999; Okano et al., 1998). Knock-out mice for the DNMTs die at E9.5 (DNMT1-/-) (Li et al., 1992), E14.5-18.5 (DNMT3B-/-) and 4 weeks (DNMT3A-/-) (Okano et al., 1999). Transcription silencing by DNA methylation of imprinted genes, transposable elements and genes located on inactive X chromosome, is essential to maintain chromosome stability (Jin and Robertson, 2013). Also, dynamic expression of DNMTs is observed during embryonic development and differentiation (Watanabe et al., 2002). For example, the promoter of transcription factor Oct4, which is required to maintain undifferentiated state, is hypomethylated in mouse embryonic stem (ES) cells and is hypermethylated in trophoblast stem cells (Hattori et al., 2004).

DNA methylation also plays an important role in skin development. In particular, levels of DNMT1 are enriched in the basal keratinocytes (Sen et

al., 2010). Depletion of DNMT1 leads to premature differentiation and exit from the progenitor function, which results in tissue loss (Sen et al., 2010). UHRF1 is a protein that targets DNMT1 to hemi-methylated DNA after replication, and is also required to prevent premature differentiation. During differentiation de-methylation of the promoters belonging to large number of epidermal differentiation genes occurs (Sen et al., 2010). For this process, Gadd45 (A11, A12 and A13) promoting DNA de-methylation is required (Sen et al., 2010). Therefore, dynamic DNA methylation pattern are required for both progenitor and somatic cell maintenance in the epidermal tissue. Recently, it has been shown using human samples that aging of the epidermis is associated with methylation changes which are localised to the promoter and enhancer regions which were linked to modified transcriptional activity (Raddatz et al., 2013).

Even though methylation of DNA is considered as a transcriptionally repressive mark (**Fig. 1.4.c**), in some instances 5mC is able to recruit C/EBPα, which is able to bind 5mC and functions as a transcriptional activator. In the epidermis, C/EBPα is expressed predominantly in the suprabasal layers (Perdigoto et al., 2014). The importance of this transcriptional activator in epidermal differentiation is demonstrated by hyperplasia of the basal layer and increased apoptosis in the suprabasal layer *in vivo* (Oh et al., 2007) and inhibition of differentiation *in vitro* (Rishi et al., 2010), when normal activity of C/EBPα is repressed.

Regulation of the DNA hydroxy-methylation by TET proteins

The TET protein family comprise TET1, TET2 and TET3 which emerged in jawed vertebrates due to triplication of a common ancestor gene (Iyer et al., 2009). First evidence validating that hydroxy-methylation was carried out by TET1 appeared in 2009 (Tahiliani et al., 2009). Eventually, it was shown that TET2 and TET3 are also able to make 5hmC (Ito et al., 2010; Ko et al., 2010). The structure of TET proteins consists of iron and oxoglutarate binding domains and possibly DNA binding domain which is cysteine-rich (Iyer et al., 2009). Interestingly, the distribution of 5hmC in the genome is distinct from 5mC and is associated with promoters, Polycomb mediated gene silencing and gene expression (Branco et al., 2012). Furthermore, it is considered that 5hmC exists as an intermediate modification before demethylation of 5mC. Currently, there is not enough evidence to determine further steps that lead to demethylation. One theory is that during replication the hemi-hydroxy methylated DNA is not remethylated by DNMT1 (Inoue and Zhang, 2011). However, it was shown that UHRF1 that targets DNMT1 to hemi-methylated DNA has similar affinity for both 5hmC and 5mC (Frauer et al., 2011), which indicates that an other mechanism of demethylation might be present.

Interestingly, demethylation of methylated cytosine might involve further oxidation of the 5hmC by TETs to make formylcytosine (5fC) and carboxylcytosine (5caC) (Branco et al., 2012). Both 5fC and 5caC can be removed by glycosylases, such as thymine DNA glycosylase (TDG) (Maiti and Drohat, 2011). The TDG enzyme has been previously implicated in

removal of thymine in the T:G base mismatch and activation of base excision repair (BER) (Branco et al., 2012). Surprisingly, the TDG enzyme has a stronger affinity to 5fC than to T:G site and is also able to remove 5caC (Maiti and Drohat, 2011). The accompanying BER mechanism is able to insert un-methylated cytosine. Therefore, multiple methods are likely present in demethylation of DNA. The role of TETs in epidermal differentiation is not yet understood and requires further research.

1.3.2. Covalent histone modifications and Polycomb-dependent gene silencing

The genome is organized in a hierarchical manner. Firstly, the genome is made up of chromosomes, which represent a largest unit of genome organization. Secondly, the chromosomes are made up of nucleosomes. Thirdly, one nucleosome consists of ~ 146 bp of DNA coiled around a histone octamer protein complex composed of two H2A-H2B and two H3-H4 histone heterodimers (Perdigoto et al., 2014).

Gene transcription is affected by histone modifications which usually occur in the amino-terminal part (histone tail) and can involve acetylation, methylation, phosphorylation, ADP-ribosylation, arginine deamination, proline isomerization, sumoylation and ubiquitination (Perdigoto et al., 2014). Depending on the location and the type of modification will determine the expression state of a gene (**Fig. 1.6**) (Perdigoto et al., 2014) because these modifications alter histone-DNA and histone-histone interactions

thereby influencing the accessibility of transcriptional machinery to the DNA (Perdigoto et al., 2014).

Histone methylation and acetylation are the most characterised modifications in the epidermis. While methylation is associated with both transcriptional activation and repression, acetylation is mostly correlated with positive regulation of gene expression (**Fig. 1.6.b**) (Perdigoto et al., 2014). These modifications are established by histone methyltrasferase and acetyl transferase enzymes and are removed by demethylase and deacetylase enzymes (Perdigoto et al., 2014).

Histone acetylation

Histone acetyl trasferases (HATs) and histone deacetylases (HDACs) are the enzymes which regulate histone acetylation (Campos and Reinberg, 2009). Hyper- and hypo-acetylation of lysine is associated with activation and repression of transcription, respectively, because of the changes in chromatin compaction (Campos and Reinberg, 2009). For example, chromatin from cells treated with an inhibitor for HDAC, trichostatin A (TCA), are less resistant to digestion by endocnucleases (Campos and Reinberg, 2009). Interestingly, the types of acetylation modifications of an active gene differ between the promoter and the coding region of the gene. The promoter is enriched with H3K9ac, H3K18ac and H2B12ac and the gene has H4K12ac and H4K16ac (**Fig. 1.6.c**) (Botchkarev et al., 2012). TCA treatment decreases cell proliferation in the epidermis (Markova et al., 2007) and induces the expression of involucrin in primary keratinocytes (Saunders et al., 1999). Deletion of HDAC1 and HDAC2 results in failure of the

epidermal stratification and ectopic expression of p21, 14-3-3σ and p16 in the ectoderm. (LeBoeuf et al., 2010). The aryl hydrocarbon receptor nuclear translocator (ARNT) was found to control expression of epidermal differentiation genes through HDAC and EGFR-dependent pathway (Robertson et al., 2012).

Histone methylation

Mono-, di-, and try-methylation are three types of modifications that can occur at histone tails and thereby regulate gene expression. Just like with acetylation, genes that are transcriptionally active or silenced also show preferential enrichment of specific methylation markers. For example, silenced genes are enriched with di- and try-methylation of histone H3 lysine 9 (H3K9me2/3) and H3K27me3 (**Fig. 1.6.c**) (Botchkarev et al., 2012; Wang et al., 2009). In active genes, these sites are monomethylated along with H3K20me1, also H3K4me3 and H3K4me1/2 are present at and around the transcriptional start site (Botchkarev et al., 2012; Wang et al., 2009). In addition, active genes can have H3K79me2/3 and H3K36me3 at 5' region and at 3' region, respectively (**Fig. 1.6.c**) (Botchkarev et al., 2012). Furthermore, some gene promoters are enriched in both H3K4me3 and K3K27me3 which puts gene transcription in a paused state (**Fig. 1.6.c**) (Botchkarev et al., 2012; Perdigoto et al., 2014; Wang et al., 2009).

The H3K20me1 histone modification has been studied in more detail during epidermal development (Driskell et al., 2012). This mark is catalysed by Setd8-mediated histone methylation and is present at transcriptionally active genes. Loss of Setd8 results in absence of proliferation and aberrant

differentiation of the epidermis (Driskell et al., 2012). The reason for this is because Setd8 is a transcriptional target of c-Myc and the absence of p63 transcription, which is mediated by H3K20me1 (Driskell et al., 2012). However, the main reason for loss of proliferation is due to increased expression of p53, which promotes cell apoptosis (Driskell et al., 2012). Therefore, Setd8 is essential for epidermal proliferation and differentiation.

The H3K27me3 is a repressive mark which is present at the promoters of many genes involved in epidermal differentiation (Sen et al., 2008). One of the enzymes that is capable to demethylate this mark and induce gene expression is a member of Jumonji C (JmjC) domain-containing proteins, JMJD3 (Agger et al., 2007). JMJD3 is crucial for proper regulation of epidermal development because depletion of this protein blocks differentiation (Sen et al., 2008).

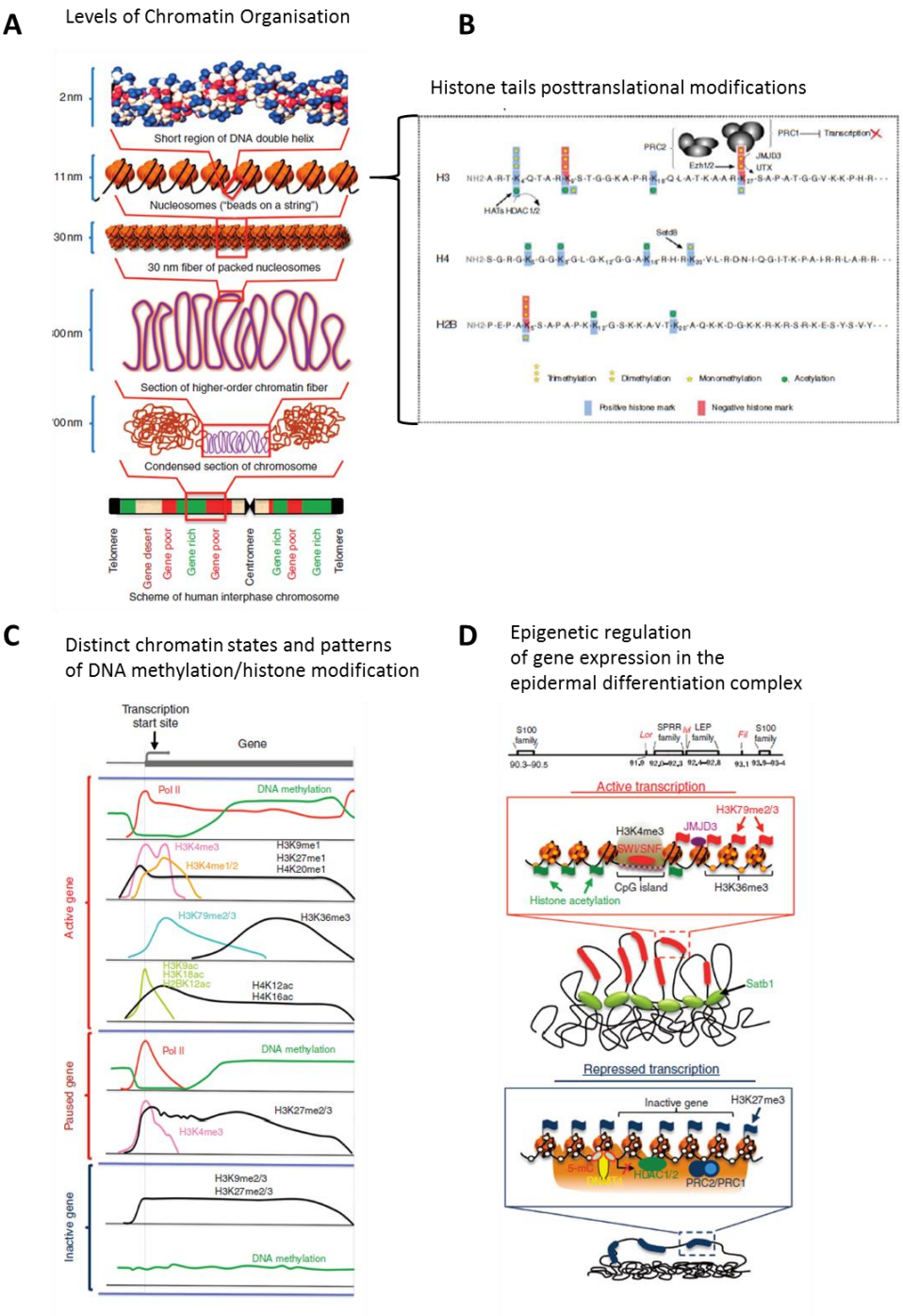

Figure 1.6. Distinct levels of chromatin organization. (A), post translational modification in histone tails (B), characteristics of the active and inactive chromatin domains (C), and epigenetic control of gene expression in the epidermal differentiation complex locus (D). Modified from (Botchkarev et al., 2012; Perdigoto et al., 2014).

1.3.3 Polycomb-dependent gene silencing

Gene silencing characterised by presence of H3K27me3 is medicated by different Polycomb group proteins (PcGs) (Di Croce and Helin, 2013). PcGs are able to block RNA polymerase 2 elongation by modulating chromatin compaction (Di Croce and Helin, 2013). They perform this functions by assembling into larger structures called Polycomb repressive complexes (PRCs) (Di Croce and Helin, 2013). Currently, there are two types of well-studied PRC complexes that are formed from PcGs, which are PRC1 and PRC2 (Di Croce and Helin, 2013). PRC1 is made from four core PcGs components, which are RING1, CBX, PCGF and HPH, while PRC2 consists of three PcGs components, which are EZH, EED and SUZ12 (**Fig. 1.7**). An overview of our current understanding of how PRCs carry out their gene silencing activity, how they are targeted to chromatin sites and their role in epidermal development is described below.

Mechanisms of PRC recruitment and regulation of gene silencing

Components of the PRC2 complex, specifically EZH1 and EZH2 are responsible for the mono-, di- and tri-methylation of H3K27 (Margueron et al., 2008). EZH1/2 require EED and SUZ12 for a functional methyl-transferase activity (Cao and Zhang, 2004). Genome-wide analysis identified a correlation between CpG rich-DNA and H3K27me3 (Ku et al., 2008). However, only CpG islands which were largely un-methylated and did not have any binding sites for transcriptional activators were able to recruit PRC2 by unknown mechanism (Mendenhall et al., 2010). Interestingly, TETs might be involved in recruitment of PRC2 due to their

ability to modify 5mCpG DNA (Wu et al., 2011). A zinc-finger binding protein, AEBP2, was found to bind to DNA and recruit PRC2 (Kim et al., 2009). Furthermore, another member of Jumonji C (JmjC) domain-containing proteins, JARID2, was found to enhance recruitment of PRC2 (Li et al., 2010) and is important in maintaining epidermal homeostasis (Mejetta et al., 2011).

The H3K27me3 provides a docking site for canonical PRC1 because this modification mark is recognised by the chromo-domain of the CBX component from PRC1 complex. After docking, the E3 ligases RING1a/b from PRC1 catalyse mono-ubiquitilation of H2A on K119 (H2AK119ub1), which leads to chromatin compaction (Wang et al., 2004). Compacted chromatin prevents accessibility of transcription factors and ATP-dependent chromatin remodelling machinery (SWI/SNF) (Bantignies and Cavalli, 2011). Also, it has been shown *in vitro* that H2AK119ub1 prevents methylation of H3K4 (Nakagawa et al., 2008). However, H2AK119ub1 is required for reactivation of PRC-silenced genes because this modification mark is recognised by zuotin-related factor 1 (ZIF1), which is able to displace PRC1 from chromatin and initiate gene transcription (Richly et al., 2010).

Until recently, it was believed that the mechanism of Polycomb dependent gene silencing consisted of PRC2 mediated tri-methylation of H3K27 and then subsequent recruitment of PRC1. However, this view has become outdated after the discovery of non-canonical PRC1 which do not have the CBX and HPH components (Schwartz and Pirrotta, 2014).

Furthermore, it was found that certain CpG islands can recruit PRC1 in addition to PRC2 (Wu et al., 2013). Specifically, a non-canonical PRC1 component called KDM2B targets RING1b via a CXXC zinc finger domain to specific loci containing CpG islands in mouse embryo stem cells (Wu et al., 2013). KDM2B is unable to bind methylated CpG (Simon and Kingston, 2013). Therefore, TETs in addition to recruiting PRC2, might, also be involved in recruiting non-canonical PRC1 (Wu et al., 2011). Interestingly, non-canonical PRC1 mediated ubiquitination of H2AK119 is able to recruit PRC2 (Blackledge et al., 2014; Cooper et al., 2014). Remarkably, Kalb *et al* (2014) were able to identify AEBP2 and JARID2 along with PRC2 to be present on nucleosomes containing H2AK119ub1. The authors concluded that PRC2 complexes containing AEBP2 and JARID2 are able to specifically interact with H2AK119ub1 and promote methylation of H3K27 (Kalb et al., 2014). Also, ablation of PRC1-mediated H2AK119 ubiquitination impairs genome-wide PRC2 binding and disrupts mouse development (Schwartz and Pirrotta, 2014).

The role of PRC2 component EZH2 has been studied in the development of mouse epidermis. Analysis of genes targeted by PRC2 in basal epidermal cells identified the H3K27me3 mark to be associated with promoters of almost 4000 genes that are normally expressed in muscle, neuronal and hematopoietic cells (Ezhkova et al., 2009). The H3K27me3 mark was not present among genes that are specifically expressed in the basal and early epidermal differentiation cells (Ezhkova et al., 2009). However, it was present at numerous promoters of genes involved in late epidermal differentiation, which are normally expressed in granular and

cornified layers (Ezhkova et al., 2009). Furthermore, EZH2 was highly expressed in the proliferative cells of basal layer and was down-regulated in the differentiated cells of the suprabasal layer (Ezhkova et al., 2009). Absence of EZH2 in the epidermal progenitor cells resulted in up-regulation of skin differentiation genes only and accelerated development of skin barrier formation (Ezhkova et al., 2009). This data indicated that other mechanisms of suppressing non-skin lineage genes must be present. Of the most up-regulated genes in the EZH2 depleted basal cells many were from the Epidermal Differentiation Complex (EDC), which included genes specific to the granular layer such as fillagrin, loricrin, involucring and genes of the late cornified envelope family (Zhang et al., 2012). Interestingly, EDC locus is the subject of higher order chromatin remodelling due to the activity of p63 and Satb1 (**Fig. 1.6.d**) (Fessing et al., 2011). Additionally, EZH2 mediated repression of epidermal differentiation genes was achieved by prevention of transcription factor (AP1) binding to the target genes (Perdigoto et al., 2014).

Analysis of PRC1 component CBX4 in the human epidermis revealed that it regulates proliferation and differentiation of epidermal progenitor cells (Luis et al., 2011). Interestingly, Luis et al (2011) have found that SUMO ligase activity of CBX4 inhibits stem cells activation and differentiation, while, the polycomb activity of CBX4 is responsible for maintaining anti-senescence. In murine epidermis, Cbx4 plays a crucial role in maintaining the epithelial identity and proliferative activity in keratinocytes via repression of the selected non-epidermal lineage and cell cycle-inhibitor genes (Mardaryev et al., 2016).

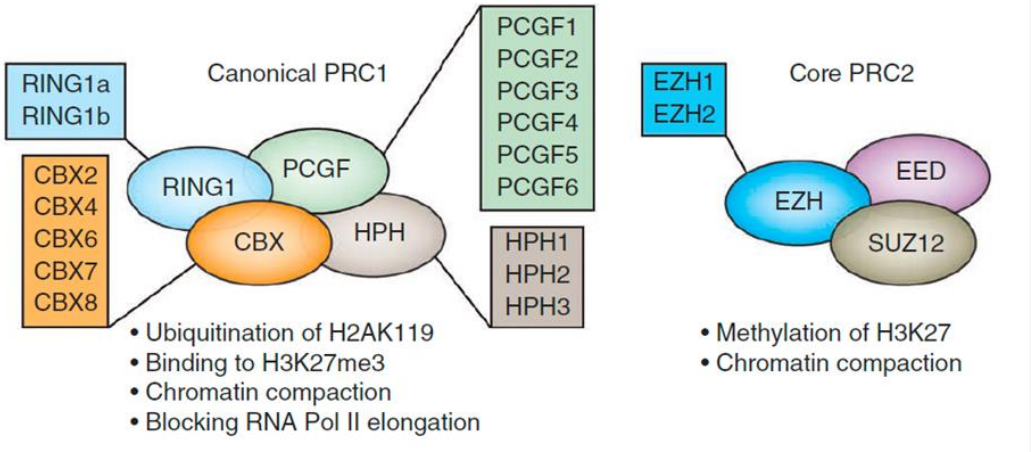

Figure 1.7. Composition and function of the main Polycomb complexes. Modified from (Di Croce and Helin, 2013)

1.3.4. Higher order chromatin remodelling and 3D genome organisation

"Higher order chromatin folding or structure" is a term that depicts chromatin organization after "beads on a string" model (**Fig. 1.6.a**) (Ferrai et al., 2010). Previously, it has been shown that the 3D organization of chromatin within the nucleus is not random. In fact, over a century ago light microscopy investigation of the nuclei stained with basic dyes identified regions of chromatin that were brighter, therefore, more condensed (heterochromatin) and dimmer regions representing expanded chromatin (euchromatin). Also, the features of the two chromatin types are different, euchromatin is transcriptionally active, contains large number of genes and replicates early in the cell cycle, while heterochromatin has low transcriptional activity, low number of genes and replicates later in the cell cycle (Dimitri et al., 2009). Furthermore, heterochromatin can be split into at least two stages: constitutive heterochromatin, which consists of silent repetitive regions, centromeres and telomeres, and facultative heterochromatin consisting of specific gene loci that can have variable states of repression in some cells or activation in other cells depending on the cellular context (Dimitri et al., 2009).

Recent research into the 3D genome organization has revealed that the chromosomes in the interphase nucleus take up distinct areas (chromosome territories) and genes within a particular chromosomal territory are located relative to each other and other nuclear sub-organelles in non-random arrangement (Albiez et al., 2006; Cremer and Cremer, 2010;

Naumova and Dekker, 2010; Sanyal et al., 2011). These observations have been possible due to two experimental techniques. First technique involves the analysis of 3D images generated by confocal microscopy of nuclei processed using fluorescent in situ hybridization (FISH) or fluorescent DNA binding chimeric proteins (Chuang et al., 2006; Joffe et al., 2010; Kumaran et al., 2008). Second technique exploits chromosome conformation capture technologies such as 3C which involves cross-linking chromatin followed by restriction, ligation, PCR and sequencing to identify intra-molecular products (Naumova and Dekker, 2010).

Analysis of the data obtained from chromosome conformation capture technologies enable the identification of topologically associated domains (TADs). TADs have been defined as “linear units of chromatin that fold as discrete three-dimensional (3D) structures tending to favor internal, rather than external, chromatin interactions” (Ciabrelli and Cavalli, 2015). TADs have been proposed as invariant building blocks of chromosomes. Furthermore, chromatin interactions within TADs are cell type-specific, thereby linking 3D genome structure with phenotype. Surprisingly, TADs were found to be conserved in different animal cell types but absent in yeast and plants (Feng et al., 2014; Grob et al., 2014; Moissiard et al., 2012; Tanizawa et al., 2010; Tjong et al., 2012).

It has been demonstrated that genes which are actively transcribed are often found associated with each other in active chromatin domain, while silent genes also tend to cluster together in the silenced chromain domain (Lieberman-Aiden et al., 2009). Furthermore, the process of gene

activation or silencing can involve adjustments to the location of the gene relative to other domains and/or nuclear bodies (Misteli, 2007; Schoenfelder et al., 2010a).

1.3.4.1. Transcription factories

Various evidence obtained from immunohistochemistry of phosphorylated Serine-5/2 RNA Polymerase 2 isoforms indicated that transcriptional factories can form after RNA Pol II-containing pre-initiation complexes assembled next to each other in the nuclear space (Cook, 1999; Schoenfelder et al., 2010a). Furthermore, large number of genes located on the same or different chromosomes which are transcriptionally active at the same time sometimes share a single transcriptional factory made from a unique combination of transcription factors and transcription facilitating molecules (Eskiw et al., 2010; Razin et al., 2011). Remarkably, such an event does occur in the erythroid cells where Hbα/β globin genes and hundreds of transcribed genes from various chromosomes aggregate in transcription factories enriched by a transcription factor Klf1 (Schoenfelder et al., 2010b). Therefore, specific transcription factories may function as hubs where tissue and cell-type specific inter- and intra-chromosomal interactions occur to coordinate expression of genes required for differentiation programs (Chakalova and Fraser, 2010).

Cell type-specific repositioning of genes from the nuclear periphery to nuclear interior is frequently seen through the course of development (Egecioglu and Brickner, 2011). This has been observed in human primary keratinocytes where the EDC located on chromosome 1 forms a loop

outside of the chromosomal territory (Williams et al., 2002). Repositioning, however, might not apply to all active genes because many of them are expressed inside the chromosomal territories (Mahy et al., 2002a; Mahy et al., 2002b). Gene repositioning during development could be interpreted as a way to reach an environment that is suitable to maintain or regulate gene expression (Lanctot et al., 2007). In developing mouse epidermis, EDC locus show remarkable developmentally regulated repositioning from nuclear periphery towards nuclear interior, which is associated with marked increase of transcription of terminal differentiation genes (Mardaryev et al., 2014). In differentiating epidermalin keratinocytes, EDC tends to cluster around nuclear speckles localized in the interchromatin compartments (Mardaryev et al., 2014) possibly because speckles provide a permissive environment for transcription, also, they are enriched with RNA splicing machinery (Hu et al., 2008; Spector and Lamond, 2011). Interestingly, it was shown that the relocation of genes promoting proliferation from repressive Polycomb bodies to speckles is associated with the methylation and demethylation of CBX4 component of the canonical PRC1 protein complex. Methylated and demethylated forms of CBX4 can attach to non-coding RNA TUG1 and non-coding RNA MALAT1/NEAT2, located at Polycomb bodies or speckles, respectively (Yang et al., 2011). MALAT1/NEAT2 mediated interactions with many transcription and/or splicing factors results in gene activation after their relocation to the speckles (Yang et al., 2011).

It was recently demonstrated that genetically engineered mice with ablation of either Keratin type I or type II loci from chromososmes 11 and

15, respectively display perinatal mortality and severe barrier (Kumar et al., 2015). Absence of keratins seriously compromises epidermal development and prenatal (E18.5) pups display a hyperthickened, fragile epidermis with smaller and fewer desmosomes, leading to intercellular adhesion defects (Bar et al., 2014). Epidermis of KtytII-/- showed a compact stratum corneum and apparent absence of filaggrin and locricrin-positive keratohyalin granules confirmed by electron microscopy, compared to controls (Kumar et al., 2015). Global gene expression analysis of back skin RNA from KtyII-/- and control littermates at E18.5 showed that of the 61 genes located on the EDC (de Guzman Strong et al., 2010), 15 encoding structural CE components, among them loricrin, filaggrin 2, hornerin (Hrnr) and late cornified envelope group1 genes (Lce1), were strongly downregulated in KtyII-/- mouse skin. However, 22 genes including small proline-rich genes (Sprrs), S100A8 and late cornified envelope group 3 genes (Lce3), connected to oxidative stress, barrier defects and hyperproliferative skin conditions, were upregulated upon Keratin type II locus ablation (Kumar et al., 2015). This study suggests the complexity of interactions between lineage-specific gene loci in the nucleus that link keratin scaffolds to epidermal barrier formation and maintenance.

1.3.4.2 Long-range chromatin interactions

"Transcriptional interactome" refers to cell type specific transcriptional profile which is the outcome of long-range inter- and intra-chromosomal associations that occur between different genomic regions (Cope et al., 2010; Schoenfelder et al., 2010a). These kind of interactions can be observed during Ca^{2+}-stimulated primary keratinocyte differentiation where

enhancer and promoter of the peptidylarginine deiminase 3 gene, which regulates metabolism of fillagrin, come together (Chavanas et al., 2008). Energy dependent process of gene relocation or other distant interactions with in the nucleus is mediated, at least partially, by actin-myosin nuclear motor complexes (Botchkarev et al., 2012; Chuang et al., 2006). Furthermore, a number of proteins are associated with the function of genome organization by creating loop-like structures inside (cis-) the chromosomes and between (trans-) the chromosomes. These proteins include Ctcf, cohesin and Satb1 (Cai et al., 2006; Merkenschlager, 2010; Ohlsson et al., 2010).

Satb1 plays an important role in governing tissue-specific gene expression programs by regulating 3D chromatin conformations via the targeting of remodeling enzymes and transcription factors to distinct genomic regions (Cai et al., 2006). The role of Satb1 has been studied during epidermal development and it was found to control conformation of the EDC locus, which contains differentiation genes (Fessing et al., 2011). Deletion of Stab1 causes the elongation of EDC within the 3D nuclear space, as a consequence gene expression and epidermal morphology are aberrant (Fessing et al., 2011). Therefore, 3D organization of tissue-specific genomic loci plays a role in the regulation of transcription programs and gene expression outcomes. Other key proteins implicated in generating 3D loop structures are Ctcf and cohesin.

1.3.4.3. CTCF as a master chromatin architectural protein involved in 3D genome assembly

CTCF is able to bind DNA and is likely involved in the formation of thousands of loops in the genome (**Fig. 1.8**), which can bring genes from different chromosomes into close proximity (Ohlsson et al., 2010). Also, CTCF recruits cohesin which is crucial for regulating chromosomal segregation during mitosis (Hadjur et al., 2009). Furthermore, cohesin controls conformation and gene expression as described in T-cell receptor locus where CTCF-cohesin complex mediates promoter-enhancer associations and maintains transcription and boundary of the locus from scattered elements and neighboring housekeeping genes (Merkenschlager, 2010; Seitan et al., 2013).

Much evidence has been generated to implicate CTCF in TAD formation. Firstly, TAD borders were found to be enriched for CTCF biding sites. Secondly, CTCF depletion in cells results in decrease in intradomain interactions, while, interaction between adjacent TADs are increased (Reviewed in Ong and Corces, 2014). Thirdly, this 11 zinc finder DNA binding protein is heavily conserved among animals, while it is absent in yeast and plants (Reviewed in Ong and Corces, 2014).

The CTCF target consensus DNA binding sequence (**Fig. 1.9**) contains CpGs indicating that methylation of cytosine can play a role in CTCF binding selectivity (Engel et al., 2004). This has been confirmed with one study showing that in 19 human cell types 41% of cell type specific CTCF-binding sites are linked with methylation status (Wang et al., 2012).

Surprisingly, CTCF itself can maintain a de-methylated state of DNA by binding and activating PARP1 which in turn turns off DNMT1 (Guastafierro et al., 2008; Zampieri et al., 2012). Hydroxymethylation of 5mC by the TET enzymes provide another level of complexity to this process (Ito et al., 2011; Kriaucionis and Heintz, 2009; Tahiliani et al., 2009).

Presence of CTCF biding sites that are not methylated suggest another regulatory mechanism of DNA occupancy by this protein. Posttranslational modification of CTCF is another mechanism. For example, incorrect poly(ADP-ribosy)lation of CTCF has been linked with CTCF removal from the tumour suppressor CDKN2A locus resulting in silencing of the p16(INK4a) gene in human breast cancer due to methylation of CpG by DNMT1 (Witcher and Emerson, 2009).

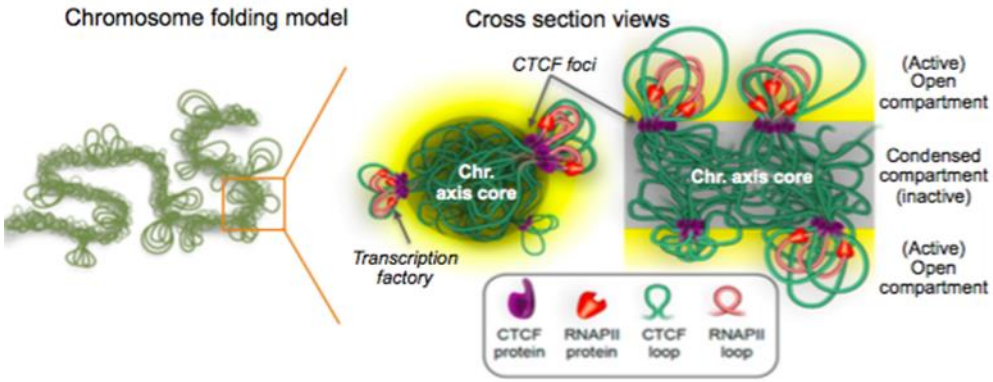

Figure 1.8. Model of chromosome folding involving CTCF and RNA Polymerase II. Modified from (Tang et al., 2015).

Further mechanisms of CTCF targeting to DNA sites can be due to interactions with other proteins. A number of proteins have been confirmed in CTCF function such as PARP1, YY1, MAZ, JUND, ZNF143 (Reviewed in Zlatanova and Caiafa, 2009). However, only cohesin has been found to be essential for stabilizing most CTCF-chromosomal contacts (Reviewed in Ong and Corces, 2014). The SA2 subunit of cohesin can interact with the carboxy-terminal part of CTCF (Xiao et al., 2011). Disruption of cohesin expression also alters intrachromosol interactions mediated by CTCF (Hadjur et al., 2009; Hou et al., 2010; Nativio et al., 2009). Interestingly, another protein that can possibly interact with CTCF is TFIIIC, which along with RNA polymerase III is involved in transcription of tRNAs, 5S rRNA, non-coding RNA (ncRNA) and B2 short interspersed nuclear elements (SINEs) (**Fig. 1.9**) (Kirkland et al., 2013). CTCF and cohesin have been found associated with genomic locations containing tRNA genes as well as TFIIIC bound sites that are devoid of Pol III in mouse and human cells (Carriere et al., 2012; Moqtaderi et al., 2010; Oler et al., 2010).

Other data has showed that RNAs are also involved in stabilizing CTCF interactions with other proteins. For example, CTCF had been implicated in binding to both the DEAD-box helicase p68 and its associated ncRNA (Yao et al., 2010). The ncRNA was found to be important for the correct CTCF function (Yao et al., 2010). This data indicates that ncRNAs do play a role in stabilizing CTCF-mediated interactions.

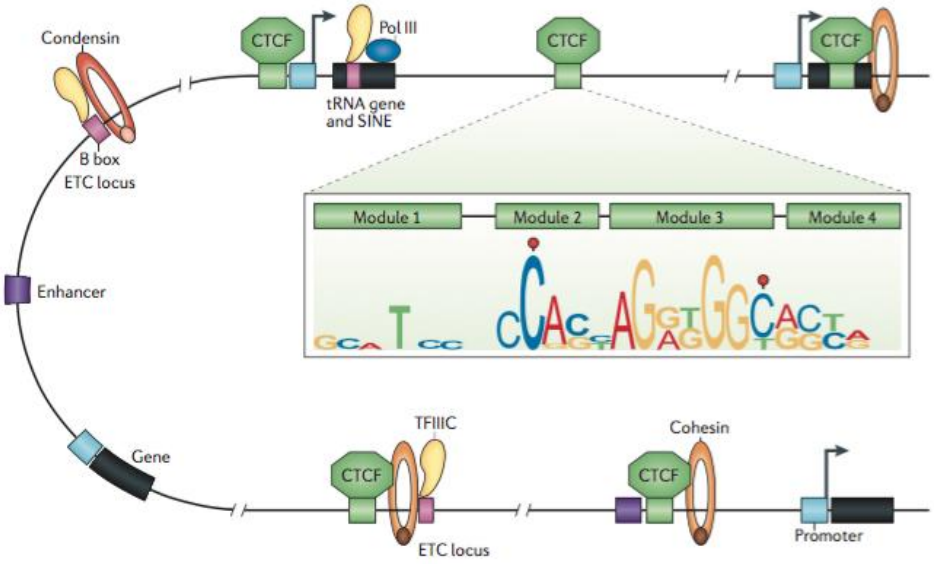

Figure 1.9. Key features of Ctcf binding sites. (Modified from Ong and Corces, 2014).

Ctcf has also been implicated in inter-chromosomal associations that are able to regulate gene expression. This has been shown in CD4+ T cells, which upon antigen stimulation can differentiate into three types of helper cells, Th1, Th2 and Th17 which express IFN-gamma, IL-4, and IL-17, respectively (Kim et al., 2014). Interestingly, using 3D-FISH it was shown that the locus containing IFN-gamma has been found to be associated with Th2 locus, and Th2 locus can associate with IL-17 locus (Kim et al., 2014). Differentiation into Th17 cells was found to be restrained by the association with the Th2 locus and this was orchestrated by Oct-1 and CTCF (Kim et al., 2014). The association was found to require an Oct-1 biding site at the DNase I hypersensitive region (RHS6) of the Th2 locus and the IL-17 promoter of IL-17 locus. Deletion of RHS6, Oct-1 or CTCF deficiency all impaired the association, which resulted in enhanced IL-17 expression, paralleled by an increased frequency of IL-17-producing cells during early during differentiation of naive T cells toward the Th17 lineage (Kim et al., 2014).

Whether gene expression in the keratinocyte-specific genomic loci is affected as a result of CTCF-mediating inter-chromosomal associations is yet to be determined. Also, the phenotype of skin deficient for CTCF is unknown. However, some data exists for cohesin-SA1 in skin development. The cohesin-SA1 null embryos (E17.5) had thinner skin with reduced number of hair follicles (Remeseiro et al., 2012). Mircroarray analysis of cohesin-SA1 null mouse embryonic fibroblasts identified that expression of

gene cluster involved in skin function was affected (Remeseiro et al., 2012). These clusters were predominantly located in the keratin type I and keratin type 2 locus. Furthermore, Ctcf Chip-Seq data obtained by Dr Andrei Mardaryev (University of Bradford) had showed Ctcf biding sites within various regions of the EDC locus (**Fig. 1.10**). Thus, the data suggest that CTCF is likely to also be involved in the control of skin development and keratinocyte differentiation.

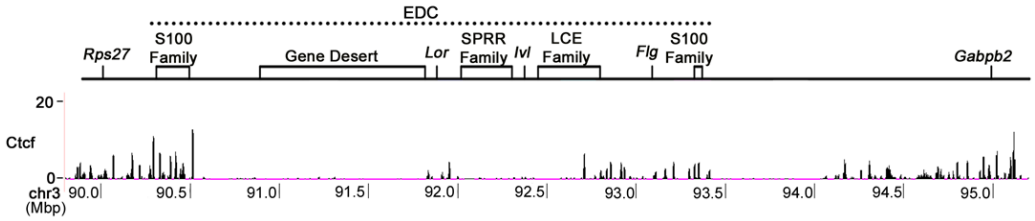

Figure 1.10. Ctcf Chip-Seq Peaks on the Epidermal Differentiation Complex. Experiment carried out by Dr Andrei Mardaryev (University of Bradford) and analyzed by Dr Krzysztof Poterlowicz (University of Bradford).

1.3.4.4. Heterochromatin

Heterochromatin is closely linked with repressive epigenetic marks such as 5meCpG and H3K9me3, as well as other proteins that participate in chromatin remodeling, such as Heterochromatin Protein 1 (HP1) (Kwon and Workman, 2011; Probst and Almouzni, 2011). Interestingly, there are three specific heterochromatic domains which are not transcriptionally active. First, domains associated with centromeres is depicted by DNA methylation, H3K9me3, H3K20me3 and α/β/γ HP1 isoforms. Second, domains enriched by H3K9me2 and HPα/β associated with nuclear lamina. Third, domains depicted by H3K27me3 and PcGs (Meister et al., 2011; Probst and Almouzni, 2011). Even though all of the heterochromatins contain some genes that are actively transcribed majority of the genes present there are silenced either permanently at the centromeres or temporarily in a manner that is developmentally-regulated by PRCs or lamina association (Meister et al., 2011).

HP1 isoforms α, β and γ, which are encoded by chromobox genes CBX5, CBX1 and CBX3, respectively, play vital roles in the heterochromatin formation. HP1α/β binds H3K9me3 and Lamin B receptor thereby maintaining lamina-associated heterochromatin and transcriptional repression, in contract HP1γ interacts with euchromatin by binding to the elongating of Polymerase II via histone chaperone FACT and positively regulating transcription (Black and Whetstine, 2011; Kwon and Workman, 2011).

Polycomb proteins are indispensable when it comes to maintaining a repressed state of the chromatin. Polycomb proteins interact with polycomb response elements and gene promoters to form repressive structures and maintain gene silencing (Lanzuolo et al., 2007). In fact, the silenced chromatin loops might be organized in the nucleus into Polycomb bodies which can be considered as chromatin silent factories that contain repressors of transcription such as non-coding RNA TUG1 (Aamodt et al., 2011; Yang et al., 2011). So far it is unclear how such repressive factories contribute to differentiation of the epidermis.

To summarize, there are two key epigenetic mechanism that modulate local and higher order chromatin architecture of keratinocytes. These include: 1) controlling the expression of genes associated with terminal differentiation; and 2) regulating cell-cycle associated gene expression. For example, repressive chromatin regulators (DNA methyltransferase DNMT1, histone deacetylases HDAC1/2, Polycomp components Cbx4, Bmi1, Ezh1/2) function by stimulating proliferation of progenitor cells via repression of the genes encoding cell-cycle inhibitors p16INK4A, p15INK4B, p21 and p19ARF. Furthermore, several repressive chromatin regulators (DNMT1, Ezh1/2, Jarid2) also prevent premature activation of terminal differentiation-associated genes, whereas HDAC2 inhibits expression of deltaNp63 and interfere with deltaNp63-regulated gene expression program in keratinocytes.

Conversely, terminal keratinocyte differentiation is promoted by chromatin remodelers that generally support active transcription and exhibit

effects on cell proliferation (histone demethylase Jmjd3, ATP-dependent chromatin remodeler Brg1, genome organizer Satb1). Most likely expression of genes associated with terminal differentiation including EDC genes of epidermal keratinocytes involves highly coordinated action of several epigenetic regulators that operate at both levels of local (DNMT1, Ezh1/2, Bmi1, Jarid2, Jmjd3, Brg1) and higher-order (Satb1) chromatin structures.

In this Thesis, the mechanisms regulating higher-order chromatin remodeling in skin epithelial cells are explored using a complex approach including microarray and qRT-PCR gene expression analyses, 3D-FISH studies of gene topology in the nucleus, keratinocyte-specific gene targeting and in vivo analyses of skin phenotype in genetically engineered mice. In particular, the results of analyses of three-dimensional organization of lineage-specific gene loci in epidermal keratinocytes using 3D-FISH technique are presented in Chapter 3.1. Furthermore, the effects of the genetic ablation of the gene encoding chromatin architectural protein Ctcf on skin development and post-natal regeneration are described in the Chapters 3.2-3.4. The results of these experiments are discussed in the Chapter 4 and conclusions are summarized in Chapter 5.

1.3. Aims and Objectives of this study

The aims of this study are to study three-dimensional organization of the lineage-specific gene loci in keratinocytes and explore the mechanisms that control higher-order chromatin remodelling and activity of lineage-specific genes in the skin epithelium.

These aims will be achieved via three distinct Objectives:

1. To study three-dimensional organization of lineage-specific gene loci (Keratin type I/II loci, Epidermal Differentiation Complex locus) in epidermal keratinocytes and define how genetic ablation of the Keratin type II locus in mouse epidermis affect three-dimensional nuclear architecture and nuclear positioning of the Epidermal Differentiation Complex locus.
2. To explore the mechanisms that control higher-order chromatin organization and remodeling in epidermal keratinocytes during murine skin development and define the role of Ctcf in the control of epidermal development and keratinocyte differentiation in mouse skin.
3. To delineate the role of Ctcf in the control of epidermal barrier maintenance and terminal keratinocyte differentiation in the epidermis of postnatal skin.

2. MATERIALS AND METHODS

2.1. Animals and tissue collection

Skin samples of Keratin Type I and Type II knockout mice (P0-P9) for 3D-FISH analyses were provided by Thomas Magin's laboratory (Leipzig University, Germany) as part of collaboration. All other skin samples were obtained from mice being housed at the University of Bradford animal facility under the approval of PPL 40/2989 licence.

The skin samples were collected from the embryos (E14.5, E16.5, E18.5) or postnatal wild-type C57Bl6 mice (P1.5-P19.5). Hair cycling was induced in 8 week-old mice by depilation and skin was collected at different time points post-depilation (days 0 p.d. – 21 p.d.).

Targeted keratinocyte-specific *Ctcf* deletion using Cre-Lox recombination technology was used to study the role of Ctcf in the control of skin development and postnatal homeostasis. *Ctcf* fl/fl mice (generated by Heath et al., 2008) were crossed with tamoxifen-inducible transgenic mouse expressing Cre recombinase/estrogen receptor under the control of Cytokeratin 14 promoter. The *K14-Cre/ER-Ctcf* fl/fl mice were intraperitoneally injected with tamoxifen. This included injecting time-mated mice at E12.5 for three days, followed by the harvesting of embryos at E16.5 and E18.5. Furthermore, 8-week old adult mice were shaved and tamoxifen was applied topically, as well as by intraperitoneal injection for three days and skin samples were collected at 5, 7, 9 and 12 days after the start of treatment. All embryos and skin samples were embedded in OCT (Optimal Cutting Temperature compound), quickly frozen in liquid nitrogen and stored at -80^{o}C until use.

2.2. Immunohistochemistry

2.2.1. Sample preparation

Skin samples were cut using cryostat Microm HM550 (Thermo Scientific) at -30ºC (section thickness - 10µm), which were collected onto adhesive SuperFrost Plus slides (VWR International, Cat. No: 631-0447) and then stored at -80ºC.

2.2.2. Immunofluorescence procedure

Slides with tissue sections selected for immunostaining were removed from the freezer and air-dried at room temperature (RT) for 10 minutes (min). In addition, PAP pen was used to highlight areas around the sections. Tissue was fixed in 4% (w/v) paraformaldehyde for 10 min at RT in a coupling jar. Slides were washed 3 times for 5 min in 1xPBS plus 0.05% (v/v) Triton X-100. Primary antibody diluted in a loading buffer, prepared as described below, was then applied onto sections and incubated overnight at +4ºC.

Antibody loading buffer consisting of 1% (w/v) BSA (Bovine Serum Albumin), 0.1% (v/v) Triton X-100, 0.1% (w/v) Saponin, 1xPBS (10mM PO_4^{3-}, 137mM NaCl, 2.7mM KCl) was prepared and antibodies with appropriate dilution factor were added (Table 2.2).

After incubation with the primary antibody, sections were washed in 1xPBS 3 times for 5 min. Secondary antibody diluted in 1% (w/v) BSA was then applied onto sections and incubated for 1 hour at +37ºC. Slides were

washed again in 1xPBS 3 times for 5 min. Vectashield mounting medium with DAPI and cover slip were then applied onto slides.

Table 2.1. List of primary and secondary antibodies used

Primary antibody	**Dilution**	**Origin**
Rabbit anti-Ctcf	(1:1000)	Cell Signaling (2899S)
Guinea pig polyclonal anti-K14	(1:100)	Abcam
Rabbit polyclonal anti-K10	(1:100)	Abcam (AB76318)
Rabbit polyclonal anti-Lor	(1:100)	Covence (PRB-145p-100)
Rabbint Anti-CD3	(1:100)	Abcam ab5690
Rat Anti-CD4	(1:100)	PharMingen
Rat Anti-CD8	(1:100)	PharMingen
Goat Anti-Lhx2	(1:100)	Santa Cruz (sc-19344)
Secondary antibody	Dilution	Origin
Goat anti-rabbit/guinea pig Alexa Fluor 488/555	(1:200)	Life technologies

TUNEL staining for apoptosis was carried using ApopTag Fluorescein In Situ Apoptosis Detection Kit (Millipore, S7110)

2.2.2. Fluorescence microscopy

Immunostaining was observed using fluorescent microscope Nicon Eclipe 50i and images taken using software ImagePro Express 6.3 connected to IMAGING camera (SN: Q26824).

2.2.3. Haematoxylin and Alkaline Phosphatase Staining

Before Alkaline Phosphatase Staining (APS) the following solutions were made up:

Solution A (30 mM Tris base, 7mM TrisHCl, 100mM NaCl) made up to a volume of 60ml.

Solution B (4M Sodium Natrite, 4mM New Fuchsin) made up to a volume of 420µl if Solution A was made up to 60ml.

Solution C (600mM of Naphthol dissolved in Dimethylformamide) made up to 360 µl if Solution A was made up to 60ml.

Staining for Alkaline Phosphatase was carried out as previously described (Lewis et al., 2014; Sharov et al., 2006). First, slides with cryosections were air-dried at RT for 10min, fixed in acetone at -20^{o}C for 10 min and washed twice in PBS, and were then placed into the APS solution (prepared immediately before staining by first mixing solution A and solution B, then by adding solution C) in a coupling jar for 15 min. Then, slides were washed, in 2xPBS for 5 min, and 300-500µl of haematoxylin was added to each slide for 40-60 seconds. The slides were then washed under running water for 5 min in a coupling jar and the sections were sealed with mounting medium and cover slip.

2.2.4. Bright-field microscopy

Slides were visualised using Brightfield Microscopy (Nicon Eclipe 50i) at 10X magnification using ACT-2U software connected to Nikon SU41 camera (Lewis et al., 2014).

2.2.5. Analysis of the epidermal thickness

Bright-field images of skin were processed and analysed using ImageJ software (NIH). Randomly selected areas of the epidermis were

used to measure distances from the basal layer up to the cornified layer of tamoxifen-treated and control skin. The mean distance was calculated from 2-3 animals and Student t-test was performed to identify any significance (Mardaryev et al., 2014).

2.2.6. Analysis of hair follicle development

Images of skin from AP stained E18.5 were collected from tamoxifen-treated and control animals. The hair follicles were counted and assigned into a stage of development category as described in (Paus et al., 1999). Then, percentage of hair follicles in each category was calculated for each animal. A mean value was determined from 2-3 animals in treatment and control groups and Student t-test was performed for each stage of hair follicle development.

2.2.7. Analysis of epidermal proliferation

Fluorescent images of E16.5 and E18.5 skin stained for Ki67 proliferation marker was analysed using ImageJ software. Number of cells with high intensity of fluorescent signal for Ki67 in the basal cells were counted from at least 2 animals in both the treatment and control groups. Mean values were obtained and Student's t-test was used to compare treatment and control groups.

2.2.8. Analyses of the epidermal barrier defects

Freshly isolated skin from adult mouse was dehydrated in the series of methanol/PBS solution (25% (v/v), 50% (v/v), 75% (v/v)) for 1 min each

followed by incubation in methanol for 1 min. The skin was rehydrated in the same series of methanol/PBS solutions, followed by rinsing in PBS. 0.1% (w/v) Toluidine Blue solution was applied on top of the skin and incubated for 15 min at RT, as described previously (Kumar et al., 2015). Skin samples were then washed extensively in PBS and water, and images were taken using digital camera.

2.3. 3D Fluorescent in Situ Hybridization (3D FISH)

The general procedure of 3D FISH experiment involved three steps. The first step involved wet laboratory experiments, in which fluorescently labelled DNA probes were applied to mouse skin sections, which hybridised to the complementary genomic DNA in the nuclei of the mouse cells. The second step involved using confocal microscopy to obtain 3D images of the mouse nuclei and the fluorescent probes. The third step involved the determination of the exact position of the fluorescent probes within the nucleus and further statistical analysis of these results.

2.3.1. Sample preparation

The mouse samples used for this study included FISH fixed dorsal skin of genetically modified mice (P0-P8) with a deletion of the Keratin Type 2 locus. These samples were provided by Prof. T. Magin (University of Leipzig, Germany). In addition, skin samples for 3D-FISH were obtained from C57Bl6 mice (E17.5, P0-P60), as well as from *Krt14-CreER/Ctcf* fl/fl mice (P60) housed at the animal centre at the University of Bradford.

The FISH fixation procedure was carried out as follows. Skin samples were rinsed in PBS pH 7.4, 2x 5 minutes, room temp. Then, each sample was transferred to a separate 15ml falcon tube and fixed overnight at 4°C in PFA 4% (w/v). The next day fixative was removed and the falcon tubes were filled with 50mM NH_4Cl solution, inverted and incubated for 5 min at room temp. Afterwards, the samples were washed twice for 10 min in 0.1 M phosphate buffer. The samples were then subjected to the following incubations with increasing concentrations of sucrose solution. First, 5 % (w/v) sucrose solution was applied to samples for 60 min at RT. Second, 10% (w/v) sucrose solution was applied 10 min at RT. Finally, samples were incubated overnight in 20% (w/v) sucrose solution at 4°C. The samples were then transferred to embedding cups and after being covered with embedding medium were completely frozen in a dry ice/ethanol bath. The samples were then transferred and stored at -80°C freezer until sectioning.

The sectioning of the samples was performed using cryostat Microm HM550 (Thermo Scientific) at -30ºC with a final section thickness of 14µm, which were collected onto adhesive SuperFrost Plus slides (VWR International, Cat. No: 631-0447) and then stored at -80ºC until further use in the FISH experiment.

Preparation of thymocytes

Thymcytes for 3D FISH experiments were extracted from 6-8 week old C57/Bl6 mice as follows. The thymus was placed on ice in a 6-well plate containing approximately 5ml of RPMI medium (Gibco) supplemented with 10% (v/v) FBS (Gibco) and epithelial tissue was mechanically removed from

the thymus. The cell lysate was filtered through a 70 µm nylon filter (BD Bioscience) and centrifuged at 200*g* for 10min at 4ºC. After discarding the supernatant, the cell pellet was resuspended in 3ml of Red Blood cells lysis Buffer (Sigma-Aldrich) and incubated for 3 minutes at RT. Cells were then diluted with RPMI medium and centrifuged at 200*g* for 10min at 4ºC. The supernatant containing lysed red blood cells was discarded and the cell pellet was resuspended in RPMI medium supplemented with 10% (v/v) FBS (~35-40ml) and filtered through a 70 µm nylon filter.

Meanwhile, microscope slides were coated with polylysine as follows. Slides were placed into 80% (v/v) ethanol for 5 min followed by 1 hour incubation with 150 µl of polylysine hydrobromide (1mg/ml) (Sigma-Aldrich) at RT. Next, slides were rinsed with ddH_2O and air dried. Approximately 1ml of culture medium, containing from ~1×10^5 to ~1×10^6 cells, was placed on a polylysine-coated slide. Slides were incubated in an incubator at 33ºC containing 8% CO_2 for 1 hour. After incubation, each slide was checked under the microscope for attachment and the medium was drained off. Slides were then incubated in 0.3X PBS for 40 seconds.

Thymocytes cells attached to slides were then fixed in 4% (w/v) PFA/0.3X PBS for 10 minutes at RT, followed by three washing in 1X PBS. Slides were then incubated in 0.5% (v/v) Triton X-100/1X PBS at RT for 20 minutes, transferred to 20% (v/v) Glycerol/1X PBS and incubated at RT for 30 minutes. Cells were frozen by dipping slides into liquid nitrogen (~ 30 seconds) and thawing them on a paper towel. As soon as the slides were thawed they were placed back into 20% (v/v) Glycerol/1X PBS solution. The

process was repeated four times. Then the slides were washed in 0.05% (v/v) Triton/1X PBS and a final incubation in 0.1 N HCl for 5 minutes followed this step.

Slides were incubated in 2X SCC/50% (v/v) Formamide from overnight up to a few weeks at 4ºC. Slides were then used for 3D FISH experiments.

2.3.2. Labelling of BAC probes

Bacterial Artificial Chromosomes (BACs) containing the desired sequences were chosen using a Clone Finder tool available at the National Center for Biotechnology Information and ordered from the mouse genomic library kept in the BACPAC Resource Center (BPRC) at the Children's Hospital Oakland Research Institute in Oakland, California. The following BAC clones were used in the study.

Table 2.2. Description of BACs used for probe synthesis.

BAC name	Chromosome	BAC size	BAC start	BAC finish	Build	gene start
RP24-61G19	3	183808	91946069	92129877	36.1	Lor
RP24-355I20	15	211830	1.02E+08	1.02E+08	36.1	krt2
RP24-171O2	15	164238	1.01E+08	1.01E+08	38.1	Ankrd33
RP24-177N5	15	175712	1.02E+08	1.02E+08	38.1	Eif4b

BACs were shipped as LB agar stab culture. Single colonies were obtained after growing overnight at 37°C on LB agar plate containing

20µg/ml of chloramphenicol. These colonies were inoculated into 3ml of LB media inside a 50ml falcon tube supplemented with 20µg/ml of chloramphenicol and grown overnight at 37°C on a shaker (300rmp). Glycerol stocks for long term storage were prepared and stored at -80°C. The rest of the LB media containing bacteria culture was used to isolate DNA as described below.

Firstly, the following solutions were prepared:

P1 solution (4ºC):	**P2 (RT):**	**P3 (4ºC)**
50mM tris, pH 8	0.2 M NaOH	3M NaOAc (Sodium Acetate)
10mM EDTA	1% (w/v) SDS	pH 5.5

Second, falcon tubes were centrifuged at maximum speed for 10 min at RT and supernatant was discarded. Then, the pellet was resuspended in 0.3ml P1 solution, transferred to 1.5 Eppendorf tube and 0.3ml of P2 solution was added. After the mixture was incubated for 5 min at RT 0.3ml of P3, solution was slowly added and the tubes placed on ice for at least 5min. Next, the tubes were centrifuged at maximum speed for 10 min at 4°C and placed on ice. Next, supernatant was transferred to a different 1.5ml Eppendorf tube containing 0.8ml of ice-cold isopropanol, the tubes were inverted and placed on ice for 5 minutes. Next, the tubes were centrifuged at maximum speed for 15 min at 4°C and supernatant discarded. The pellet was washed using 0.5ml of 70% (v/v) Ethanol. After centrifugation at maximum speed for 5 min at 4°C the supernatant was discarded. Finally, pellets were air dried at RT and resuspended in 20µl TE buffer.

Amplification of BAC DNA

BAC DNA isolated from *E.coli* was amplified with illustra GenomiPhi V2 DNA Amplification Kit according to the supplied protocol (GE Health Care Life Sciences, Cat. No: 25-6600-30). Kit contains random hexamer primers, the DNA polymerase of Bacillus phage phi29, nucleotides and buffers. The kit was used to amplify the isolated BAC DNA and the results were checked by electrophoresis on the 1% (w/v) agarose gel.

Labelling of BAC probes

Nick translation (NT) is a method of DNA labelling using DNA polymerase I. Labelled dUTPs (provided by Dr M.Fessing), including FITC-dUTP, Bio-dUTP, Dig-dUTP, were used as the DNA labelling components of the BAC probes. This method works because DNA polymerase I has a 5'-3' exonuclease activity that mediates nick translation during DNA repair, as well as the 5'-3' polymerase activity. Deoxyribonuclease I (DNase I) was used to generate random damage in the BAC probe DNA resulting in single strand nicks. The DNA polymerase I repairs these nicks using the labelled dUTPs.

The following solutions for NT were prepered:

i) dNTP mixture (400µl):

100µl	2mM dATP
100µl	2mM dGTP
100µl	2mM dCTP
20µl	2mM dTTP
80µl	H_2O

ii) 10xNT buffer (100ml):

50ml	1M Tris-HCl pH 7.5
5ml	1M MgCl2
50mg	BSA
45ml	H_2O

iii) 0.1M Mercaptoethanol:

0.1ml	Mecaptoethanol
14.4ml	H_2O

iv) DNase I (grade II, from bovine pancreas) Roche: Cat No: 104 159 (100mg):

1mg/ml in 0.15M NaCl in 50% (v/v) glycerol

v) Stop Mixture:

50mg	Bromphenolblue
250mg	Dextanblue
1ml	5M NaCl
2ml	0.5M EDTA pH8
1ml	1M Tris-HCl pH7.5

The DNase I was diluted to a ratio of 1:250 in cold water and kept on ice, it was then used in the following NT reaction prepared on ice in a 0.2ml PCR tube:

Reagent	**Amount**	**Final Concentration**
2ug DNA (GenomiPhi BAC amp)	5µl	
NT-buffer 10X	10µl	50mM Tris-HCl, pH7.5; 5mM MgCl2; 50ug/ml BSA

β-mercaptoethanol (100mM)	10µl	10mM
dNTPmix(0.5mM ACG, 0.1mM T)	10µl	50µM for ACG, 10uM for T
Modified dUTP 1mM	5µl, 10µl (fluoro-dUTP)	20µM; 40µM for flurochrome labelled nucleotide
ddH_2O	To 100µL	-
DNase 1 (2,000U/ml)	2µl	0.008U in 100µl reaction
Polymerase 1 (Promega, #M205A)	2µl	0.1U/µL

The above reaction was incubated at 15°C for 90 min-120min. The length of the resulting DNA fragments was checked with an aliquot of 5 µL on a 1% (w/v) agarose gel (See Figure 3.1 for an example).

2.3.3. Chromosome Painting

The second amplification of flow sorted DNA of the mouse chromosomes 3 and 15 (obtained from Prof. T. Cremer, Munich University, Germany) was firstly amplified by DOP-PCR method in which DNA is amplified by PCR reaction with degenerated 6MW primers. Similar method was used to label the amplified chromosomal DNA with labelled dUTPs.

Chromosomal amplification with DOP-PCR

The 6MW primer with the following sequence, 5'–CCGACTCGAGNNNNNNATGTGG -3' (Eurofins MWG GmbH, Ebersberg, Germany), was used to amplify chromosomes 3 and 15. The reaction was set up as described below

Single reaction:	1µl	DNA (e.g. chromosome 3 or 15)
	10µl	10x PCR buffer (No $MgCl_2$)

8µl	25mM $MgCl_2$
2µl	100uM 6MW primer
8µl	2.5mM dNTPs
70µl	H_2O
1µl	*Taq* pol
100µl	**Total**

The reaction was placed in a thermocycler with the program below:

Number of Cycles	Reaction	Temperature	Time
1	Initial denaturation	96°C	3min
35	Denaturation	94°C	1min
	Annealing	56°C	1min
	Extension	72°C	2min
1	Final extension	72°C	5min

Next, 2µL of amplification product was run on a 1% (w/v) agarose gel with appropriate size markers to identify if a visible smear ranging between ~200bp and 1.5 kb was present. If the smear was present then chromosome labeling with DOP-PCR was carried out.

Chromosome labelling with DOP-PCR

Amplification and labeling of the chromosomes was performed by setting up the following reaction:

Single reaction: 2µl DNA (e.g. chromosome 3 previously amplified by DOP-PCR)

10µl	10x PCR buffer (No $MgCl_2$)
8µl	25mM $MgCl_2$
2µl	100uM 6MW primer
5µl	2mM of ATP, GTP, CTP mix
8µl	1mM of TTP

6µl	labelled-UTP
58µl	H_2O
1µl	*Taq* pol

The reaction was placed in a thermocycler with the program below:

Number of Cycles	Reaction	Temperature	Time
1	Initial denaturation	96°C	3min
35	Denaturation	94°C	1min
	Annealing	56°C	1min
	Extension	72°C	2min
1	Final extension	72°C	5min

Finally, 2µL of the solution was checked on a 1% (w/v) agarose gel.

2.3.4. Probe validation (2D FISH)

Preperation of nuclei from* newborn *mouse primary fibroblasts

Approximately 4 million cells of mouse primary fibroblasts were seeded into 4 Petri Dishes with complete culture medium containing FBS, 20µg/ml of chloramphenicol and grown for 2 days. Cells were then incubated for 30 min in cell culture medium containing 0.1µg/ml of colcemid at 37°C. After washing cells with pre-warmed 1xPBS (37°C) they were incubated in 2ml of trypsin (2.5g/L) for 3-5min. After cells were detached from substratum 4ml of medium was added. Single cells suspension was obtained by pipetting up and down, transferred to 15ml Falcon tubes and centrifuge at 200×*g* at RT for 6min. 80-90% of supernatant was removed and the cell pellet was mixed with the remaining medium.

Afterwards, 10ml of hypotonic 0.56% (w/v) KCl solution was added dropwise while the solution was being vortexed. The tube was then filled up to 15ml with the hypotonic solution and incubated at 37°C for 25 min. Next it was centrifuge at 200×*g* at RT for 6min and supernatant discarded. Then the nuclei were resuspended in 2ml of fixative (ice cold methanol : acetic acid with a ratio of 1:3) and transferred to a new 15ml Falcon tube. Next, the tube was completely filled with fixative and centrifuged at 200×*g* at RT for 6min. Next, the supernatant was replaced with 14ml of fresh fixative solution, the pellet was resuspended, incubated at RT for 10min and then centrifuged at 200×*g* for 6min. This process was repeated ten times. For storage, the cell pellet was resuspended in 2ml of fixative solution and stored at -20°C.

Metaphase spreads

The previously prepared mouse fibroblasts were centrifuged at 250×*g* for 6min, supernatant was discarded and a new fixative consisting of methanol and acetic acid with a ratio of 3:1 was added. A metal tray was pre-heated in a water bath to 55°C after the water level was adjusted so that 23% of air volume was left under the water bath cover. Microscopic slides were placed on metal tray. Two drops of mouse primary fibroblast suspension was applied onto each slide and left in the water bath until complete evaporation of the fixative. The slides were then checked under phase contrast microscope and if at least 3 metaphase spreads were observed then the slide was placed into a Coplin jar with 70% (v/v) ethanol and left overnight. The next day the 70% (v/v) ethanol solution was replaced

with a fresh 100% ethanol solution and incubated for 10min. Next, the slides were air dried at RT for one week in a closed container. The slides were then incubated for 2 hours at 60°C. Just before the end of the incubation a pepsin solution was prepared by adding 50µl of 10% (w/v) pepsin stock solution to prewarmed (37°C) 0.01M HCl. At the end of the incubation slides were placed into Coplin jar with pesin solution and incubate for additional 10 min at 37°C. Slides were washed 3 times for 5 min in 1X PBS. Then slides were placed consequently ethanol solution, first 70% (v/v) ethanol and then 100% ethanol. Finally, the slides were air dried at RT and stored in a slide box at -20°C.

Validation of the probe specificity and labelling efficiency

After checking for a product expected to be present in the probe by PCR using specific primers, 2D FISH was carried out on the previously generated metaphase spreads as follows. These components were mixed together in 1.5ml Eppendorf tube:

7µl	chosen labelled chromosome (e.g. chromosome 3 or 15)
25µl	labelled BAC probes (from 1 to 3 BACs labelled)
10-25µl	Cot1 DNA (depending on BAC's DNA amount)

Next, ethanol precipitation of DNA was carried out by adding 2.5 volume of 100% ethanol and leaving the mixture at -20°C for 30-60min. The tubes were spun down at maximum speed for 15 min at 4°C. The supernatant was discarded and the pellet air dried. The pellet was then dissolved in 2.5 µl deionized formamide using a shaker set to 37°C for 30 min. To complete the mounting probe, additional 2.5µl of 20% (w/v) dextran

sulphate in 4× SSC (Saline-Sodium Citrate Buffer, at 20× contains 3M NaCl in 0.3M sodium citrate at pH7.0) was added and mixed.

The probe was then mounted onto the slide containing the highest density of metaphase spreads and covered with a 15x15 mm cover slip. A rubber cement was used to seal the cover slip. The slide was left in dark condition at RT for 15-20 min until the rubber cement was completely dry. Next the slides were incubated at 75°C for 2 min. Hybridization chamber on a water bath set to 37°C was used to incubate the slides for 24-48 hours.

The cover sleep along with the rubber cement was carefully removed and the slides were then washed 3 times using 2xSSC for 10 min at 37°C and once in 0.1xSSC for 10 min at 60°C. A secondary detection system was assembled as follows:

Solution: 4xSSC

4% (w/v) BSA

For Bio-dUTP: Streptavidin-Cy5 (1:100)

For Dig-dUTP: Cy3-anti-Dioixigenin (1:100)

For FITC: anti-FITC-FITC conjugated (1:50-1:100)

A PAP pen was used to isolate the region on the slide exposed to the probe. Next, 100 µl of the secondary detection system was mounted onto this region and left in an. Incubator for 60 min at 37°C. The slides were then washed in 4xSSC (0.1% (v/v) Triton) 3 times for 5 min. DAPI with a concentration of 0.2µg/ml (1mg/ml stock -> 5ug/ml second stock -> 0.2ug/ml

working solution) was applied to the section for 10 min. The slides were washed in 2xSSC for 5 min at RT. A mounting medium without DAPI was applied and sealed with a 0.17mm cover slip. Results were checked using a microscope.

2.3.5. 3D FISH

In a 1.5-ml tube, all the labeled DNA probes that were previously prepared for the hybridization were mixed together along with unlabeled competitor DNA, e.g., Cot-1 DNA with 5-, 10-, or 50-fold the concentration of probe DNA.

To the probe DNA mixture 100% of ice cold EtOH (2.5× volumes) was added and kept for at least 30 min at −80°C. Then the tube was spun down at 15,000×g for 20 min. The supernatant discarded and the pellet air dried at RT. Afterwards, the pellet was resuspended in 50% (v/v) formamide/2× SSC/10% (w/v) dextran sulphate as follows. First, the pellet was dissolved in the appropriate amount (15µl) of 100% formamide and incubated at 37°C for 30min (vortexing every 10min). Second, an equal volume (15µl) of 4× SSC/20% (w/v) dextran sulphate was added to the resuspended pellet. Finally, the contents of the tube were briefly mixed and incubate at 37°C for 10 min. The hybridization probe was then stored at −20°C or used immediately.

The slides were removed from the -80°C and left to thaw and dry for 30 min at RT. The fallowing optional step was performed to increase probe/antibody penetration in very dense tissues, permeabilize in 1×

PBS/0.5% (v/v) Triton X-100 at RT for 20 min. Slides were placed in a microwave safe Coupling jar, which was filled with 10 mM sodium citrate buffer (1L = 2.94g sodium citrate dissolved in distilled water, pH 6). The tissue was left to rehydrate in this solution for 10 min at RT.

DNA unmasking was carried out by heating the Coupling jar container in a microwave oven until first signs of boiling appeared, the microwave was then switched off and the jar was left for 2 min at RT to cool. The jar was then heated again until first signs of boiling and left to cool down for 2 min at RT. This process was repeated 7 times. Next, the slides were transferred to 2× SSC. Next, the slides were equilibrated in 50% (v/v) formamide/2× SSC solution for at least 4 at 4°C (or stored up to 2–4 months at 4°C).

The probe was mounted under small glass chambers specifically designed for DNA hybridization on relatively thick tissue sections (see **Fig. 2.1** for details). First, slides were taken out of the 50% formamide/2× SSC solution, excess liquid around section removed using soft paper. Next, the section was covered with the glass chamber and the chamber filled with the probe. Rubber cement was used to seal the chamber and left to dry at RT.

The slide was prehybridized with the mounted probe at 37°C overnight to allow infiltration of the section with the probe. The next day the slide was incubated on a hot block at 80 °C for 5 min to enable simultaneous denaturation of cellular DNA and probe. Hybridization was carried out by incubating slides at 37°C in humid dark chambers (e.g, metal boxes floating in a water bath) for 2–3 days. Next, post-hybridization washings were carried after the rubber cement along with the glass chamber were carefully

peeled off the slide. The slide was then transferred slides to 2× SSC and washed 3 times for 10 min at 37°C. Final high stringency wash was carried out in 0.1× SSC at 60°C for 10 min.

The detection of hybrizised regions of DNA was carried out by carrying out additional immunostaining for the labelled DNA. First blocking solution consisting of 4% (w/v) BSA and 4xSSC was applied onto the section for 15 min. Next, antibodies tagged with fluorescent fluorophores were diluted in 4% (w/v) BSA and 4xSSC as follows: for Bio-dUTP Streptavidin-Cy5 (1:100); for Dig-dUTP Cy3-anti-Dioixigenin (1:100); for FITC anti-FITC-FITC conjugated (1:50-1:100)

The antibody solution was then applied onto the slide and left in an incubator at 37°C for 60min. The slide was then washed in 4xSSC (0.1% (v/v) Triton) 3 times for 5 min. DAPI with a concentration of 0.2µg/ml was applied to the section for 10 min. The slides were washed in 2xSSC for 5 min at RT. A mounting medium without DAPI was applied and sealed with a 0.17mm cover slip. Results were checked using a microscope.

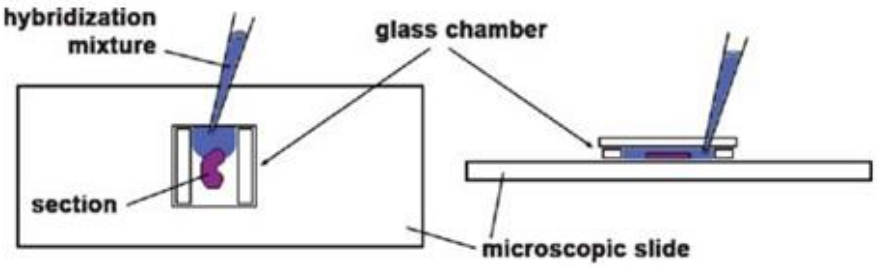

Figure 2.1. Schematic representation of a glass chamber used for hybridization. The glass chamber was prepared by cutting strips of glass from a coverslip using a diamond cutter and glueing them parallel on two borders of an intact coverslip using a nail polish. The DNA probe was mounted by capillary action once the glass chamber was correctly placed over the tissue. (Figure modified from Cremer et al., 2008)

2.3.6. 3D Image generation using confocal microscopy

3D images of the tissue processed for FISH were generated using Confocal Laser Scanning Microscope (ZEISS, 2013). This microscope has a pinhole which prevents out of focus light coming from the tissue sample from reaching the detector. This drastically improves the contrast and enables to scan layer by layer through the tissue sample. These layers are stacked generating a Z-axis in addition to the X-axis and Y-axis. The information booklet from ZEISS provides more information (ZEISS, 2013).

2.3.7. Mass Image Refining and Analysis

To obtain useful information from the 3D FISH images a number of steps were performed. First, it was important to identify the XYZ-axis coordinates of all the BAC signals present in the nucleus. This required refining the images to decrease background signals and identify the specific signals in the image. These images were then analysed. For this, the centre of each specific signal within the 3D space was identified and represented as an XYZ coordinate. Due to the fact that up to four different lasers were used in generating one 3D image chromatic aberration was introduced. Therefore, the amount of aberration was determined by using fluorescent beads.

Image Refining

Refining of 3D images was performed through the use of a java based programme called ImageJ (v1.47), which was specifically designed for working with images (Abramoff et al., 2004) and has been used for image

analysis for over 25 years. By adjusting brightness and contrast as well using a range of build in filters, if required, it was possible to improve the specific signal quality. One of such filters was Gaussian Blur 3D, which uses a normal distribution curve to blur and thereby produce a more uniform distribution of the signal.

To calculate the distance between the detected signals within a nucleus a Pythagoras' theorem was used (Equation 2.1).

Equation 2.1. Pythagoras' equation to determine distance between two points

$$d^2 = (X1-X2)^2+(Y1-Y2)^2+(Z1-Z2)^2$$

$$d = \sqrt{d^2}$$

Even though the distances themselves could provide some useful information as they are in metric units, they by themselves are not complex. This is because nuclei have different volumes between themselves in one tissue type and even more so between different cell types. Therefore the distances were normalised to take this into account. Normalisation was carried out to the mean nuclear radius. In this case all the nuclei for which data was collected previously were further analysed to determine their average radius. This was achieved by randomly selecting at least 200 points throughout the whole nucleus and recording their XYZ coordinates. After calculatin a mean value for X, Y and Z from the 300 random points a hypothetical coordinate for the centre of the nucleus was obtained. Then distances between the 300 random points and the hypothetical centre were

measured using Equation 2.1. The mean value of the 300 calculated distances represents the mean nuclear radius, which was used for normalization of the distances between BACs or chromosomal territories (Equation 2.2).

Equation 2.2. Normalised distance/% of mean nuclear radius

Normalised distance = distance/(mean nuclear radisu)×100

After normalising the distances further analysis was carried out using R/RStudio to determine any statistical significance between different tissue samples. Statistical analysis was performed by identifying if data was normally distributed and accordingly Student t-test or Wilcoxon signed-rank test was used if data was parametric or non-parametric, respectively.

Additional analysis was performed on observational data. For this Pearson's Chi Squared test was used.

2.4. Laser Capture Microdissection and Microarray analysis

The quick frozen samples of the skin of *KrtCre-14ER/Ctcf fl/fl* mice skin and control samples were cut using a cryostat as described above (Sharov et al., 2006). Skin sections of 10µm thickness were collected onto membrane slides (MMI, part-Nr: 50103) and stored in RNase free environment at -80ºC overnight. These were subsequently stained according to the protocol supplied with the H&E RNase free kit (MMI, Product Nr: 70302) and epidermis was isolated into 0.5ml collection tube using Nikon T2000 laser capture microscope. Laser capture was performed for one hour to minimize RNA degradation and immediately 100µm of BL (lysis buffer) and TG (1-Thioglycerol) from ReliaPrep RNA Cell Miniprep System Kit (Promega, Z6010) was added to the 0.5ml tube and RNA isolation was carried out accordingly to the supplied protocol and stored at -80ºC. The RNA then underwent two rounds of amplification using Arcturus® RiboAmp® HS PLUS RNA Amplification Kit. Mouse reference RNA (Agilent Technologies, 750600) was also amplified and used as universal control during microarray analysis. All RNA samples were sent to Mogene Co. (USA), the company performed all the microarray analysis based on Mouse SurePrint G3 GE 60K whole genome microarray (manufactured by Agilent Technologies) as described previously (Fessing et al., 2011; Mardaryev et al., 2014; Sharov et al., 2006).

3. RESULTS

3.1. Optimization of Fluorescent In Situ Hybridization for Three Dimensional Imaging

3.1.1. DNA Probe labeling

Nick Translation (NT) was a technique used to generate labeled DNA probes, which were subsequently used during In Situ Hybridization as described in Chapter 2. During NT reaction, DNase I was used to digest large DNA fragments, the size of which were checked using 1% (w/v) agarose gel (**Fig. 3.1**). In fact, a perfect NT should yield a smear of DNA fragments ranging from ~300–1,000bp. Therefore, if further digestion was necessary (e.g. BAC RP24-68P2 in **Fig. 3.1**) another 1 µL of diluted DNase I was added for 5–10 min at 20°C and the resulting DNA fragment size was checked again on an agarose gel (**Fig. 3.1**). Once optimal NT products were obtained the probe was generated as described in previous chapter.

3.1.2. Utilization of computation tools for automation of 3D FISH analysis

To automate the detection of all the signals within the nuclei of the 3D images an imageJ plugin, Object Counter 3D, was used to facilitate this process. Object Counter 3D measured the pixel density of the signals in the image stack, locate the geometric centre of the signal and produce a file with a list of XYZ values (**Fig. 3.2**). Also, each coordinate was tagged with a unique ID number, which was also plotted next to the signal on the image. This enabled visual identification of the signals of interest and the retrieval of their XYZ values (**Fig. 3.2**) using programming language R. (Bolte and Cordelieres, 2006).

3.1.3. Compensating for chromatic shift aberration during 3D FISH Analysis.

All the ID numbers present next to specific signals within the nuclei of interest were recorded and their XYZ coordinates retrieved using a script written in R/RStudio. The XYZ values were then adjusted for the chromatic shift. This process was accomplished by scanning 0.5 µm fluorescent beads. The LSM microscope had four lasers and four filters and therefore could excite and detect 4 channels with the light wavelength of 360 (excitation)/460nm (emission) (DAPI), 495/520nm (FITC), 550/570nm (Cy3) and 650/670nm (Cy5). The fluorescent beads were able to emit light at all of the excitation wavelength and enable the observation of the shift of each channel (**Fig. 3.3**). The mean chromatic shift in the X,Y and Z direction for each channel in relation to the reference channel, which was selected to be DAPI (channel 1), was determined from approximately 20 beads. The X,Y and Z values of the BAC signals determined previously were adjusted using these mean values. Chromatic shift was measured on a regular basis especially after any calibrations or servicing were carried out on the microscope.

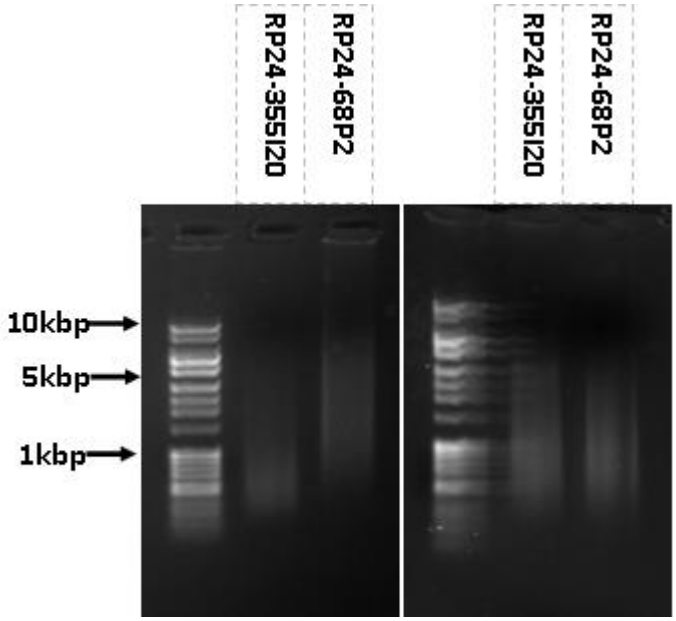

Figure 3.1. Example of the labelled BAC probes after Nick Translation.

The BAC called RP24-68P2 was digested further to produce DNA fragments of the desired length as shown in the right image.

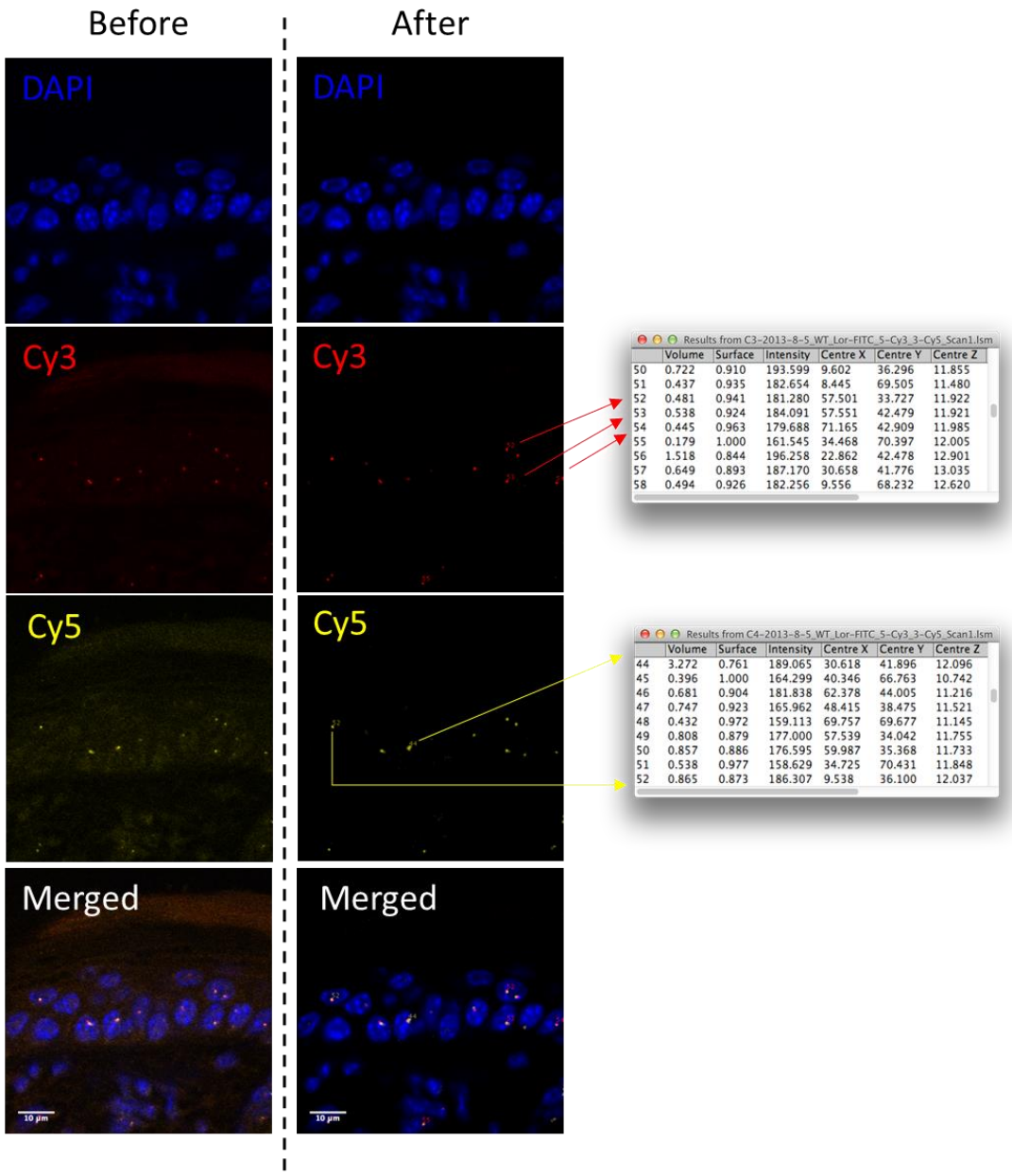

Figure 3.2. The process of refining 3D FISH images and obtaining signal coordinates for labelled BACs using ImageJ. Before and after images are shown after refining them and obtaining coordinates of each signal using Object Counter 3D plugin. The plugin also generates a separate file with the coordinates of all the signals for each fluorescent channel file tagged by a number that is also plotted on an image.

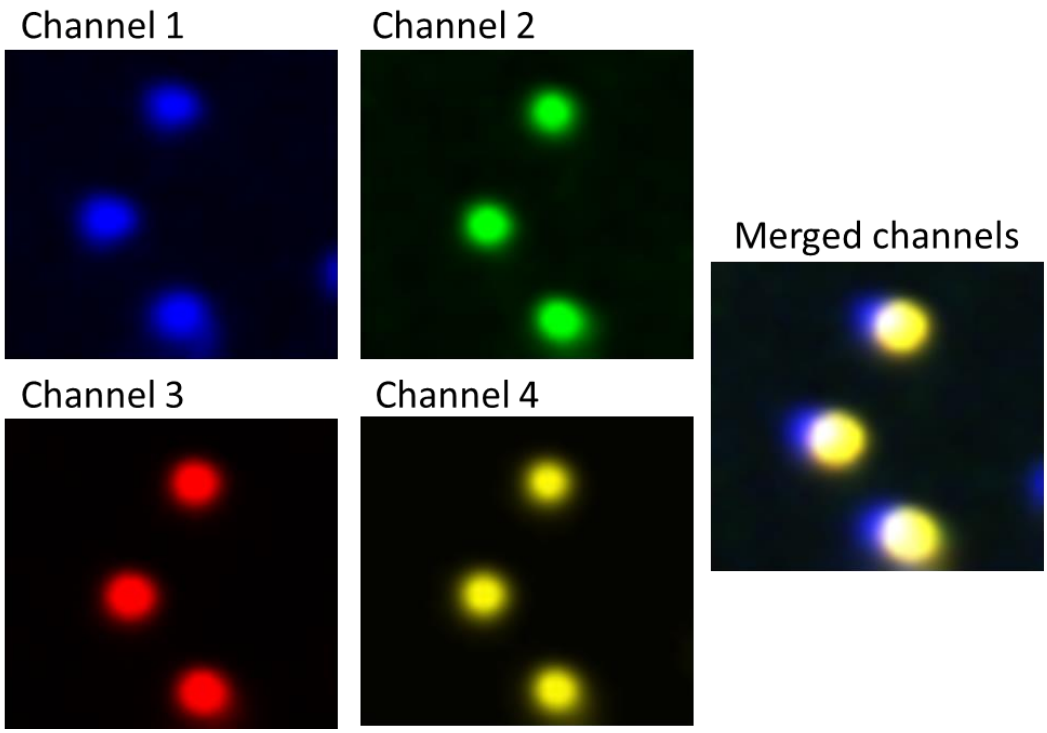

Figure 3.3. Representation of chromatic shift obtained by LSM using 0.5 µm fluorescent beads. The merged image of four different channels shows that they do not completely overlap with each other.

3.2. Analysis of higher order chromatin organisation in the epidermis of genetically engineered mice with ablation of the Keratin type 2 locus

During development, the genome of multi-potent stem cells becomes reorganized in 3D nuclear space to establish a proper spatio-temporal regulation of transcription underlying execution of lineage-specific gene expression programs (Bickmore and van Steensel, 2013; Dekker et al., 2013; Schoenfelder et al., 2010a; Wei et al., 2013). However, mechanisms coordinating transcription in lineage-specific gene loci located on different chromosomes during cell differentiation are poorly understood. Differentiation of the epidermis is accompanied by tightly-balanced expression of the keratinocyte-specific genes that are clustered in the mammalian genome into several loci including the Keratin type I (KtyI) and type II (KtyII) gene loci located on mouse chromosomes 11 and 15, respectively, as well as the Epidermal Differentiation Complex (EDC) locus located on mouse chromosome 3 (Blanpain and Fuchs, 2009; Koster and Roop, 2007; Watt and Huck, 2013). Chromosomal conformation capture techniques, such as 3C, 4C and 5C, have shown that genes tend to form inter- and intra-chromosomal interactomes required for establishment of lineage-specific gene expression programs (Schoenfelder et al., 2010b).

Data obtained from Prof. Thomas Magin's laboratory (University of Leipzig, Germany) revealed that genetically engineered mice with ablation of Keratin type II locus from chromosomes 15 display severe epidermal

barrier defects (Kumar et al., 2015). Epidermis of KtytII-/- showed a compact alterations in expression of 37 genes in the EDC locus and apparent absence of filaggrin and locricrin-positive keratohyalin granules, compared to controls (Kumar et al., 2015). Global gene expression analysis of back skin RNA from KtyII-/- and control littermates at E18.5 showed that of the 61 genes located on the EDC (de Guzman Strong et al., 2010), 15 encoding structural CE components, among them *loricrin*, *filaggrin 2*, *hornerin* (*Hrnr*) and late *cornified envelope group 1* (*Lce1*) genes, were strongly downregulated in KtyII-/- mouse skin. However, 22 genes including small proline-rich genes (*Sprrs*), *S100A8* and *late cornified envelope group 3* (*Lce3*) genes, connected to oxidative stress, barrier defects and hyperproliferative skin conditions, were upregulated upon Keratin type II locus ablation (Kumar et al., 2015).

To better understand the topological relationships between the EDC and Keratin type II loci in the nucleus, the 3D-FISH analyses of the nuclear positioning of these loci was performed in epidermal keratinocytes of WT mice and genetically engineered mice with ablation of KtyII locus obtained from Magin's lab, as well as in thymocytes (selected as the control), in which gene expression in both loci is markedly decreased compared to keratinocytes. Because nuclear morphology in the epidermal keratinocytes is markedly changed during cell transition from the basal to granular layer (Gdula et al., 2013), only nuclei of non-proliferating basal epidermal keratinocytes containing diploid number of genomic loci were selected for 3D-FISH analyses.

3.2.1. 3D FISH analysis of keratinocyte-specific gene loci in epidermal keratinocytes of wild-type mice and thymocytes

For 3D-FISH analyses, distinct DNA probes were generated from BAC clones covering the entire EDC or KtyII loci, as well as the genes that constitute as components of these loci (*Lor* and *Krt5*, respectively), or located in the immediate vicinity to either 3'- or 5'- ends of the KtyII locus (*Ankrd33, Eif4b*) (Table 2.3). In addition, positioning of the EDC and KtyII loci was assessed relative to the corresponding chromosome territories 3 and 15, as described previously (Fessing et al., 2011; Mardaryev et al., 2014).

The analysis of the 3D FISH data determined that the chromosomal region containing *Loricrin* gene is found closer to the keratin type 2 locus in epidermal keratinocytes than in thymocytes. This conclusion is based on the shorter distances observed between *Loricrin* and Keratin Type 2 locus in epidermal keratinocytes than in thymocytes (**Fig. 3.4.a**). Further statistical analysis determined that a statistically significant difference was present within the actual distances (**Fig. 3.4.b**). As the size of the nuclei varies within a specific tissue and between different cell types, as measured with mean nuclear radius (**Fig. 3.4.c**), the distances were normalised to the mean nuclear radius. The normalised distances were also significant (**Fig. 3.4.d**).

The position of chromosomes themselves in different tissue types might be different thereby contributing to the previous results. In both cell types, chromosome 3 was always located more peripherally in the nucleus compared to the chromosome 15, which was located more centrally. Both

chromosomal territories (3 and 15) showed quite close localization in keratinocytes and thymocytes, and the distances between the centres of chromosomal territories 3 and 15 were analysed (**Fig. 3.5.a**). It was determined that the mean distance between centres of the Ch3 and Ch15 was shorter in thymocytes (**Fig. 3.5.c**) after normalization of the raw data (**Fig. 3.5.b**). Therefore, chromosomal location was eliminated as a factor to explain the longer distances observed between *Lor* and Keratin Type II locus in thymocytes.

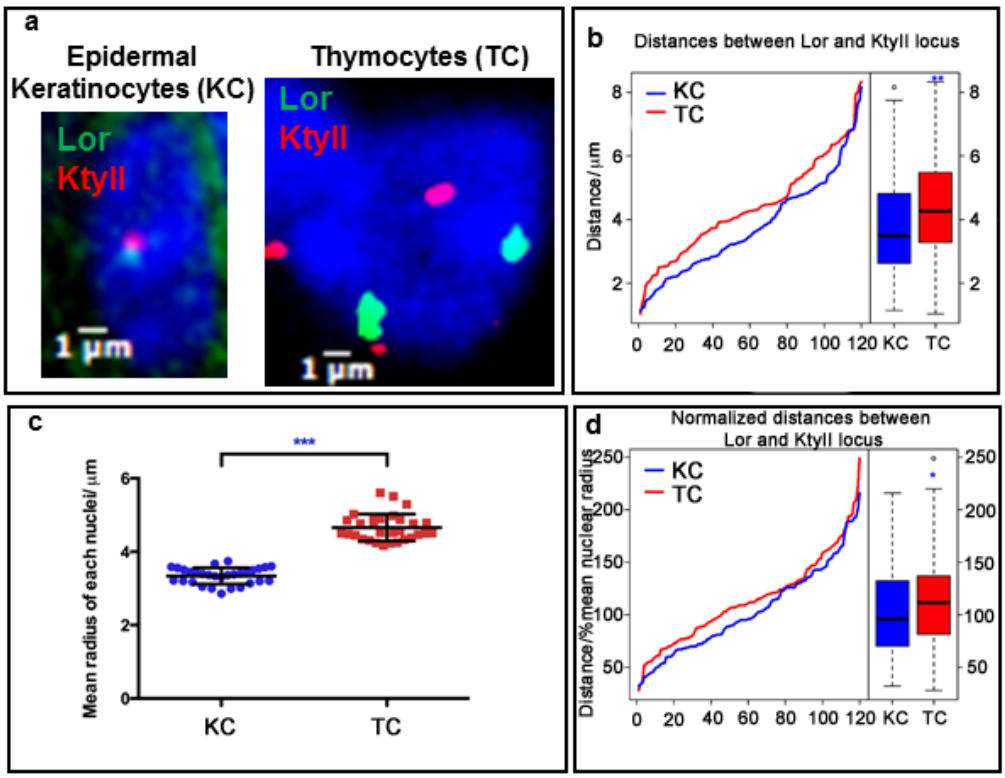

Figure 3.4. *Lor* shows closer positioning to the Kty2 locus in epidermal keratinocytes (KC) compared to thymocytes (TC). (**a**) Multicolour 3D FISH with BACs depicting *Lor* and KtyII locus in epidermal keratinocytes and thymocytes with arrows indicating the location of the detected signals. (**b**) Distribution of distances between *Lor* and KtyII locus in µm (Wilcoxon test, **p<0.01, n=120 from 30 nuclei, box and whisker distribution). (**c**) mean radius of each nucleus from epidermal keratinocytes and thymocytes (t-test, ***p<0.001, n=30 nuclei). (**d**) Distribution of distances normalised to mean nuclear radius between *Lor* and KtyII locus (Wilcoxon test, **p<0.01, n=120 from 30 nuclei, box and whisker distribution).

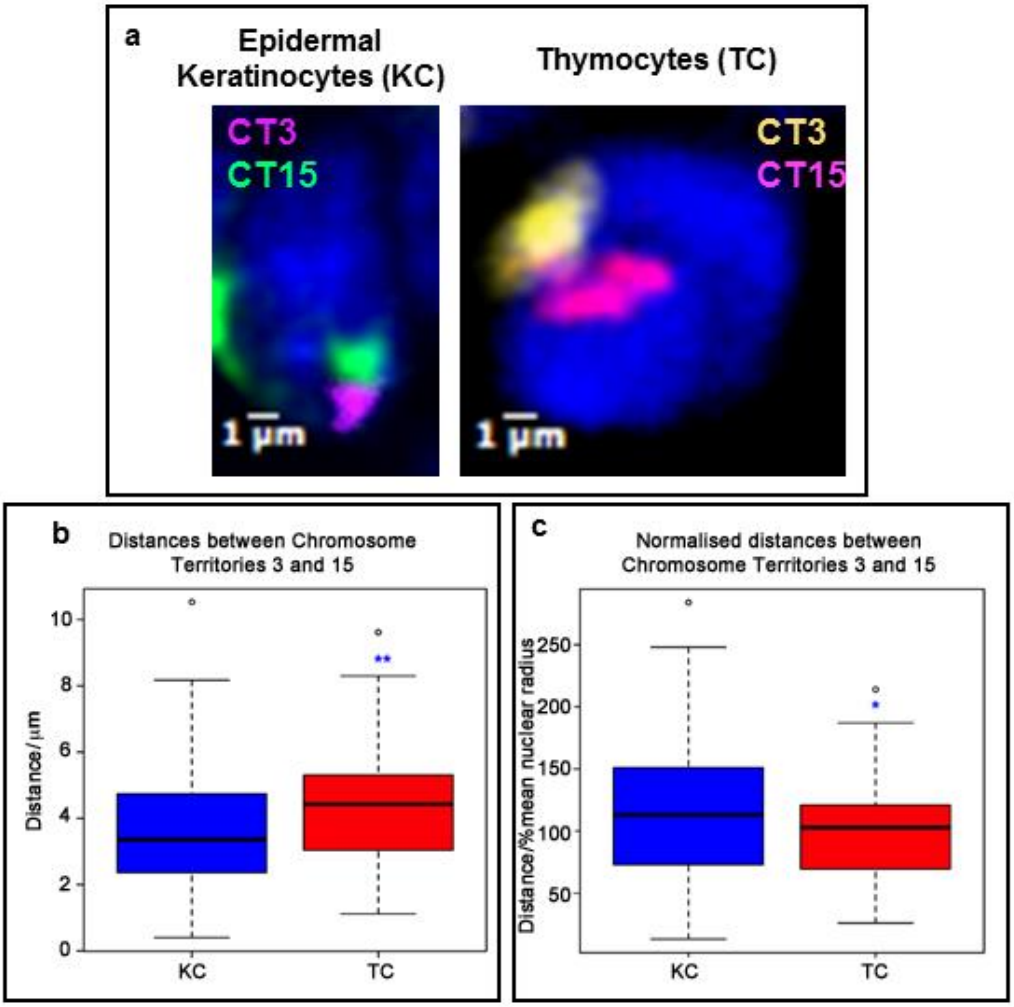

Figure 3.5. Distances between centres of the chromosomal territories 3 and 15 are shorter in thymocytes (TC) compared to epidermal keratinocytes (KC). (**a**) Multicolour 3D FISH with arrows indicating the localisation of chromosomal territories 3 and 15. (**b**) Distribution of distances between Ch3 and Ch15 in µm. Analysis performed on 84 loci obtained from 21 KC nuclei versus 120 loci obtained from TC nuclei (Wilcoxon test, $p<0.01$). (**c**) Distribution of distances normalised to mean nuclear radius between Ch3 and Ch15 (Wilcoxon test, $p<0.05$).

3.2.2. 3D FISH analysis of keratinocyte-specific gene loci in epidermal keratinocytes of wild type mice and keratin type 2 locus knock out mice

Firstly, KtyII ablation in the KtyII knockouts was confirmed by determining if the distances between the 3'- and 5'-flanking regions of the KtyII locus were shorter in KtyII locus KO mice as compared to WT epidermis (**Fig. 3.6.a**). Statistical analysis of the distances between the flanking regions of the KtyII locus after normalising to the mean nuclear radius (**Fig. 3.6.c**) showed significant differences between WT and KtyII locus KO mice (**Fig. 3.6.d**), thus documenting the ablation of the KtyII locus at the 3D nuclear organization levels.

Also, our 3D-FISH analyses revealed that in contrast to basal epidermal keratinocytes of WT mice, a significant repositioning of the Lor gene away from the genes that constitute 3' or 5' ends of the KtyII locus occurred in KtyII locus-deficient mice. The distances between the *Lor* and the KtyII locus flanking regions in epidermal keratinocytes of WT mice were significantly shorter compared to KtyII locus KO mice (**Fig. 3.7.b,c**). The reposition of the *Lor* gene away from the KtyII locus flanking regions was accompanied by significant changes in the positioning of the *Lor* gene relative to the chromosomal territory 3 (from internal to peripheral), suggesting a marked remodeling of the higher-order chromatin structure in the EDC locus upon KtyII locus ablation (**Fig. 3.9**).

However, the distances between centres of chromosomal territories 3 and 15 (**Fig. 3.8**) were unchanged in KtyII locus KO mice versus WT

controls, suggesting that the positioning of the chromosomal territories 3 and 15 was unchanged upon the KtyII locus ablation. Interestingly, epidermal keratinocytes in KtyII locus KO mice showed less frequent associations of the EDC locus and flanking regions of the KtyII locus with SC35-positive nuclear speckles (**Fig. 3.10**). Because nuclear speckles and the associated proteins/RNAs are involved in facilitating the transcription of lineage-specific genes (Spector and Lamond, 2011), relocation of the EDC locus away from the nuclear compartment enriched by nuclear speckles might explain alterations in expression of the EDC genes in KtyII locus KO mice.

Thus, ablation of the KtyII locus result in the remodeling of the higher-order chromatin structure of the EDC locus and its neighboring regions on chromosome 3. Because KtyII locus ablation results in marked changes in the EDC gene expression (Kumar et al., 2015), these data also suggest that KtyII locus might contain specific enhancers for the EDC genes, which might physically interact with the EDC gene promoters and facilitate their expression in epidermal keratinocytes of WT mice.

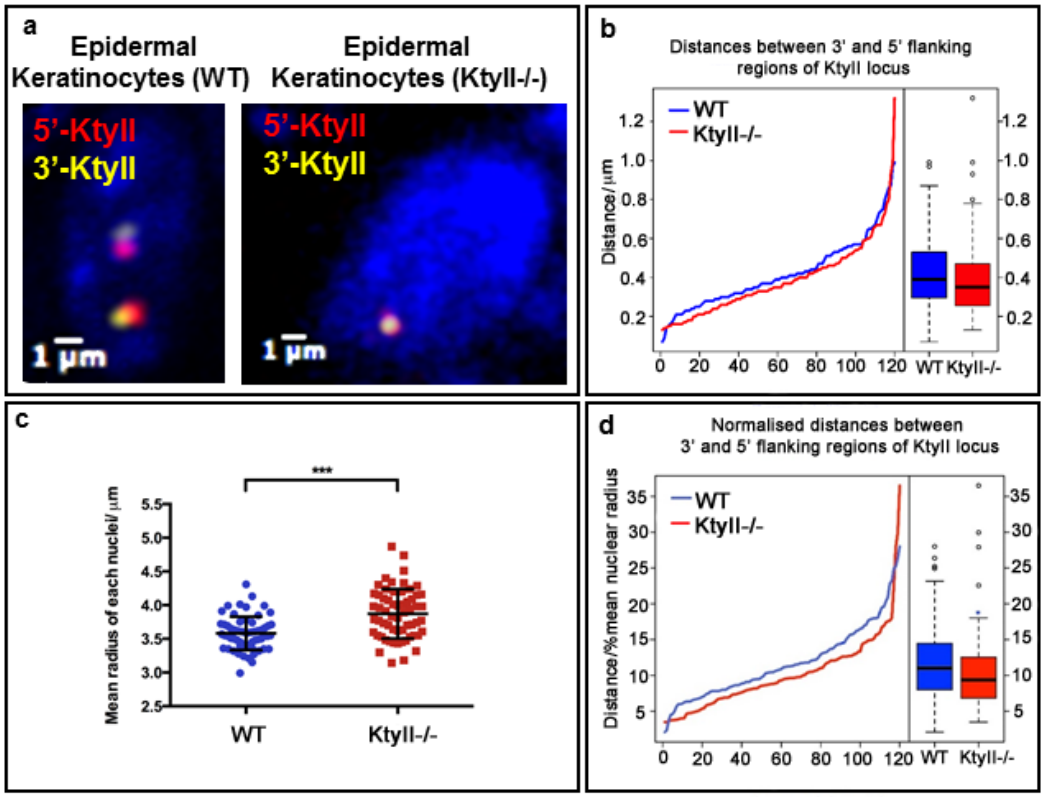

Figure 3.6. Distance between flanking regions of the Keratin Type 2 locus (KtyII) is shorter in epidermal keratinocytes of KtyII locus knock out mice compared to wild-type mice. (**a**) Multicolour 3D FISH with BACs depicting 5' and 3' flanking regions of KtyII locus in wild type and KtyII KO epidermal keratinocytes (P8) and with arrows indicating the location of the detected signals. (**b**) Distribution of distances between 5' and 3' of KtyII locus in µm. (**c**) mean radius of nuclei from Wild Type and KtyII KO epidermal keratinocytes (t-test, ***p<0.001, n=120 from 60 nuclei). d-Distribution of distances normalised to mean nuclear radius between 5' and 3' of KtyII locus (Wilcoxon test, **p<0.01, n=120 from 60 nuclei, box and whisker distribution).

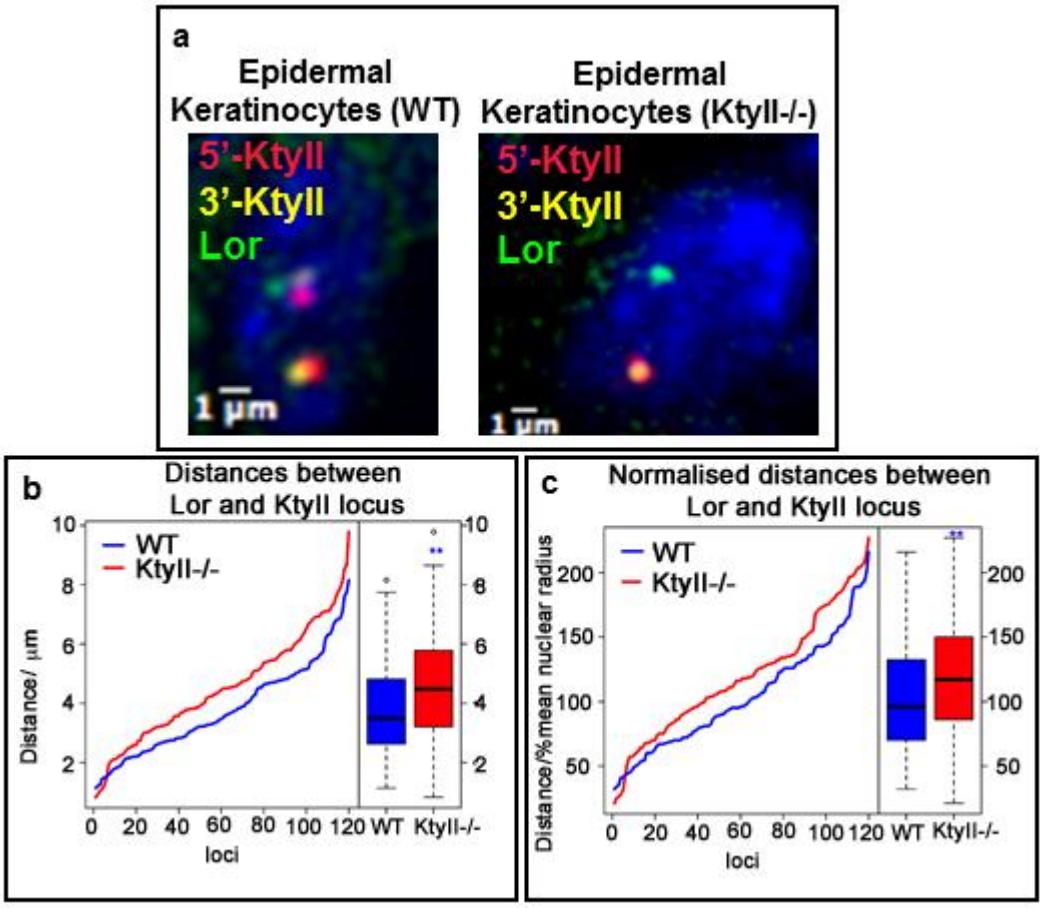

Figure 3.7. *Loricrin* gene is localized in the vicinity of the KtyII locus in keratinocytes, while KtyII locus ablation results in the *Lor* repositioning away from the KtytII locus flanking regions. (**a**) Multicolour 3D FISH with BACs depicting Lor, 5' and 3' flanking regions of KtyII locus in wild type and KtyII KO epidermal keratinocytes with arrows indicating the location of the detected signals. (**b**) Distribution of distances between Rps27 and KtyII locus in µm. (**c**) Distribution of distances normalised to mean nuclear radius between Rps27 and KtyII locus (Wilcoxon test, **p<0.01, 120 loci from 30 nuclei, box and whisker distributions).

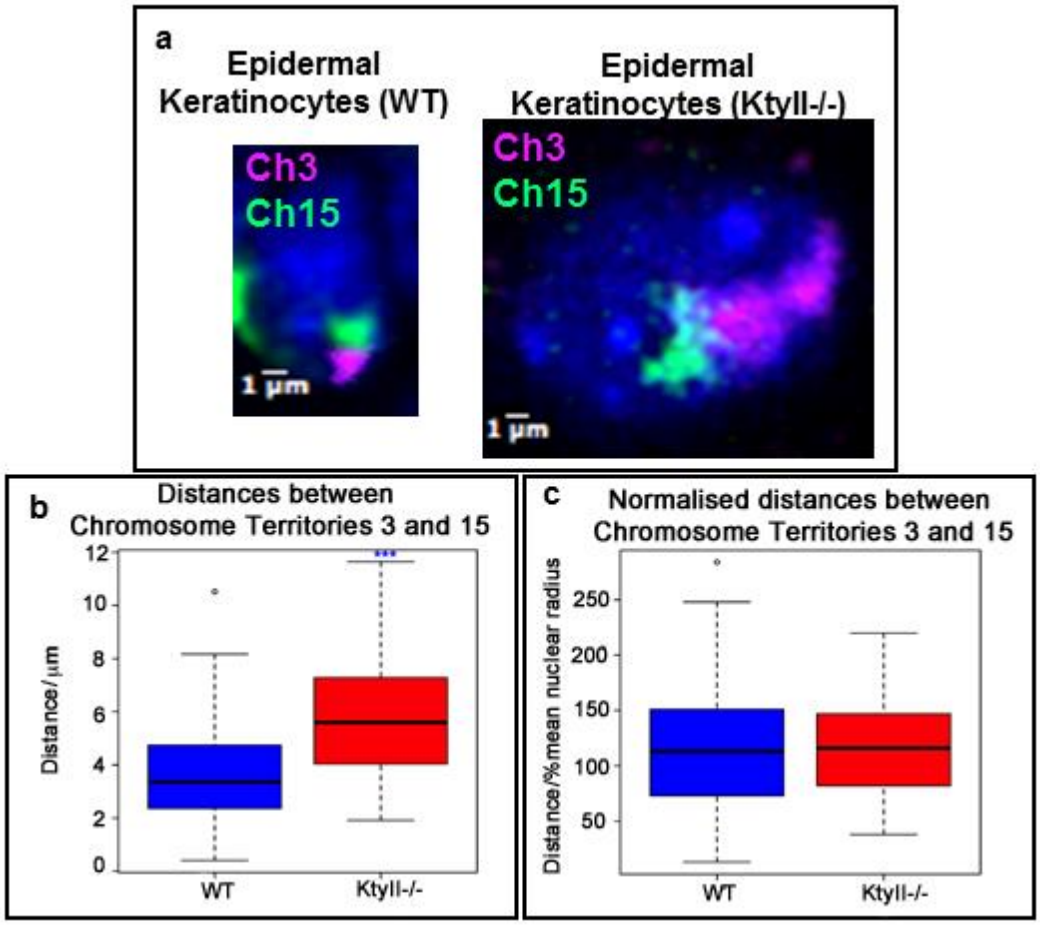

Figure 3.8. Distances between the centres of chromosomal territories 3 and 15 are unchanged in epidermal keratinocytes of WT and KtyII KO mice. (**a**) Multicolour 3D FISH with arrows indicating the localisation of chromosomal territories (CT) 3 (purple) and 15 (green) in epidermal keratinocytes. (**b**) Distribution of the distances between CT3, CT15 in µm. Analysis was performed based on data from 84 loci obtained from 21 WT nuclei and 108 loci obtained from 27 KtyII-/- nuclei, data represented as box and whisker distribution (***p<0.001). (**c**) Normalised to mean nuclear radius distribution of the distances between CT3 and CT15, no significance.

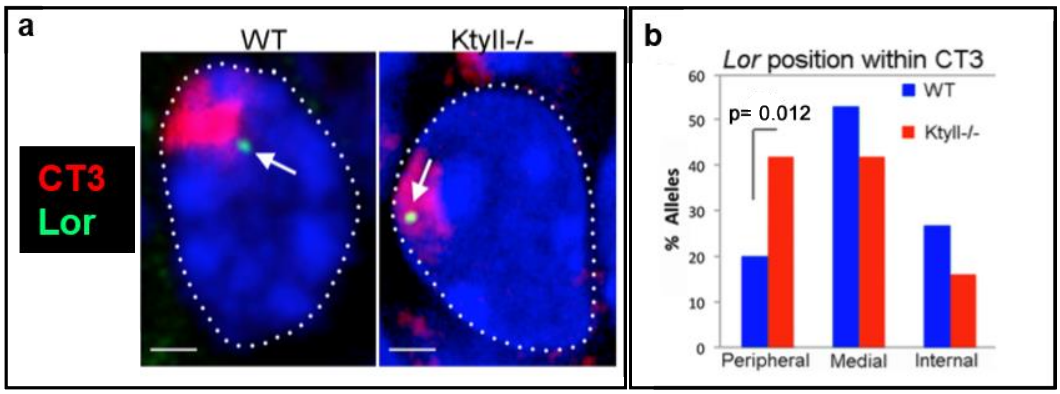

Figure 3.9. *Lor* positions within the Chromosome Territory 3 change from the internal to peripheral in epidermal keratinocytes of KtyII locus knockout mice. (**a**) Multicolour 3D FISH with arrows indicating the localisation of *Lor* (green) within Chromosome Territory 3 (CT3) (red) relative to the nucleus (DAPI), Scale = 2µm. (**b**) Analysis of *Lor* position within CT3, data obtained by analysing 35 nuclei (70 loci) of WT and 35 nuclei (70 loci) of KtyII-/- image stacks, the location of each Lor loci within the CT3 was assigned to Peripheral (P), Median (M) or Internal (I). WT = 14(P), 37(M) and 19(I); KtyII-/- = 30(P), 29(M), 11(I). Analysis was performed using Pearson's Chi-Squared test (p=0.012).

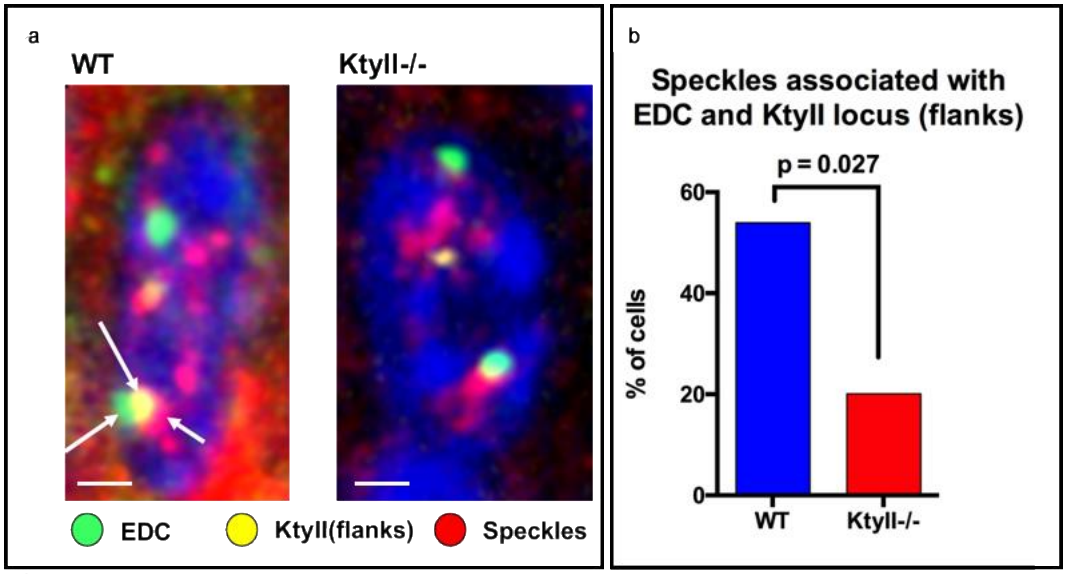

Figure 3.10. Localization of the EDC, Keratin Type 2 locus and SC35+ speckles in the nucleus. (**a**) 3D-FISH for EDC and KtyII locus combined with immunostaining for SC35 (Speckles), **arrows** show co-localization of EDC, KtyII and Speckle. Scale = 2µm. (**b**) Analysis of number of cells showing co-localization of EDC, KtyII genomic loci and speckles, shown as a percentage (WT = 14 out of 26 total nuclei analysed showed co-localization between EDC, KtyII and Speckles; KtyII-/- = 5 out of 25 total nuclei analysed showed co-localization between EDC, KtyII-/-(flanks) and Speckles; Analysis was performed using Pearson's Chi-Squared Test).

3.3. Analysis of Ctcf expression during skin morphogenesis

Ctcf gene is a member of a special class of chromatin architectural proteins important for organizing 3D chromatin structure and enhancer-promoter interactions (Ohlsson et al., 2010). Even though *Ctcf* is one of the best characterized chromatin remodeling genes, its role in the control of skin development has not been previously demonstrated. Immunohistochemistry using anti-Ctcf antibody was carried out on the skin of wild-type mice in order to elucidate the expression of this protein during skin development, postnatal growth and hair follicle cycling (**Fig. 3.11** and **Fig. 3.12**).

3.3.1 Ctcf expression in the skin during embryogenesis

At embryonic day (E14.5), when basal layer and intermediate layer are present in skin epithelium, the Ctcf expression was observed in all nuclei of the epidermal and dermal cells (**Fig. 3.11.a**). By E16.5, when granular layer is established, the levels of Ctcf expression had increased in the epidermis. Furthermore, early hair follicle placodes became positive for Ctcf, which expression was also seen in the mesenchymal cells beneath the epithelial placodes (**Fig. 3.11.b**). At E18.5, when cornified layer is formed, the Ctcf expression was strongest in the basal layers of the epidermis and papillary layer of the dermis (**Fig. 3.11.c**). Furthermore, the hair follicle at later stages of development showed higher levels of Ctcf expression in both epithelium and mesenchyme (e.g. in stage 5 hair follicle shown in **Fig. 3.11.c**).

3.3.2. Ctcf expression in the skin during postnatal development

At day 1.5 after birth (P1.5) Ctcf expression remained strong in the epidermis and the dermis. Levels of Ctcf were strongest in the bulb of developing hair follicles (**Fig. 3.11.d**). Similar pattern of expression was observed at P3.5. Furthermore, strong Ctcf expression was observed in the hair follicle infundibulum, outer root sheath and interfollicular epidermis, while lower levels of Ctcf were visible in the inner root sheath (**Fig. 3.11.e**). At P10.5 and P17.5, the cells of the basal layer remained positive for Ctcf (**Fig. 3.11.f,g**). However, in hair follicles during catagen (**Fig. 3.11.g**) the levels of Ctcf in the shrinking hair bulb and outer root sheath remained high (**Fig. 3.11.g**). At P25.5, when the hair follicles progressed through catagen, telogen and entered new anagen, the Ctcf expression remained strong including the hair follicle epithelium and the derma papilla (**Fig. 3.11.h**).

Figure 3.11. Expression of Ctcf in normal skin during mouse development. Immunihistochemistry performed on mouse skin at different developmental time-points during embryogenesis and after birth. Embryogenesis (E) stages shown are E14.5 (**a**), E16.5 (**b**) and E18.5(**c**). Post-natal developmental stages are P1.5 (**d**), P3.5 (**e**), P10.5 (**f**), P17.5 (**g**) and P25.5 (**h**). Arrows point towards the following structures: IFE – interfollicular epidermis, IRS – inner root sheath, ORS – outer root sheath, Bulb, DP – dermal papilla, Inf - infundibulum. Scale bar = 100μm.

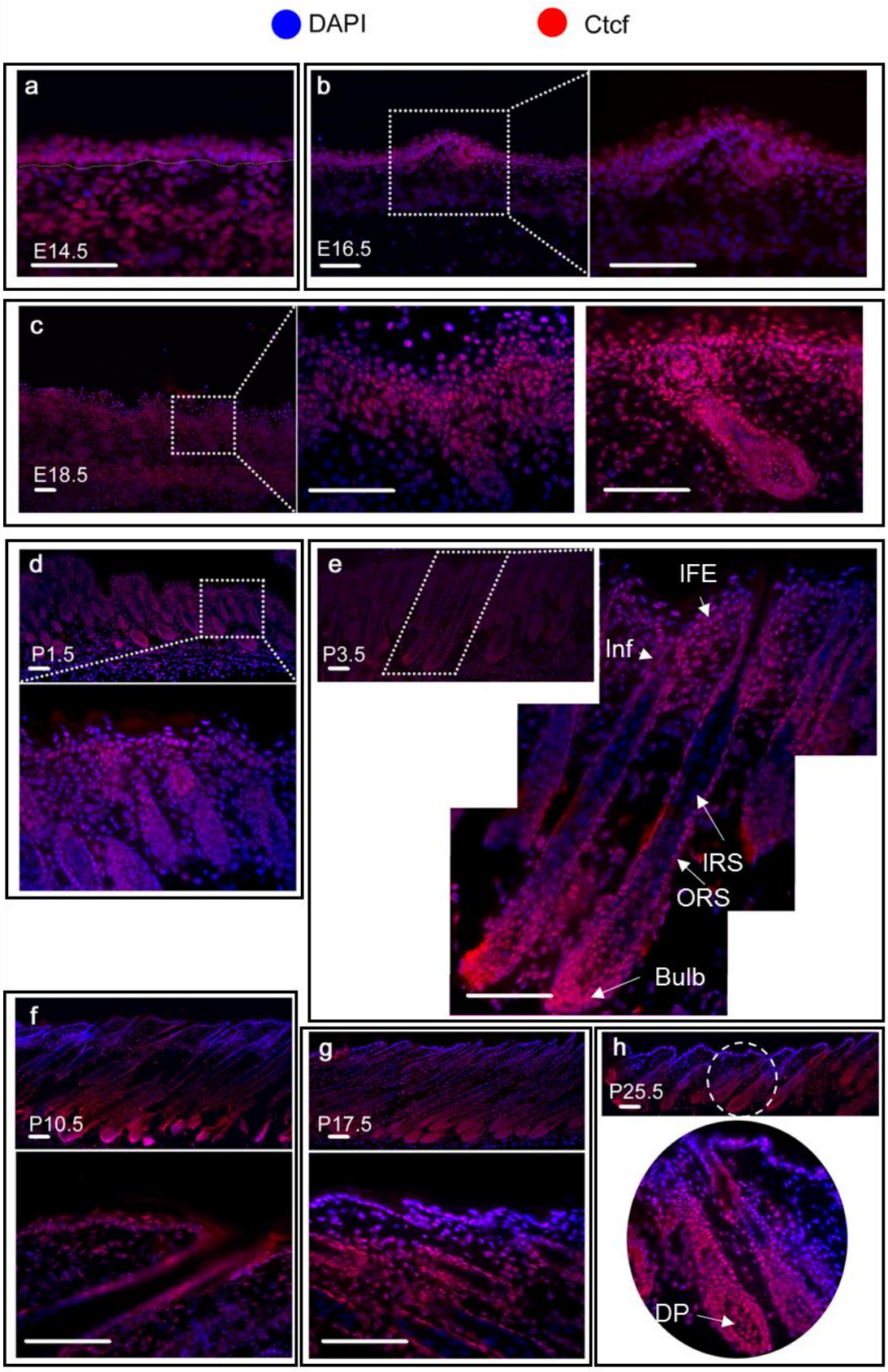

Figure 3.11. For Legend See Facing Page

3.3.3. Ctcf expression in the skin during postnatal hair follicle cycling

To further understand how Ctcf expression levels change during hair follicle cycling, wild-type 8 week-old mice were depilated and skin was harvested at different days after the procedure. Immunohistochemistry for Ctcf expression was performed on these samples. The results showed that Ctcf was present in the cells of the telogen skin of un-depilated mice (**Fig. 3.12.a**). Interestingly, the levels of Ctcf in the anagen I hair follicles of day 3 p.d. (day 3 post depilation) appeared to be higher than in telogen (**Fig. 3.12.b**). At day 5 p.d., when hair follicles are in anagen IV, Ctcf expression was high in the bulb and dermal papilla (**Fig. 3.12.c**). On day 12 p.d., when hair follicles were in late anagen, the Ctcf expression was very strong in the bulb and dermal papilla. During catagen, expression of Ctcf in the outer root sheath remained high. Interestingly, transition from early catagen (day 16 p.d.) to late catagen state (day 19 p.d.) associated with the hair bulb shrinkage was also accompanied with decrease in Ctcf expression (**Fig. 3.12.d,e**). However, the hair follicles at day 21 p.d. (telogen) showed high levels of Ctcf expression.

The epidermis also showed high levels of Ctcf expression during hair follicle cycling. At day 3 p.d., when the epidermis became thicker, the Ctcf expression was seen in both basal and suprabasal keratinocytes (**Fig. 3.12.b**). Levels of Ctcf in the epidermis appeared to be high through anagen and early catagen (**Fig. 3.12.c,d,e,f**). At day 21 p.d., the Ctcf levels in the epidermis appeared to decrease (**Fig. 3.12.g**).

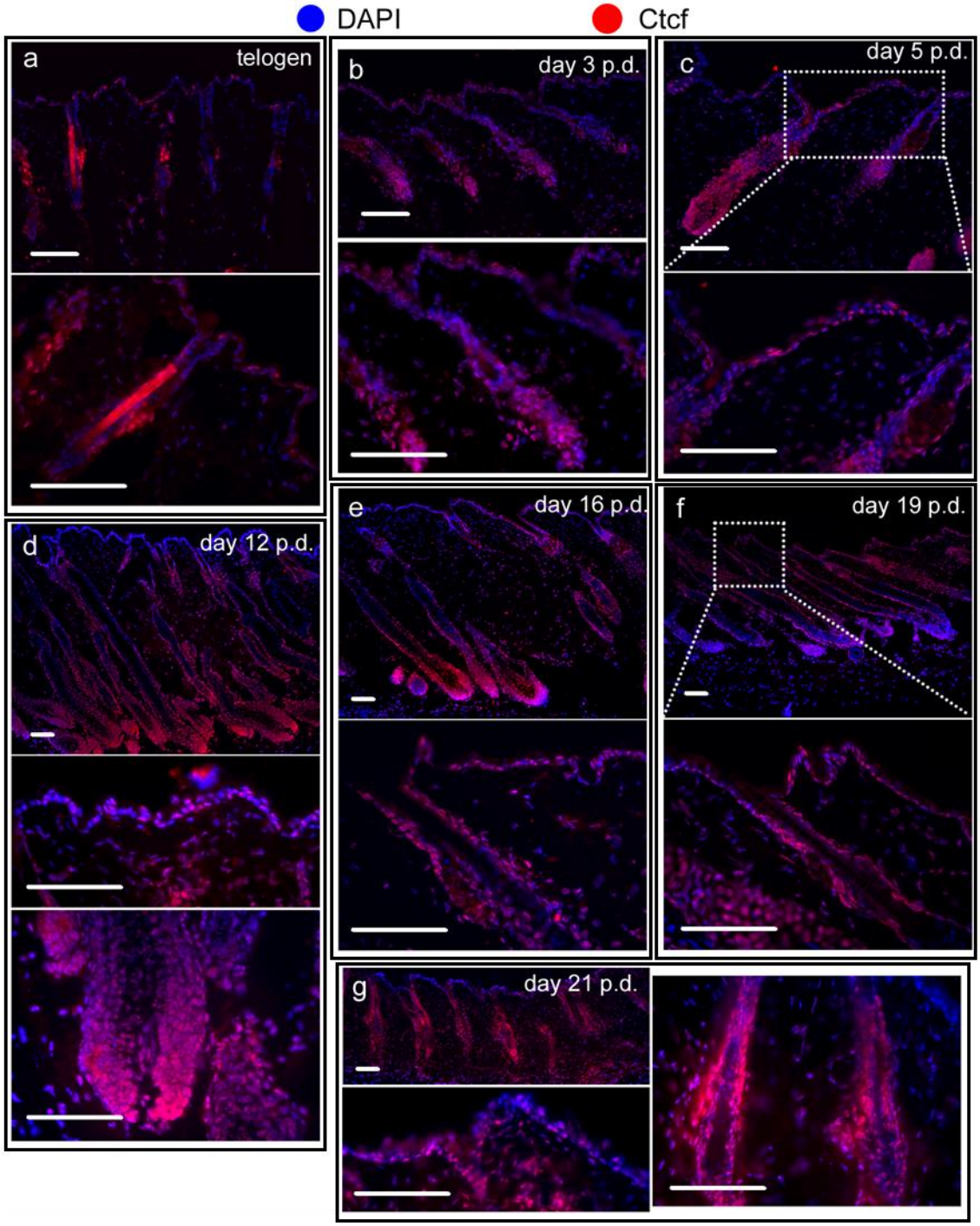

Figure 3.12. Expression of Ctcf in mouse skin during induced hair cycle. Immunohistochemistry for Ctcf was carried out on skin samples harvested from adult mice at different time points after induction of a hair cycle. The time points correspond to the distinct hair cycle stages: Telogen (**a**,**g**), Anagen at days 3 p.d (**b**), 5 p.d. (**c**) and 12 p.d (**d**) and Catagen at days 16 p.d. (**e**) and 19 p.d. (**f**). Scale bar = 100µm.

3.4. Analysis of skin development and keratinocyte differentiation in the epidermis in genetically-engineered mice with Keratin-14 driven *Ctcf* ablation

The functional importance of Ctcf in establishing organ development and cell fate decisions is demonstrated by the fact that *Ctcf*-null mice die early during embryogenesis (Moore et al., 2012). To study the role of *Ctcf* in the control of skin development, a genetically modified mice with a conditional knock out of *Ctcf* only in the skin epithelial cells have been generated. Specifically, previously created *Ctcf* fl/fl mice (described by Heath et al. 2008) were crossed with a mouse strain expressing the tamoxifen-inducible Cre-recombinase under the control of cytokeratin 14 promoter (*Krt14-CreER*), which is specific to the basal layer of the epidermis and the hair follicle outer root sheath (Koster and Roop, 2007). Upon addition of tamoxifen, *Ctcf* is ablated from the genome by the Cre-recombinase in the *Keratin-14* expressing cells.

To study the role of *Ctcf* in the control of skin of development, time-mated *K14-CreER/Ctcf* fl/fl mice were intraperitoneally injected with tamoxifen at E12.5 for three days and embryos were collected at E16.5 and E18.5. Immunohistochemistry using anti-Ctcf antibody showed a downregulation of Ctcf protein in the tamoxifen treated cells, indicating that *Ctcf* gene had been indeed ablated in keratinocytes (**Fig. 3.13.a**). However, Ctcf protein was seen in the skin mesenchymal cells of both *K14-*

CreER/Ctcf fl/fl and WT mice, indicating for the specific *Ctcf* ablation in the basal epidermal cells induced by tamoxifen (**Fig. 3.13.a**).

In skin cryosections stained for alkaline phosphatase at E16.5 (**Fig. 3.13.b**) and E18.5 (**Fig. 3.13.c**), a significant increase in the epidermal thickness was seen upon *Ctcf* ablation compared to WT controls (**Fig. 3.13.d,e**). Furthermore, analysis of hair follicle development in E18.5 embryos showed a significant retardation of their development in *Ctcf*-deficient skin compared to controls (**Fig. 3.13.f**). However, the number of hair follicles was not significantly different (number of hair follicles per mm of epidermal length: Ctcf_KO=10, WT=12, p=0.50).

To determine if the differences in epidermal thickness were due to an increase of proliferation in the *Ctcf*-deficient keratinocytes immunohistochemistry for proliferation marker Ki67 was carried out. Interestingly, *Ctcf*-deficient epidermis showed ectopic presence of Ki67 positive cells in the suprabasal layer of the epidermis, while in WT controls Ki67-positive cells were only seen in the basal epidermal layer (**Fig. 3.14.a**). Also, the number of cells positive for Ki67 in the basal layer was significantly higher in the *Ctcf*-deficient epidermis of both E16.5 and E18.5 skin samples than in the corresponding controls (**Fig. 3.14.b**).

To identify if *Ctcf* ablation had an effect on the keratinocyte differentiation, immunostaining was carried out against key differentiation markers (cytokeratin 14, cytokeratin 10 and Loricrin) on E16.5 embryos. Fluorescent microscopy showed that in addition to basal epidermal layer, cytokeratin 14 expression was ectopically seen in the suprabasal layer of

Ctcf-deficient epidermis (**Fig. 3.15**). Furthermore, Krt10 expression was expanded in the *Ctcf*-deficient epidermis as compared to control (**Fig. 3.15**). Finally, a weaker expression of Loricrin, the marker of terminally differentiating keratinocytes was seen in *Ctcf*-deficient epidermis as compared to controls (**Fig. 3.15**).

Thus, *Ctcf* ablation in the epidermal keratinocytes during skin development results in increased epidermal proliferation and thickness, as well as in alterations of terminal keratinocyte differentiation and retardation of hair follicle development.

Figure 3.13. Development of the epidermis and hair follicles in Ctcf deficient mice. (**a**) Immunohistochemistry against Ctcf in the *Krt14CreER/Ctcf* fl/fl embryos treated with tamoxifen (Ctcf-/-) and DMSO treated control mice, scale bar = 100µm. (**b**) Staining for alkaline phosphatase (AP) in E16.5 DMSO treated (WT) and tamoxifen-treated (Ctcf-/-) embryos, scale bar = 25µm. (**c**) Staining for AP in E18.5 DMSO treated (WT) and tamoxifen-treated (Ctcf-/-) embryos, scale bar = 100µm. (**d**) Mean thickness of dorsal skin was determined from two *Ctcf*-deficient embryos and two WT embryos at E18.5 as follows. For each embryo five images were taken of the different areas of the dorsal skin and thickness randomly measured. These technical replicates were averaged for each animal. The mean was then calculated for two animals per treatment group. Student t-test was used to compare the means. (**e**) Analysis was carried out as described in **d** for E16.5. (**f**) Percentage of the mean number of hair follicles at different stages of development in E18.5. Analysis was performed from two *Ctcf*-deficient embryos and two control embryos. For each embryo five images were taken of the dorsal skin. All hair follicles in the images were counted and each hair follicle was assigned to most appropriate stage of development (1-5). Then, number of hair follicles per stage was determined, converted to percentage, and a mean calculated between two embryos per group. Student t-test was carried out to compare the means of each stage (*$P < 0.05$, ** $P < 0.01$).

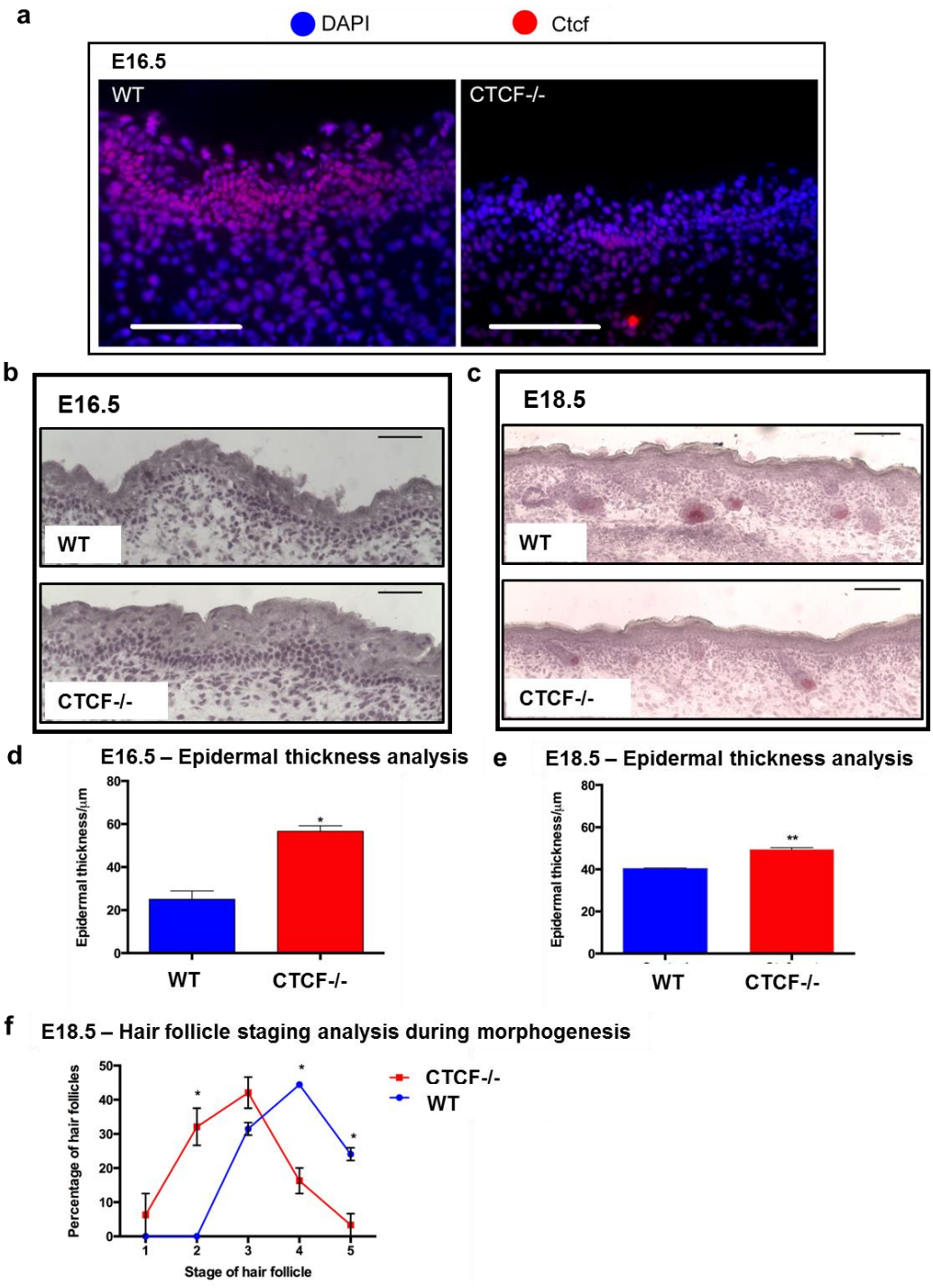

Figure 3.13. For Legend See Facing Page

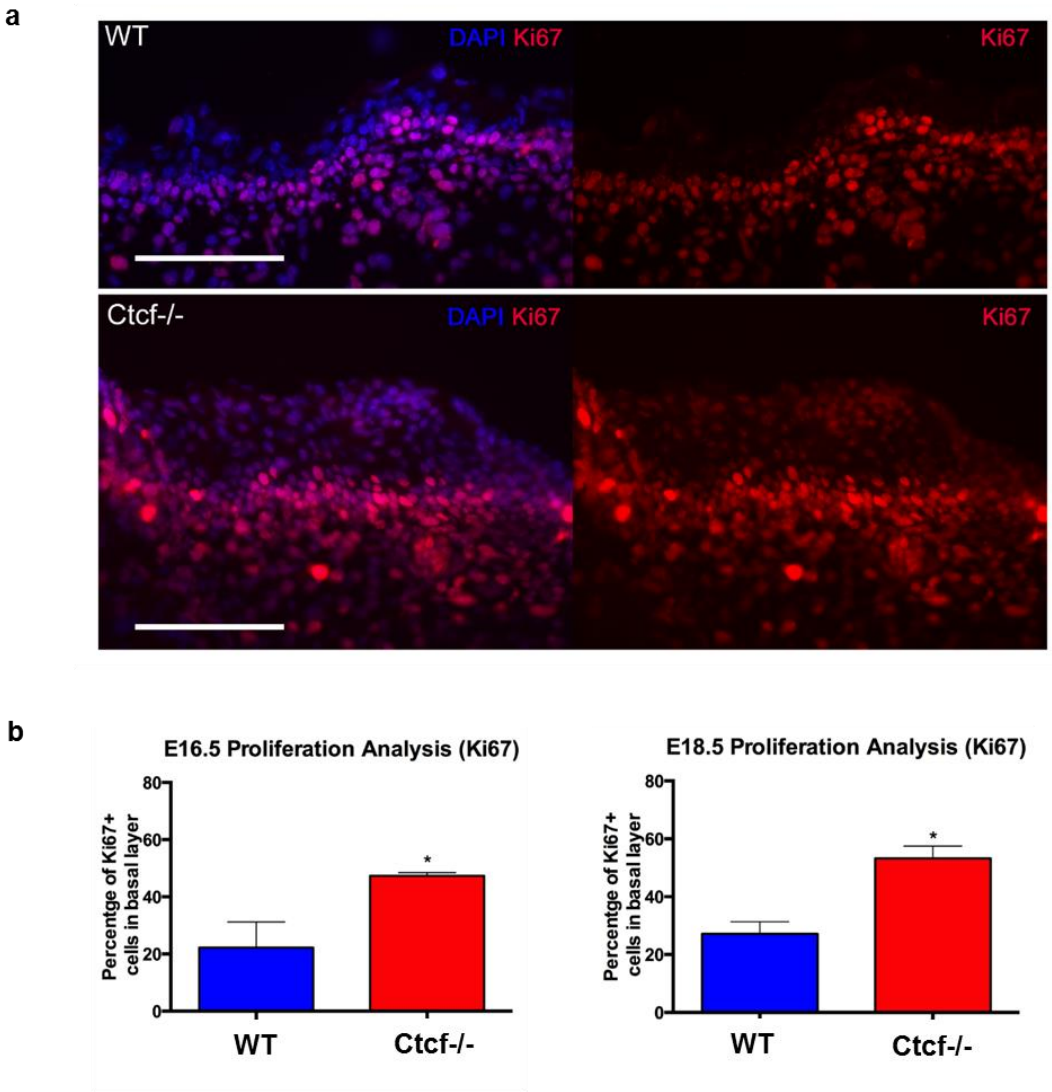

Figure 3.14. Cell proliferation analysis in the epidermis of *Ctcf*-deficient and control mice. (A) Immunostaining for proliferation marker Ki67 in DMSO- (WT) and tamoxifen-treated (Ctcf-/-) E16.5 embryos. (B) Analysis of Ki67-positive cells in basal layer of *Ctcf*-deficient epidermis vs controls based on mean value obtained from two animals (E16.5 and E18.5). Student t-test was used to compare the means * $P < 0.05$.

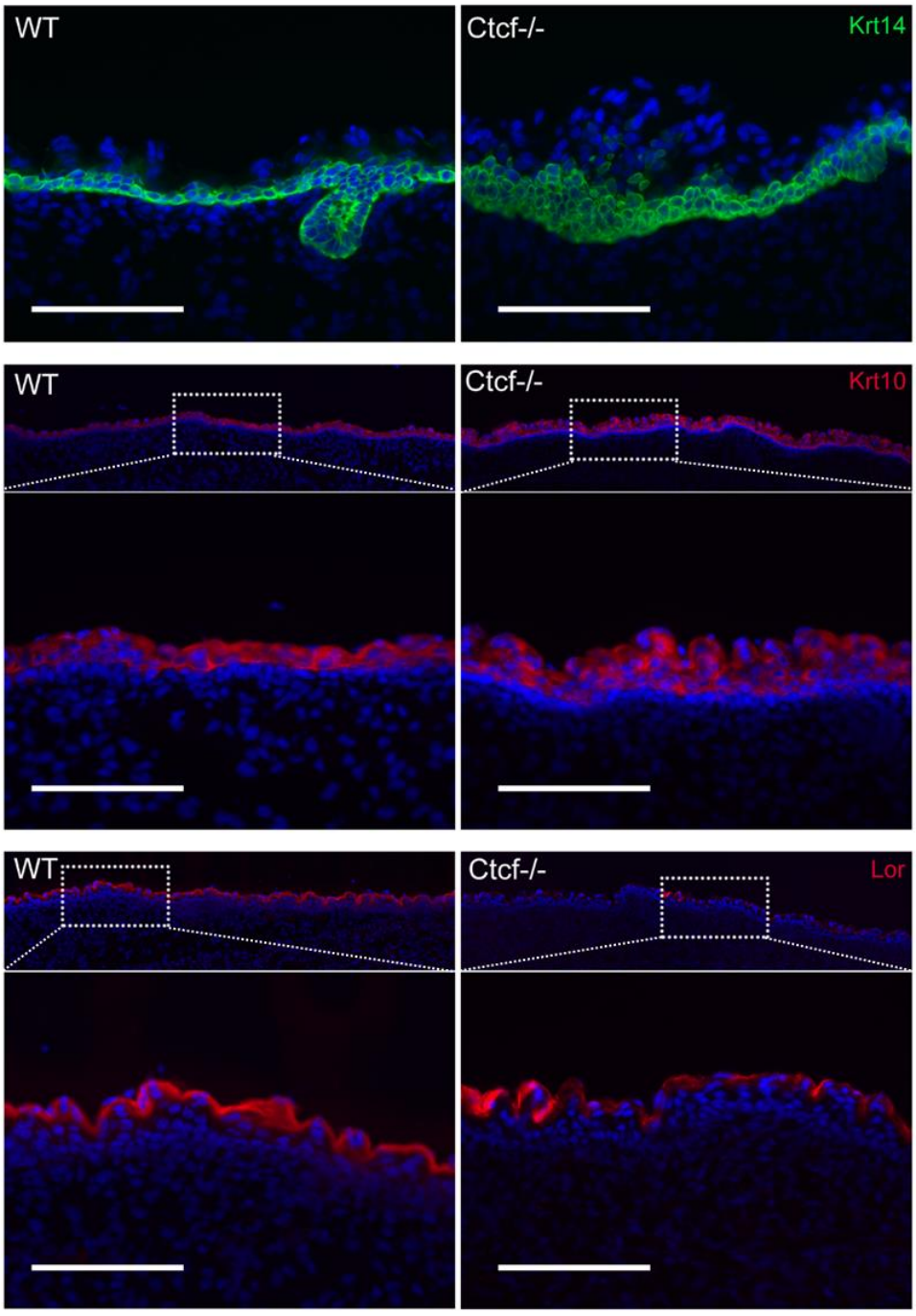

Figure 3.15. Expression of keratinocyte differentiation markers in the epidermis of Ctcf-deficient and control mice. Immunohistochemistry for the markers of keratinocyte differentiation (Krt14, Krt10, Loricrin) in the epidermis of *Krt14CerER/Ctcf* fl/fl and control mice. Expansion of the Krt14 and Krt10 in the epidermis upon *Ctcf* ablation. Scale bar = 100µm.

3.5. Analysis of keratinocyte differentiation in the adult epidermis of genetically engineered mice with ablation of the chromatin architectural protein Ctcf

Because embryonic skin development was altered in *Ctcf* mutant embryos, it was logical to obtain complementary results from postnatal skin. However, we have not been able to obtain any early postnatal skin samples from *Krt14-CreER/Ctcf* fl/fl mice, possibly due to their lethality during the last day of pregnancy or during delivery. To study the role of *Ctcf* in the control of homeostasis in adult skin, 8 week-old *Krt14-CreER/Ctcf* fl/fl mice were injected and topically treated with tamoxifen for three days and their skin was harvested at days 5, 7, 9 and 12 after the start of treatment. Validation of *Ctcf* ablation was carried out by immunostaining for Ctcf and genotyping of mice. The results confirmed that the expression of Ctcf in the epidermis was markedly reduced in the tamoxifen-treated mice (**Fig. 3.16**) and deletion product was seen by PCR (**Fig. 3.16.b**) in the epidermis of treated day 7 skin as compared to control.

3.4.1 Microscopic analyses of the epidermal phenotype in adult Ctcf-deficient mice

The striking increase of epidermal thickness was seen in the skin of *Krt14-CreER/Ctcf* fl/fl mice compared to controls (**Fig. 3.17.a-d**) at days 7, 9 and 12 after tamoxifen treatment (**Fig. 3.17.e**). Surprisingly, the highest increase in the epidermal thickness was seen at day 7 after beginning of the experiment. Furthermore, toluidine blue staining showed increased

penetration of the dye in the *Ctcf*-deficient skin confirming that the epidermal barrier function is compromised in knock-out mice (**Fig. 3.17.f**).

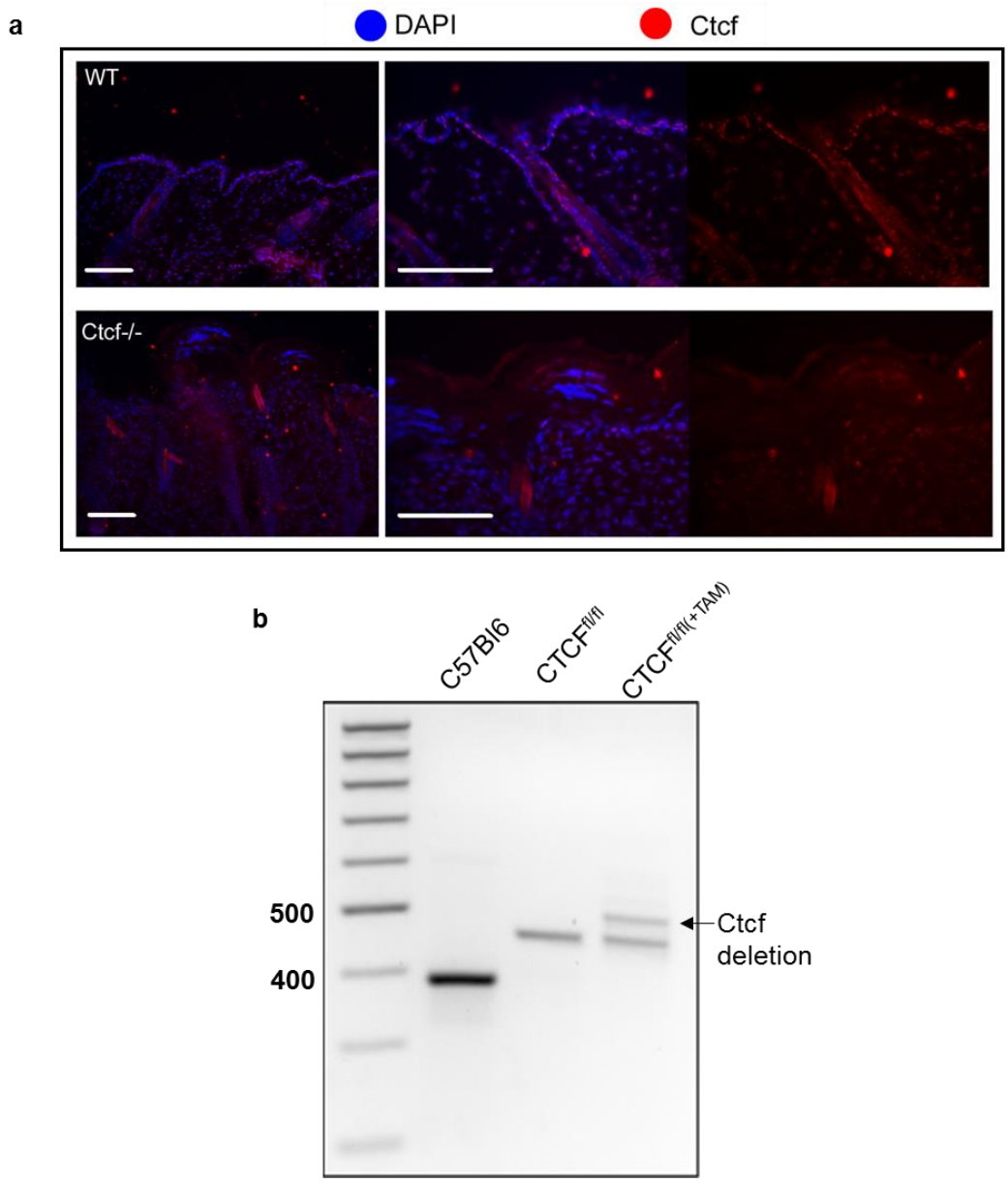

Figure 3.16. Ctcf expression in tamoxifen-treated skin of *Krt14-CreER/Ctcf* fl/fl mice. (**a**) Immunostaining for Ctcf on day 7 after tamoxifen treatment. (**b**) Genotyping for *Ctcf* deletion in tamoxifen-treated and untreated skin. PCR products cluster in the regions 400-500bp. Arrow indicated the deleted *Ctcf* product.

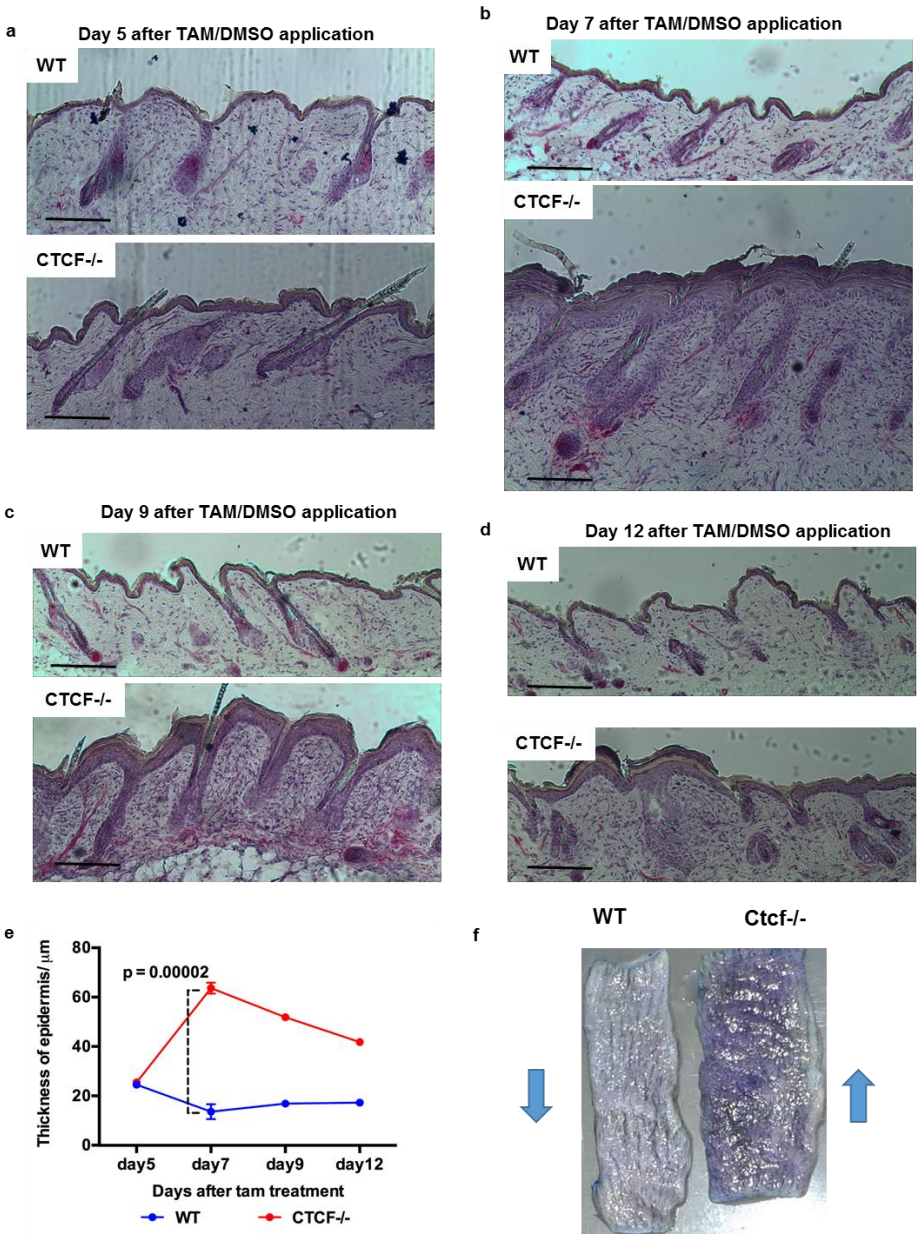

Figure 3.17. Skin phenotype of adult Ctcf-deficient mice. Skin sections at different days after tamoxifen or DMSO treatment were stained for H&AP. (**a**) 5 days after treatment, (**b**) 7 days after treatment, (**c**) 9 days after treatment, (**d**) 12 days after treatment, scale = 100µm. (**e**) Analysis of epidermal thickness of skin samples obtained from *Ctcf*-deficient and control mice at distinct time-points after tamoxifen treatment, day 7 after treatment shows the mean epidermal length from three animals for control and three animals from tamoxifen treatment, these were used for Student t-test analysis, the time points for day5, day9 and day 12 after treatment are average epidermal thickness from one animal only. (**f**) Toluidine blue demonstrate retention of the dye in the epidermis of *Ctcf*-deficient mice documenting alterations of the epidermal barrier. Lack of the dye penetration through the epidermis is seen in the control mice.

3.5.2 Expression of markers for cell proliferation and epidermal differentiation in the skin of Ctcf-deficient mice

Immunostaining for proliferation marker Ki67 showed significantly increased number of proliferating cells in the basal layer of the epidermis in tamoxifen treated *Ctcf*-deficient mice compared to controls (**Fig. 3.18.a,b**). Furthermore, some Ki67 positive cells were detected in the suprabasal layer (**Fig. 3.18.a**, arrows) of *Ctcf*-deficent epidermis, while such cells were exclusively seen in the basal epidermal layer of control mice.

Immunostaining for the markers of epidermal differentiation revealed expansion of the Krt14 expression in the epidermis of tamoxifen-treated mice, however, signal intensity of this marker was lower in both the epidermis and hair follicles than in controls (**Fig. 3.19.a**). Expression of cytokeratin 10 was expanded in the *Ctcf*-deficient epidermis (**Fig. 3.19.b**) and appeared to overlap with the expression of Krt14 (**Fig. 3.19.a,b**). Furthermore, ectopic Krt10 expression was seen in the upper portions of the hair follicle, specifically, in the infundibulum and possibly upper part of the outer root sheath (**Fig. 3.19.b**). Loricrin showed patchy expression in the *Ctcf*-deficient epidermis (**Fig. 3.19.c**). Surprisingly, un-identified DAPI positive cells were detected above the cornified layer of the epidermis and were located close to or directly above the hair follicle (**Fig. 3.19.c**). The effects of *Ctcf* ablation on hair follicle cycling were not investigated in detail and will be investigated further in the future.

3.5.3. 3D-FISH analysis of keratinocyte-specific gene loci in the epidermis of wild-type mice and Ctcf knock-out mice

Because the EDC and KtyII loci harbouring lineage-specific genes activated during keratinocyte differentiation showed close associations between each other and nuclear speckles in the nucleus (**Fig. 3.6, 3.7, 3.9**), 3D-FISH analyses of the nuclear positioning of the EDC and KtyII loci was performed on the epidermis of 8 week-old *K14-CreER/Ctcf* fl/fl mice treated with tamoxifen and corresponding control mice. 3D-FISH analyses revealed that in contrast to basal epidermal keratinocytes of control mice, a significant repositioning of the EDC locus away from the KtyII locus occurred in *Ctcf*-deficient mice. The distances between the EDC and the KtyII loci for epidermal keratinocytes of control mice were significantly shorter compared to *Ctcf*-deficient mice (**Fig. 3.20**). These data suggest that Ctcf might be involved in mediating the cross-talk between the EDC and KtyII loci in the nucleus, perhaps, via regulation of the higher-order chromatin remodelling and chromatin looping in the corresponding genomic domains on chromosomes 3 and 15, respectively.

Figure 3.18. Analyses of cell proliferation and apoptosis in the epidermis of *Ctcf*-deficient mice. (**a**) Immunofluorescence of proliferation marker Ki67 in *Ctcf*-deficient epidermis, arrows indicate Ki67+ve cells in the subprabasal layer. Scale bar = 100µm. (**b**) Analysis of the number of Ki67+ cells in basal layer, represented as mean percentage of total cells obtained from two animals, significance calculated using Student t-test. (**c**) TUNEL staining for apoptotic cells in day 7 p.t. (post treatment) and control. (**d**) Mean intensity of TUNEL fluorescence in the epidermis calculated from two control animals and two treated animals measured using ImageJ, P value calculated using Student t-test.

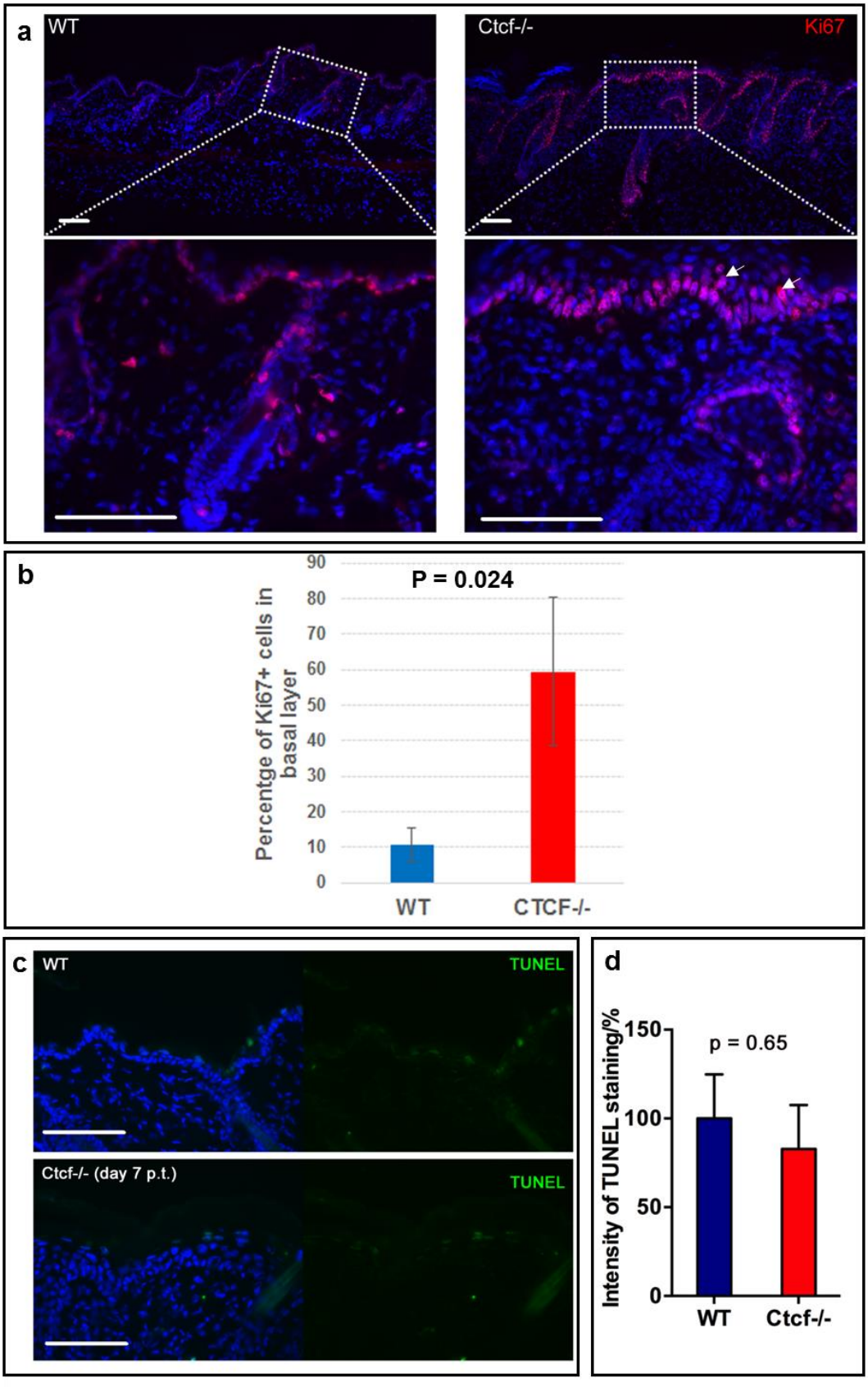

Figure 3.18. For Legend See Facing Page

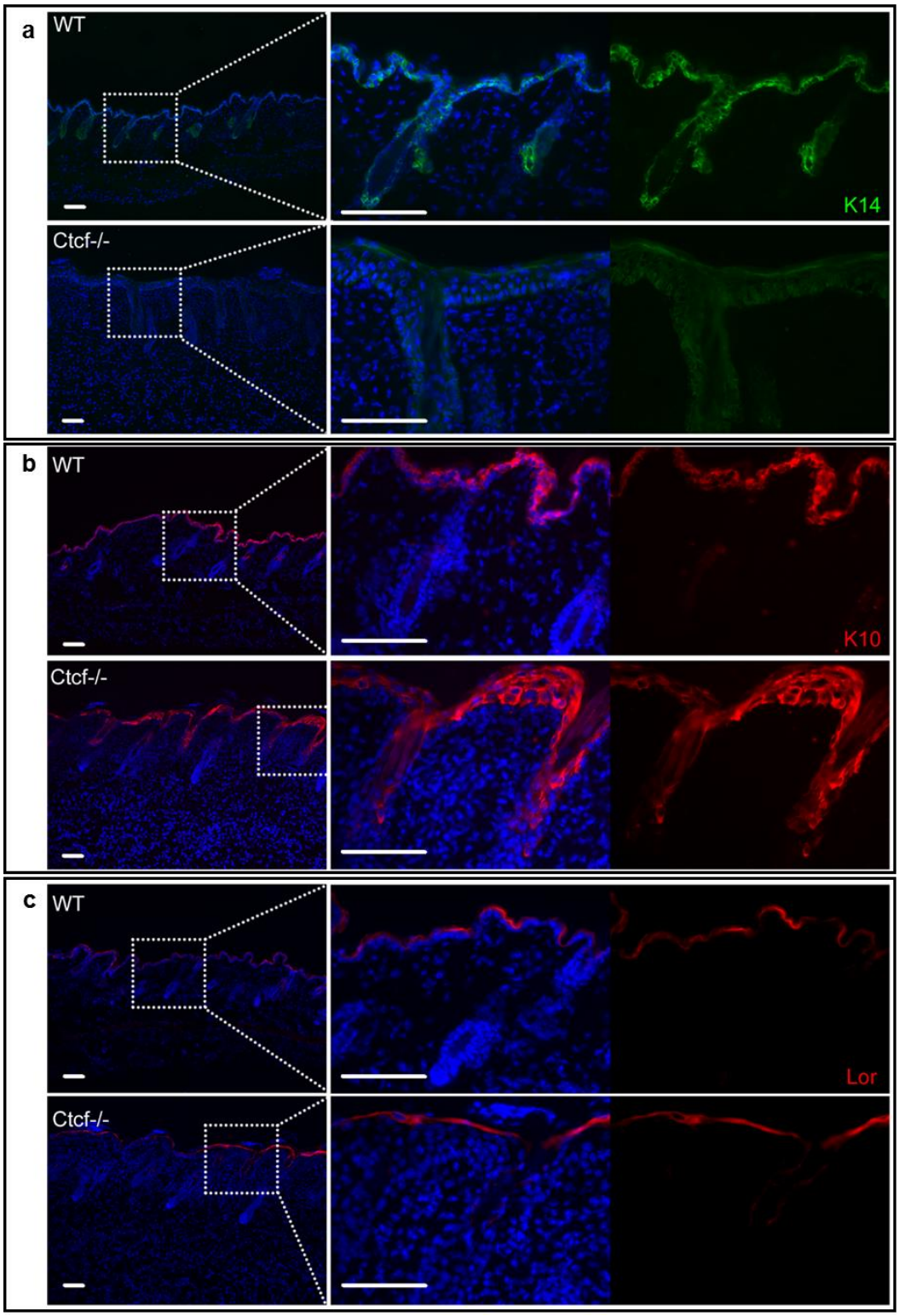

Figure 3.19. Expression of keratinocyte differentiation markers in *Ctcf*-deficient epidermis. (**a**) Immunofluorescence of epidermal differentiation marker of basal layer - cytokeratin 14. (**b**) Immunofluorescence of epidermal differentiation marker of suprabasal layer - cytokeratin 10. Expansion of cytokeratin 10 into the hair follicle infundibulum. (**c**) Immunofluorescence of epidermal differentiation marker of the granular/cornified layers – loricrin. Scale bar = 100μm.

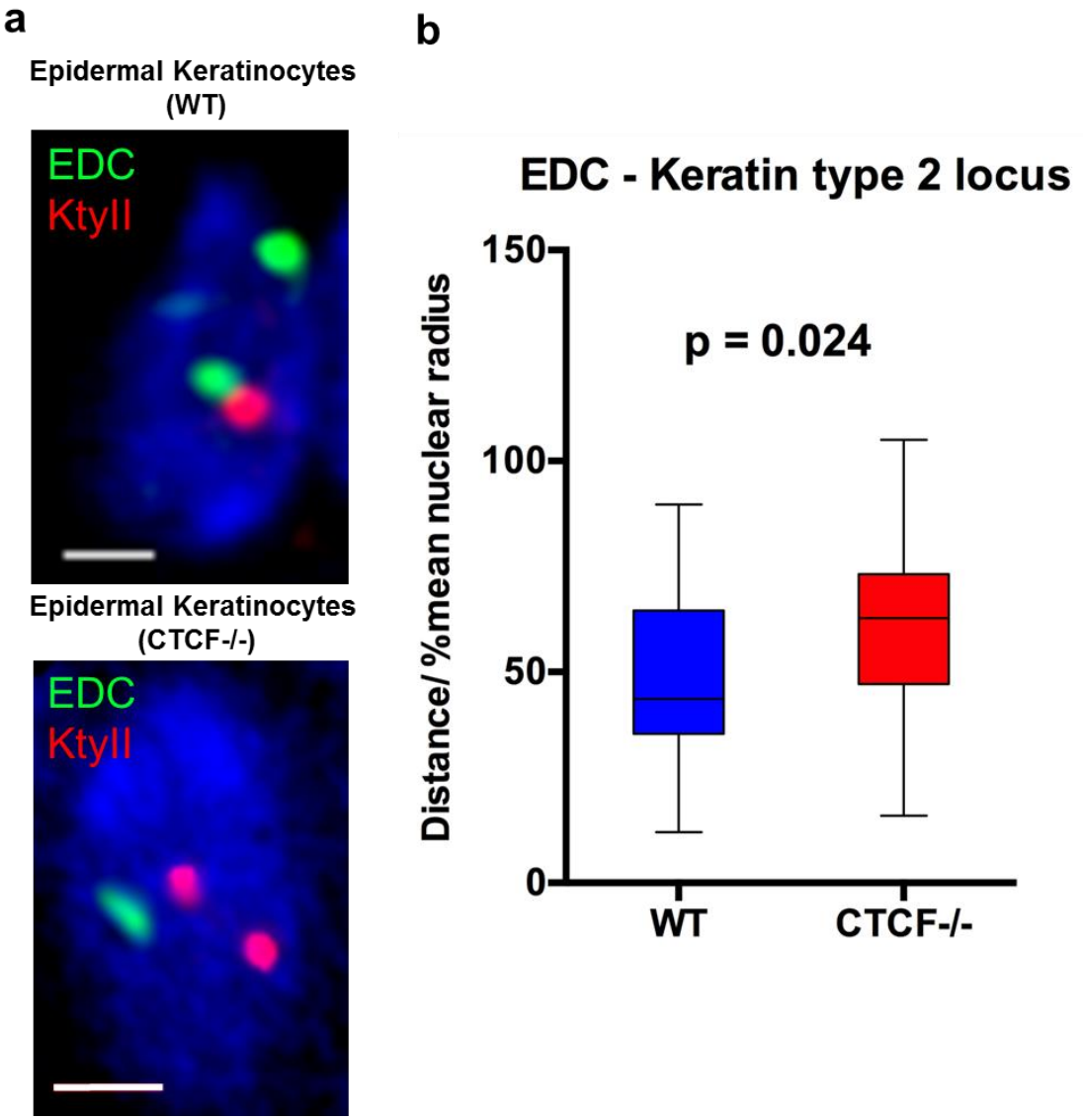

Figure 3.20. Distances between the EDC and Keratin Type 2 loci in the nuclei of basal epidermal keratinocyte of *Ctcf*-deficient mice. (**a**) 3D FISH for EDC (green) and KtyII locus (red) in 8 week old epidermal keratinocytes of day 7 p.t. and C57Bl6 (WT) mice, scale bar = 2µm. (**b**) Analysis of shortest distance between EDC and KtyII loci per nucleus from WT (35 nuclei) and *Ctcf*-deficient epidermis (30 nuclei) and normalized to mean nuclear radius, data represented in box-whisker plot and p-value calculated using Wilcoxon test.

3.5.4. Increased number of immune cells in the Ctcf-deficient skin

A defective epidermal barrier should result in an increased immune response and inflammation due to penetration of the microorganisms through the cornified layer. To show that this is the case, immunofluorescence was carried out for immune T cell markers CD3, CD4 and CD8, as described previously (Mardaryev et al., 2011). The results showed markedly increased number of CD3+ cells in the epidermis and dermis of *Ctcf*-deficient mice compared to controls (**Fig. 3.21.a,d**). Similar, pattern was seen for CD4+ cells (**Fig. 3.21.b,d**) and CD8+ cells (**Fig. 3.21.c,d**). These data demonstrate that skin of *Ctcf*-deficient mice is characterized by the epidermal and dermal inflammatory response, most likely due to the alterations of the epidermal barrier followed by the influx of harmful micro-organisms and activation of anti-inflammatory genes.

3.5.5. Expression of epidermal markers is detected in the hair follicles of tamoxifen treated K14-CreER/Ctcf-floxed mice.

Interestingly, a few K14-CreER/Ctcf-floxed samples which were treated with tamoxifen, showed abnormal expression of epidermal markers in the hair follicles. For an unknown reason, time-mated mice treated with tamoxifen for three days before expected day of delivery consistently did not produce viable pups. However, by chance some dead pups were found, which upon immunohistochemistry showed a great decrease in the number of hair follicles (not analyzed), and the hair follicles that were present where greatly reduced in size and showed expression of Keratin 10 and Loricrin

(**Fig. 3.22.a**). Staining for Lhx2 hair follicle stem cell marker showed some positive cells still present at the bottom part of the hair follicles (arrows, **Fig. 3.22.a**).

During another experiment, which involved tamoxifen treatment of 8-week-old K14-CreER/Ctcf-floxed mice for three days by Intraperitoneal injection followed by depilation, aberrant expression of K10 was seen in the hair follicles. Specifically, part of the skin from day 5 post depilation sample showed K10 expression in both epidermis and the hair follicles, while, control samples only showed K10 expression in the epidermis as expected. Both experiments independently verify that levels of Ctcf expression in the hair follicle stem cells might play an important role in regulating their fate.

Figure 3.21. Analyses of expression of the immune cell markers in the epidermis of *Ctcf*-deficient skin. (**a**) Immunofluorescence for T-cell markers CD3, (**b**) CD4 and (**c**) CD8 in the skin of *Ctcf*-deficient mice versus the controls. Scale bar = 100µm. (**d**) Mean number of cells per mm length of epidermis from two *Ctcf*-deficient animals and two WT animals. Student t-test was used to compare means.

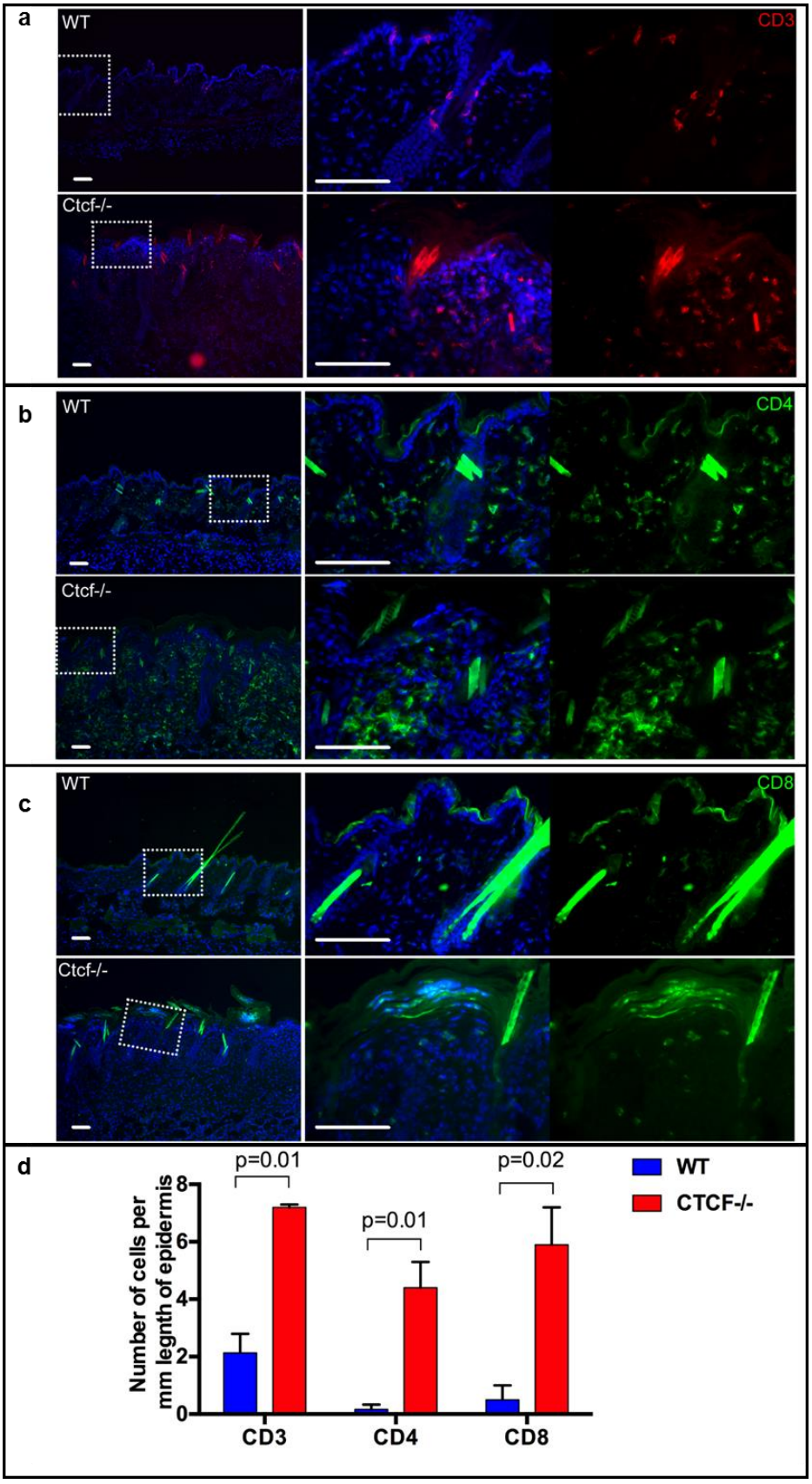

Figure 3.21. For Legend See Facing Page

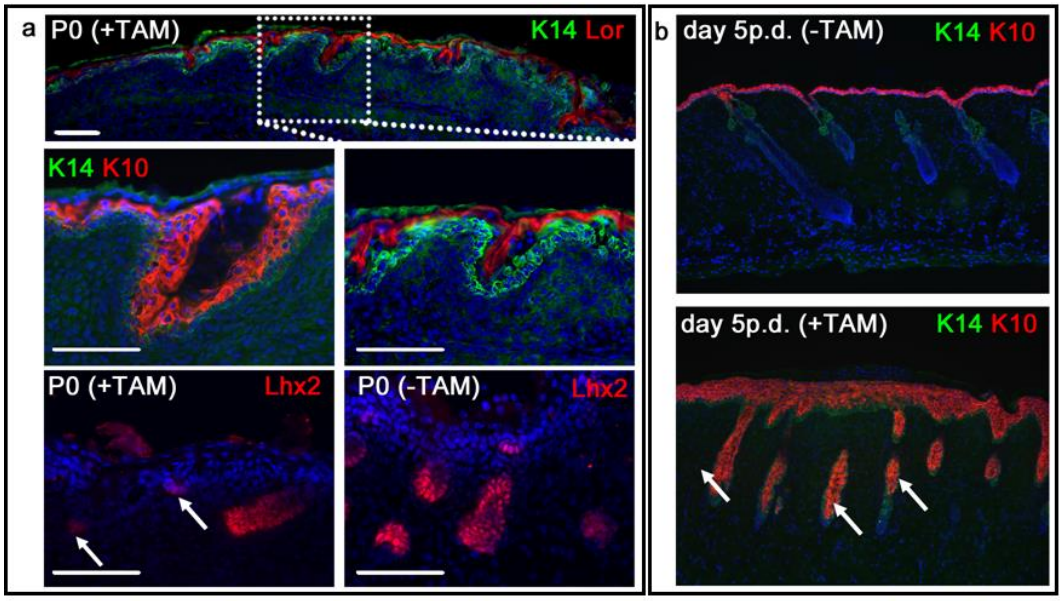

Figure 3.22. Epidermis specific genes are expressed in the hair follicles of Ctcf-deficient mice. (**a**) Pregnant female mouse was treated with tamoxifen for three days before birth by IP, immunostainings for epidermal markers (Keratin 14 (green), Keratin10 (red) and Loricirn (red)) were carried out on the collected pups, as well as hair follicle stem cell marker Lhx2 (arrows show positive Lhx2 cells). Scale = 100µm. (**b**) 8-week-old mice were treated with tamoxifen by IP, then depilation was carried out and skin collected 5 days after depilation. Arrows show staining for Keratin 10 in the hair follicles of Tam treated mouse.

3.6. Global gene expression profiling of the epidermis in *Ctcf*-deficient skin

3.6.1. Microarray analysis of gene expression in the epidermis of Ctcf depleted mice

To determine the possible biological processes that underlie the development of epidermal phenotype (increased epidermal thickness/proliferation, epidermal barriers defects, inflammation) upon *Ctcf* depletion in the skin, gene expression microarray analysis was performed.

Epidermal samples of the skin of *Ctcf*-deficient and control mice on day 7 after tamoxifen/DMSO treatment were isolated by laser capture microdissection (LCM) (**Fig. 3.23**). The RNA from the captured epidermis was amplified and processed for microarray profiling (Agilent platform), as described previously (Sharov et al., 2006, 2009; Mardaryev et al., 2014).

The number of the RNA transcripts for the genes and long non-coding RNAs showing two-fold or higher changes in expression between *Ctcf*-deficient and control mice was identified to be about 15,000. These transcripts were manually placed into one of these categories according to their most appropriate function: signaling, metabolism, proteolysis, RNA processing, cell cycle/apoptosis, nuclear and chromatin assembly, cytoskeleton/differentiation, adhesion/extracellular matrix, covalent modification of histones and non-histone proteins, long non coding RNA, transcription regulation, others and unknown (**Fig. 3.24**). Interestingly, non-

coding RNAs made about 14% of over-expressed transcripts while under-expressed consisted of 26% (**Fig. 3.24**).

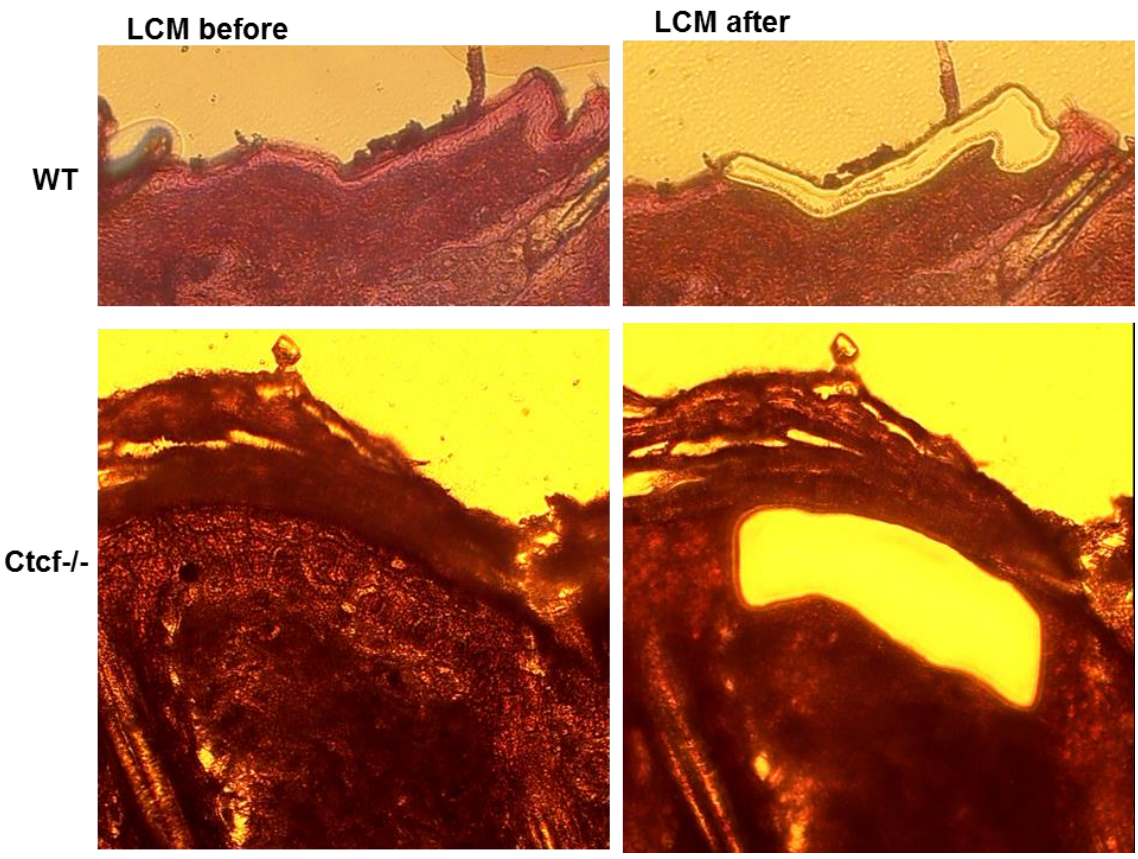

Figure 3.23. Laser capture microdissection (LCM) of *Ctcf-/-* deficient and control epidermis. Epidermal samples prior to and after LCM are shown. Illustration only (no scale).

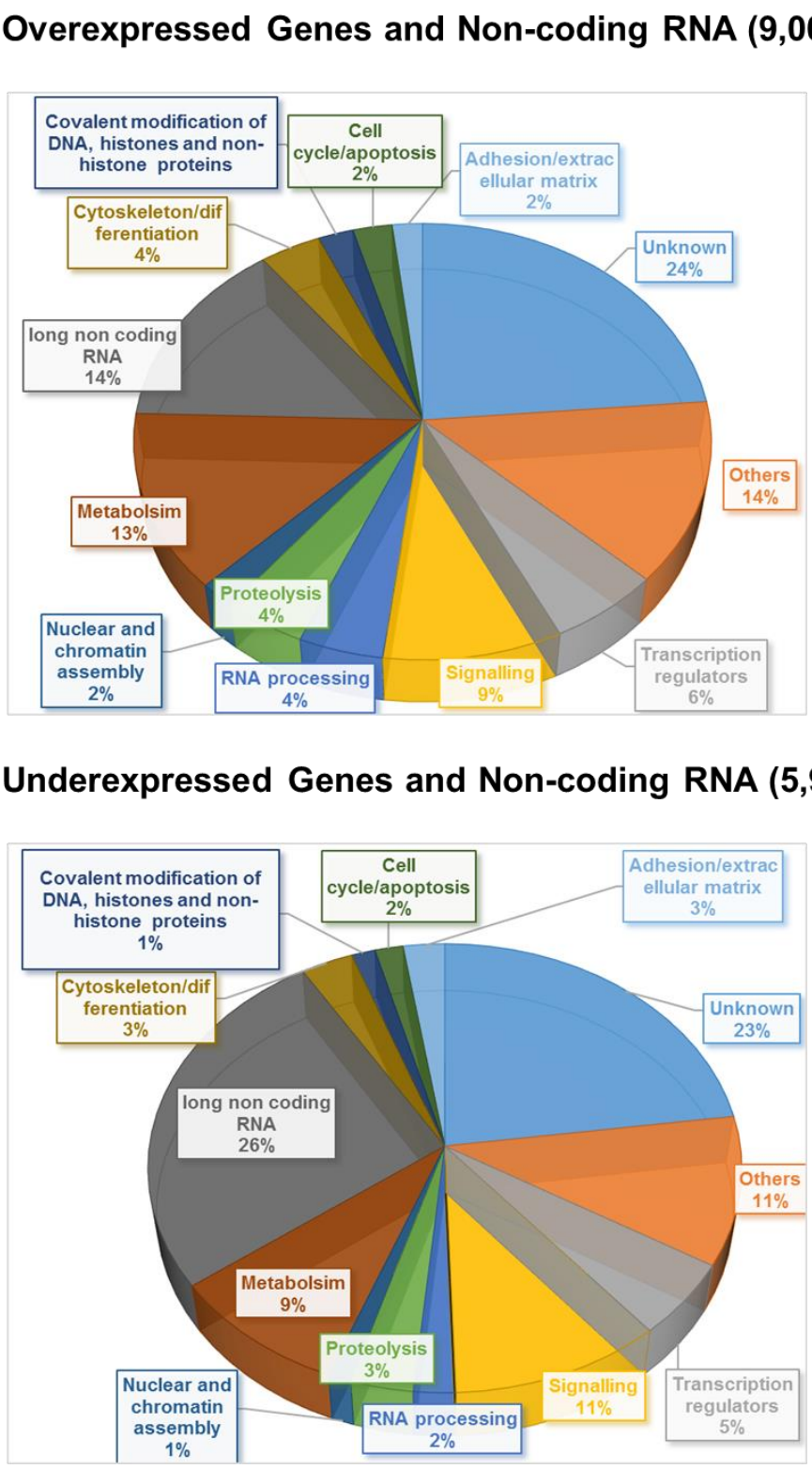

Figure 3.24. Functional annotation of over- and under-represented genomic transcripts in *Ctcf*-deficient epidermis versus the controls.

3.6.1. Analyses of expression of lineage-specific genes in the Type I, Type II Keratin Custers and the Epidermal Differentiation Complex in the Ctcf-deficient and control epidermis

Terminal differentiation of keratinocytes involves the expression of genes in the epidermal specific genomic loci located in the Keratin Type I locus, Keratin Type 2 locus and the Epidermal Differentiation Complex (Botchkarev et al., 2012). Therefore, the genes within these loci showing two-fold or higher change in expression between *Ctcf*-deficient and control mice were identified in microarrays and plotted relatively to their genomic location (**Fig. 3.25**).

According to the microarray data, the expression of *Krt10* was increased in the *Ctcf*-deficient epidermis compared to controls, thus confirming the immunostaining results (**Fig. 3.25**). However, *Krt14* did not show a difference of expression between *Ctcf*-deficient and control samples. Other keratins that were upregulated in the Keratin Type I locus included *Krt12* and *Krt13*, while *Krt23, Krt40* and *Krt15* were downregulated in *Ctcf*-deficient mice compared to controls (Appendix A).

Interestingly, large number of keratins within the Keratin Type II locus showed increased expression in *Ctcf*-deficient epidermis versus the controls including the genes located between the clusters of hair keratins and inner root sheath keratins (*Krt6b, Krt6a* and *Krt5*) (**Fig. 25.b**).

Genes that constitute the EDC locus also showed up- and down-regulation of their expressions between *Ctcf*-deficient and control mice.

Overexpressed genes were belonging to the S100 and SPRR gene families, while genes belonging to the LCE family were mostly under-expressed verus the controls (**Fig. 3.25**). Interestingly, changes in expression of the EDC genes upon *Ctcf* ablation in the epidermis were very similar to the changes seen in the epidermis of KtyII locus knockout mice (Kumar et al., 2015). Together with the similarities in the epidermal phenotypes of *Ctcf*-deficient and KtyII knockout mice, these data suggest that alterations in expression of the EDC genes can, at least in part, explain the mechanisms of the epidermal barrier defects observed in *Ctcf*-deficient mice (**Fig. 3.17.c**).

3.6.2. Analyses of expression of the genes involved in the control of inflammation and immune response in the epidermis of Ctcf-deficient mice

Firslty, large number of genes involved in the immune response were upregulated in the *Ctcf*-deficient mice, which include the following antigens: *Cd1d1, Cd2, Cd3d, Cd4* and *Cd8* (Appendix B).

Secondly, a large number of genes encoding distinct cytokines and interleukins showed higher expression in *Ctcf*-deficient epidermis versus the controls. Some of these are *Il1b, Il1f5, Il10ra, Il10rb, Il6ra*, as well as the interleukin enhancer binding factors *Ilf2* and *Ilf3*. Furthermore, a large number of TNF superfamily genes showed increased expression in *Ctcf*-deficient epidermis compared to controls. (Appendix B).

Thus, this data contributes to the previous immunofluorescence results indicating that the inflammatory response is taking place in the skin of *Ctcf*-deficient mice confirming that epidermal barrier defects probably resulted in the increased penetration of microorganisms into the skin after *Ctcf* ablation.

3.6.3. Analyses of expression of the genes involved in the control of cell proliferation and apoptosis in the epidermis of Ctcf-deficient mice

Substantial changes were also observed in the expression of the genes involved in the control of cell proliferation upon *Ctcf* ablation. Upregulated genes included *Pcna, cyclin B1, cyclin D3, cyclin E1, polo-like kinase 1, polo-like kinase 2, polo-like kinase 3, Mybl2, Bub1b, Myc, E2F1*. Expressions of anti-apoptotic genes such as *Bcl3, Bag1, Bag2, Bag3* were increased, while, expression of some pro-apoptotic genes (*Bax, Bok*) was decreased in the epidermis of *Ctcf*-deficient mice versus the controls.

In contrast to WT mice, *Ctcf*-deficient epidermis also showed marked change in the expression of the genes implicated in a number of cutaneous tumorigenesis pathways: Wnt (*Wnt1, Wnt3, Wnt4, Wnt5b, Wnt6, Wnt9a, Wnt11*), Ras/MAP kinase pathway (*Nras, Traf2, Map2k, Mapk1*, etc) as well as AP-1 transcription factor components (*Fos, Jun, Atf2, Jdp2*). Interestingly, *Jdp2* was the only AP-1 component showing reduced expression in the epidermis of *Ctcf*-deficient mice compared to controls (Appendix C).

Taken together, these data demonstrate that Ctcf plays an essential role in the control of epidermal barrier maintenance in adult skin, and is involved in the control of expression not only of the keratinocyte-specific genes, but also of the genes controlling epidermal proliferation, immune response and regulation of tumorigenesis.

Figure 3.25. Microarray data for the over- and under- expressed genes in the Keratin type I/II and EDC loci of *Ctcf*–deficient epidermis. (**a**) The location and log2 value of genes showing a 2 or greater fold change of RNA transcript levels in the region of the Keratin Type I locus on chromosomes 11 in *Ctcf*-deficient epidermis versus the controls. (**b**) The location and log2 value of genes showing a 2 or greater fold change of RNA transcript levels in the region of the Keratin Type II locus on chromosomes 15 in *Ctcf*-deficient epidermis versus the controls. (**c**) The location and log2 value of genes showing a 2 or greater fold change of RNA transcript levels in the region of the Epidermal Differentiation Complex on chromosomes 3 in *Ctcf*-deficient epidermis. Expression levels of the over- or under-expressed genes in *Ctcf*-deficient epidermis versus the controls are shown in green and red, respectively (See Appendix A for the list of genes and their expression changes).

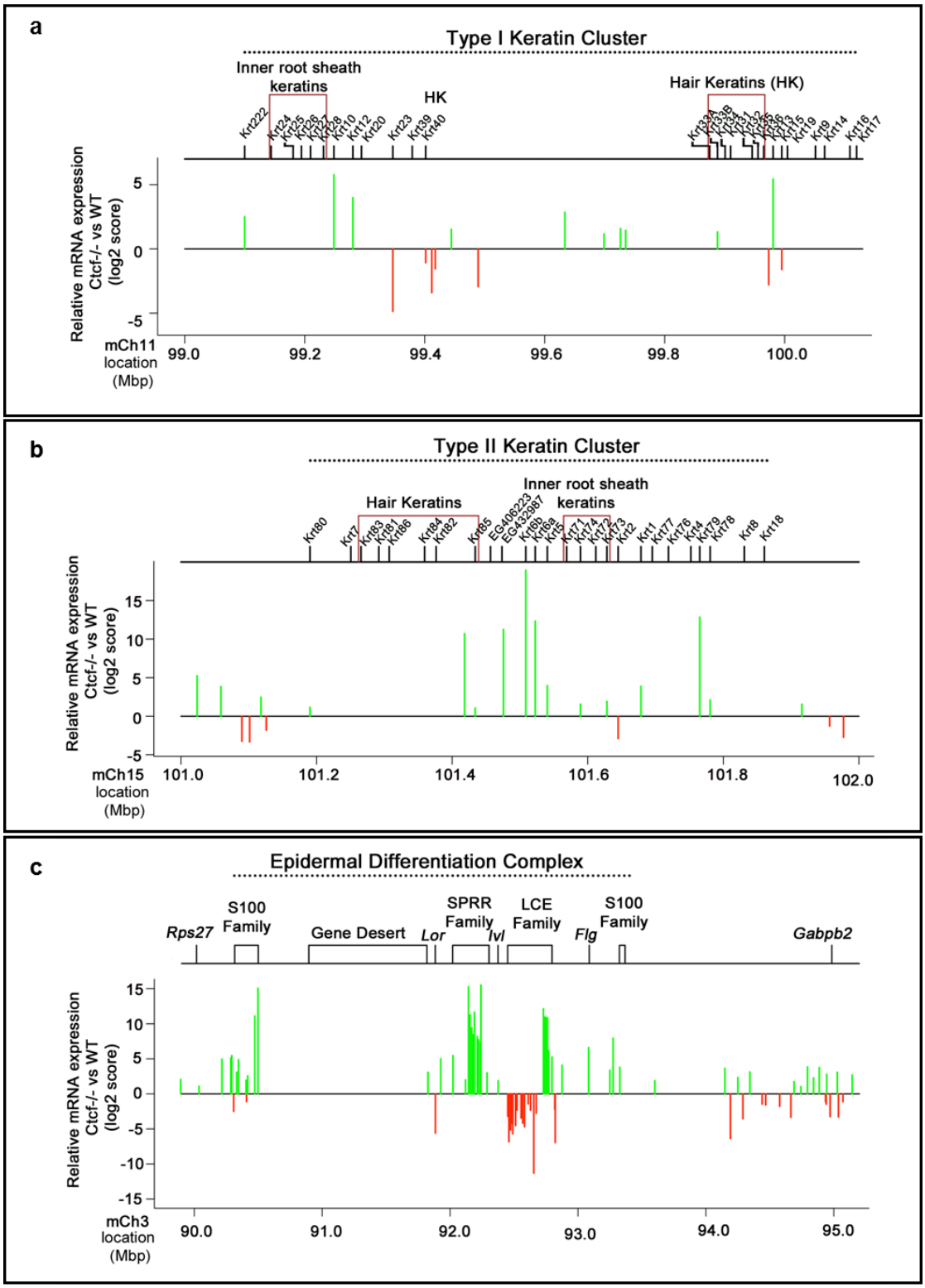

Figure 3.25. For Legend See Facing Page

4. DISCUSSION

4.1. Higher-order chromatin remodeling and control of expression of terminal differentiation-associated genes in epidermal kerationcytes

During development, the genome of multi-potent stem cells becomes reorganized in 3D nuclear space to establish a proper spatio-temporal regulation of transcription underlying execution of lineage-specific gene expression programs (Bickmore and van Steensel, 2013; Dekker et al., 2013; Schoenfelder et al., 2010a; Wei et al., 2013). However, mechanisms coordinating transcription in lineage-specific gene loci located on different chromosomes during cell differentiation are poorly understood.

The mammalian epidermis is a stratified epithelium which protects the body against mechanical injury, dehydration and infections (Blanpain and Fuchs, 2009; Koster and Roop, 2007; Watt and Huck, 2013). These functions rely on the maintenance of a basal stem cell compartment orchestrating a series of differentiation events. These result in the formation of the cornified envelope (CE), which together with tight junctions and epidermal Langerhans cells forms the protective epidermal barrier (Candi et al., 2005; Simpson et al., 2011). Members of the keratin (K) family of proteins comprise the major cytoskeleton of all epithelia and are believed to contribute to crucial keratinocyte functions by acting as cytoskeletal scaffolds undergoing protein interactions in a context- and keratin isotype-dependent manner. Of particular importance to skin cytoarchitecture are keratin interactions with cornified envelope and desmosomal proteins

(Candi et al., 2005; Simpson et al., 2011). The cornified envelope is a lipoprotein structure that consists of involucrin, loricrin, filaggrin, plakin family members, small proline-rich proteins (SPRRs), late cornified envelope proteins (LCEs), and S100 protein family members which become sequentially cross-linked to a subset of keratins during the final stages of epidermal differentiation (Segre, 2006).

Lineage-specific genes activated during the execution of the epidermal differentiation program are clustered in the mammalian genome into several loci including the KtyI and KtyII gene loci located on mouse chromosomes 11 and 15, respectively, as well as the Epidermal Differentiation Complex (EDC) locus located on mouse chromosome 3 (de Guzman Strong et al., 2010; Magin et al., 2007; Martin et al., 2004). In the epidermis, gene expression in KtyI/KtyII loci is regulated in a tightly coordinated manner: while proliferating basal keratinocytes express K5, K14 and K15, the switch to terminal differentiation is accompanied by the expression of K1, K2e and K10 in postmitotic keratinocytes (Reviewed in Fuchs, 2007). Further transition of post-mitotic keratinocytes from the spinous to granular epidermal layer is accompanied by the marked increase in expression of the EDC genes (loricirin, filaggrin, Sprrs, LCEs, etc.) (Fuchs, 2007). However, despite substantial advances in understanding of the role of signaling pathways that act on transcription factors and epigenetic modifiers to control epidermal differentiation (Reviewed in Botchkarev et al., 2012; Frye and Benitah, 2012; Perdigoto et al., 2014), it remains unclear how physically separated gene loci including the EDC and the KTyI/II are coordinated to result in the formation of a fully functional epidermal barrier.

To study the potential interactions between the distinct lineage-specific loci in epidermal cells, genetically-engineered mice with ablation of the entire Keratin type II locus located on mouse chromosome 15 were generated in Prof. T. Magin's laboratory at the University of Leipzig (Germany). The KtyII locus ablation caused dysregulated expression of 37 genes localized in the Epidermal Differentiation Complex (EDC) locus on chromosome 3, leading to severe epidermal barrier defects (Kumar et al., 2015).

During the epidermal morphogenesis and differentiation of multi-potent progenitor cells residing in the basal epidermal layer, the lineage-specific EDC locus shows marked remodelling of its higher-order chromatin structure and relocates away from nuclear periphery into the nuclear interior (Mardaryev et al., 2014). This shift in the position of the EDC is associated with an increase in the transcriptional activity of genes involved in the control of terminal keratinocyte differentiation and epidermal barrier formation (Mardaryev et al., 2014). The process of developmentally-regulated higher-order chromatin remodelling in the EDC locus is regulated by p63 transcription master regulator and includes at least two interconnected steps: i) the Brg1-dependent relocation of the EDC away from the nuclear periphery into the nuclear interior and propinquity with speckles; ii) the final, Satb1-mediated, arrangement of chromatin conformation within the central domain of the locus, which contains a large number of genes activated during terminal keratinocyte differentiation (Mardaryev et al., 2014).

3D-FISH experiments performed to define whether EDC and KtyII loci spatially interact in keratinocytes during epidermal development revealed

that in WT epidermis, the KtyII locus showed significantly closer localization to the EDC locus and *Lor* gene, compared to thymocytes, in which gene expression in both loci is shut down. In both keratinocytes and thymocytes, chromosome 15 showed more central positioning in the nucleus and contacted the internal part of the chromosome 3, which was located more peripherally.

Similarly to thymocytes and in contrast to basal epidermal keratinocytes of WT mice, a significant movement of the *Lor* gene away from the genes that constitute 3' or 5' ends of the KtyII locus was seen in KtyII-deficient mice. This movement was also accompanied by significant changes in the positioning of the *Lor* gene relative to the chromosomal territory 3 (from internal to peripheral), suggesting a marked remodeling of the higher-order chromatin structure in the EDC upon KtyII locus ablation. These data suggest that ablation of the KtyII locus result in the remodeling of the higher-order chromatin structure of the EDC locus and its neighboring regions on chromosome 3 associated with marked changes in the EDC gene expression.

However, additional studies are required to fully understand the impact of distinct protein-coding or non-protein-coding genes that control interactions between the KtyII and EDC loci in differentiating epithelial cells. In particular, the effects of long non-coding RNAs (Kretz et al., 2012; Wang and Chang, 2011) and microRNAs (Yi and Fuchs, 2011), that are present in both loci, on gene expression in both EDC and KtyII loci need to be carefully dissected.

Also, the roles of distinct transcription factors (p63, AP1, Klf4, Arnt, etc.) and chromatin regulators, such as Satb1, Brg1, Ctcf, cohesin, in the formation and maintenance of lineage-specific gene interactomes and their remodelling in differentiating cells remain to be clarified. Transcription factors promote formation of spatial gene interactomes in different cell types (Schoenfelder et al., 2010b; Wei et al., 2013), and p63 transcription master regulator control expression of Satb1 and Brg1 in epidermal progenitor cells (Fessing et al., 2011; Mardaryev et al., 2014). Satb1 controls specific conformation of the EDC locus, as well as gene expression in both EDC and KtyII loci (Fessing et al., 2011), while its expression is markedly decreased in epidermal keratinocytes of KtyII-deficien mice.

In addition, the impact of nuclear micro-environment of the EDC and KtyII loci including SC35+ speckles which are enriched in the vicinity of the EDC locus in basal epidermal cells (Mardaryev et al., 2014) on balancing gene expression in keratinocyte-specific gene loci during epidermal differentiation remain to be defined. Given that SC35+ speckles contain RNA metabolic factors and non-coding RNAs (Reviewed in Sleeman and Trinkle-Mulcahy, 2014), while non-coding RNA TINCR modulate gene expression in the EDC locus via controlling RNA stability (Kretz et al., 2013), speckles might serve as an important component of the nuclear compartment, in which EDC and KtyII loci are clustered in differentiating epidermal cells.

This data support the fundamental significance of the 3D genome organization for the coordination of gene expression and establishment of distinct phenotypic features in differentiating cells. Future advances in the

HiC technology should help to generate global 3D gene interaction maps for each cell type in the mammalian organism and to elucidate how such maps are established during development and altered during disease.

Finally, the impact of enhancer-promoter interactions in the control of gene expression in the EDC locus including the interactions of the EDC gene promoters with the putative enhancers residing in the KtyII locus need to be carefully dissected. Enhancers are the sequence modules that are preferentially located in the non-coding part of the genome at various distances from their target genes or even at different chromosomes (Symmons and Spitz, 2013). In normal differentiating cells, interactions between the genes and their enhancers are very important for execution of lineage-specific gene expression programs (Symmons and Spitz, 2013). Key regulators of development, such as *Shh* or *Nanog* genes, show looping outside the chromosomal territories, possibly to interact with their enhancers and/or to balance their expression (Amano et al., 2009; Schneider and Grosschedl, 2007).

Inter-chromosomal interactions between the enhancers and gene promoters are pretty well established, and there are several examples of eukaryotic genes located on distinct chromosomes are associating physically in the nucleus via interactions that may have a function in coordinating gene expression (for review, see Williams et al., 2010)). For instance, the region of the IFN-gamma gene on chromosome 10 interacts with the regulatory regions of the T(H)2 cytokine locus on chromosome 11 (Spilianakis et al., 2005).

Following the same line of arguments, it is shown that one allele of the insulin-like growth factor 2 (Igf2)/H19 imprinting control region (ICR) on chromosome 7 co-localized with one allele of Wsb1/Nf1 on chromosome 11 (Ling et al., 2006). Interestingly that omission of CTCF abrogated this association and altered Wsb1/Nf1 gene expression (Ling et al., 2006). These findings demonstrate that CTCF mediates an interchromosomal association, perhaps by directing distant DNA segments to a common transcription factory, and the data provide a model for long-range allele-specific associations between gene regions on different chromosomes (Ling et al., 2006).

In summary, our data support the fundamental significance of the 3D genome organization for the coordination of gene expression and establishment of distinct phenotypic features in differentiating cells. Future advances in the HiC technology should help to generate global 3D gene interaction maps for each cell type in the mammalian organism and to elucidate how such maps are established during development and altered during disease.

4.2. Role of Ctcf in the control of skin development and keratinocyte differentiation in the epidermis

4.2.1. Involvement of Ctcf in the control of epidermal and hair follicle development.

Using the chromosome conformation capture technique (3C and its modifications 4C, 5C, Hi-C), based on the formaldehyde-mediated cross-linking of closely located chromatin domains, it was shown that the mammalian genomes are organized into Topologically Associating Domains (TADs) having an average size of about 1MB and defined as the genomic regions with higher frequency of spatial chromatin contacts within TADs compared to adjacent regions (Pope et al., 2014).

In differentiating cells, spatial chromatin interactions of lineage-specific gene promoters with their distal regulatory elements occur both *in-cis* and *in-trans* within and between different TADs (Bonora et al., 2014). Enhancer-promoter gene interactomes provide functional and structural frameworks for lineage-specific transcription, which is controlled at several levels including pioneer transcription factors and chromatin architectural proteins (CTCF, cohesin, condensin, Satb1).

Chromatin architectural protein CTCF controls the establishment and maintenance of the long-range enhancer/promoter regulatory networks in differentiating cells. CTCF binding sites are enriched at the borders between distinct TADs, where CTCF together with other chromatin architectural proteins is involved in demarcating distinct TADs (Ong and Corces, 2014).

Depletion of CTCF results in the reduction of intra-TAD interactions and increase of the contacts between different TADs (Zuin et al., 2014). Importantly, CTCF DNA binding sites are asymmetrical and most CTCF-mediated chromatin contacts occur between the sites in convergent orientation (ENCODE, 2012; Rao et al., 2014). The inversion of the CTCF binding sites at the TAD boarders lead to rewiring of the chromatin contacts and changes of gene transcription in the neighboring genomic regions (Guo et al., 2015). CTCF binding sites also exist within TADs, in which CTCF is involved in organizing the smaller-sized (100-200 kb) intra-TAD chromatin loops and in mediating the enhancer-promoter contacts (Cubenas-Potts and Corces, 2015; Rao et al., 2014).

Here, the role of CTCF in the control of skin development and postnatal homeostasis was explored. Our data reveal that *Ctcf* protein is expressed in both epithelial and mesenchymal compartments of the developing and postnatal mouse skin (**Fig. 3.11, 3,12**). In particular, CTCF protein is expressed in all layers of the epidermis, hair follicles (placodes, outher root sheath, hair matrix, dermal papilla), as well as in dermal cells (**Fig. 3.11, 3.12**).

Because *Ctcf* knockout mice die during early embryonic development (Moore et al., 2012), we addressed the role of *Ctcf* in the control of epidermal and hair follicle development by generating *Krt14-Cre*ER/*Ctcf* fl/fl mice with tamoxifen-induced *Ctcf* ablation in Keratin 14-expressing basal epidermal and outer root sheath keratinocytes. *Ctcf* fl/fl mice were obtained from N. Glajart (Erasmus Medical Center, Rotterdam, Netherlands). Tamoxifen (TAM) was injected into *Krt14-Cre*ER/*Ctcf* fl/fl pregnant females

between E12.5-14.5, and *Ctcf* ablation was confirmed by lack of Ctcf protein in the isolated epidermis (**Fig. 3.10**).

Skin of TAM-treated embryos (E16.5-E18.5) showed marked increase of the epidermal thickness and proliferation, as well as the retardation of their development (**Fig. 3.10, 3.11**). Also, epidermis of E16.5 TAM-treated *Krt14-Cre*ER/*Ctcf* fl/fl mice showed marked expansion of Keratin 14 into suprabasal layers, increased Keratin 10 expression, while Loricirn expression was unchanged compared to controls (**Fig. 3.12**). These data allowed concluding that Ctcf indeed plays an essential role in the control of execution of lineage-specific differentiation programmes in skin epithelial cells during development, most likely, via global regulation of the higher-order chromatin folding and control of the enhancer-promoter interactions.

4.2.2. Invovlement of Ctcf in the control of epidermal homeostasis and barrier maintenance in adult mice.

To address the role of Ctcf in the maintenance of homeostasis in adult epidermis, TAM was injected into 8 week-old *Krt14-Cre*ER/*Ctcf* fl/fl mice, as well was topically applied onto the skin. Ctcf ablation in adult epidermis resulted in marked changes in the epidermal integrity accompanied by increase of the epidermal thickness and proliferation followed by alterations in the epidermal barrier maintenance (**Fig. 3.17**, **3.18**). These changes were accompanied by the alterations in expression of the epidermal keratins (Krt14, Krt10) and expansion of the Krt10 expression into the hair follicle infundibulum (**Fig. 3.19**).

Microarray analyses of the epidermal samples isolated from *Krt14-Cre*ER/*Ctcf* fl/fl mice reveal marked alterations in expression of the keratinocyte-specific genes that constitute the EDC, KtyI and KtyII loci upon Ctcf ablation (**Fig. 3.20**). Interestingly, the profile of changes in expression of the EDC genes including downregulation of the Loricrin, Lce family genes and upregulation of the Sprr family genes strikingly resemble changes in expression of the EDC genes seen in the KtyII locus knock-out mice (Kumar et al., 2015).

Furthermore, our 3D FISH analyses show that EDC locus in Ctcf-deficient mice moved away from the KtyII locus and relocate towards nuclear periphery (**Fig. 3.20**). Similar changes in the positioning of the EDC locus were observed in KtyII locus knock-out mice (**Fig. 3.7**), suggesting that Ctcf might be involved in the regulation of the cross-talk between the EDC and KtyII loci in epidermal cells during the execution of terminal differentiation programme. These data are quite consistent with previous reports demonstrating that CTCF controls the establishment of inter-chromosomal associations between the insulin-like growth factor 2 (Igf2)/H19 imprinting control region (ICR) on chromosome 7 and Wsb1/Nf1 gene on chromosome 11, while Ctcf ablation result in altered Wsb1/Nf1 gene expression (Ling et al., 2006).

Alterations in epidermal barrier formation upon Ctcf ablation was also accompanied by appearance of the Cd4 and Cd8 cells in the epidermis and development of the epidermal inflammatory response (**Fig. 3.21**), possibly, due to the influx of bacteria into the epidermis (Bognar et al., 2014; Darido et al., 2016). Microarray data obtained from the epidermis of *Krt14-*

*Cre*ER/*Ctcf* fl/fl mice show marked alterations in expression of numerous genes mediating inflammatory response, including cytokines (Il1b, Il1f5, Il10ra, Il10rb, Il6ra), adhesion molecules and membrane receptors (Appendix B). However, additional experiments are required to fully understand whether expression of these genes is under direct control of Ctcf or changes in their expression occur as a result of epidermal inflammation occurring after alterations of epidermal barrier integrity upon Ctcf ablation.

The same is true for the genes encoding the components of cell cycle-associated machinery and controlling keratinocyte proliferation (Pcna, cyclin B1, cyclin D3, cyclin E1, polo-like kinase 1, polo-like kinase 2, polo-like kinase 3, Mybl2, Bub1b, Myc, E2F1), as well for the genes encoding the distinct signaling molecules and transcription factors relevant to the regulation of epidermal homeostasis (Wnt pathway, RAS/MAPK pathway, TNF pathway) (Appendix B, C). Additional ChIPseq analyses are required to prove direct binding of Ctcf to the promoters of those genes and/or to the putative distal regulatory/enhancer elements that might control their expression.

These analyses will provide an important platform for obtaining novel fundamental information on how Ctcf regulates the establishment of enhancer-promoter regulatory networks in distinct epithelial cell populations in the skin during development, postnatal regeneration and response to different environmental stressors. In global context, these data will provide an important foundation for further studies on how enhancer-promoter networks of active or repressed genes and their enhancers are changed in the disorders associated with alterations of epidermal differentiation

(psoriasis) or in epidermal tumors, and how development of these disorders can be managed via targeting distinct chromatin remodeling factors and modulating enhancer-promoter interactions.

Interestingly, preliminary data shows that upon *Ctcf*-depletion because of tamoxifen treatment of K14-CreER/*Ctcf*-floxed mice the cells of the hair follicles start expressing epidermal specific genes such as Keratin 10 and Loricrin (**Fig. 2.23**). This suggests that Ctcf is important for the maintenance of skin appendages during normal homeostasis. Recently, it has been shown that during aging hair follicle stem cells acquire epidermal fate leading to the loss of the hair follicle (Matsumura et al., 2016). Due to striking similarities in phenotype it would be interesting to determine if expression of *Ctcf* might play a role in aging of the hair follicles.

5. CONCLUSIONS

Based on the generated data in this thesis the following conclusions can be made:

1) The organisation of the nucleus in keratinocytes is tissue-specific with genomic loci containing genes which are responsible for epidermal development being arranged in a non-random manner. This is evident by closer topological association detected between Epidermal Differentiation Complex (EDC) located on mouse chromosome 3 and Keratin Type II (KtyII) locus on chromosome 11 in keratinocytes, while in thymocytes the distances between these loci are significantly larger.
2) Genetic ablation of KtyII locus results in relocation of the EDC locus away from the nuclear compartment containing the flanking regions of the KtyII locus and enriched by nuclear speckles: the distances between the EDC and the flanking regions of KtyII locus are significantly increased, while the positioning of Loricrin gene within the chromosome territory 3 changes to a more peripheral location in KtyII deficient epidermal nuclei. These data demonstrate topological and possibly functional relationships between the EDC and KtyII loci, which also include nuclear speckles, likely providing the environment facilitating coordinated gene expression in the EDC and KtyII loci.
3) The chromatin architectural protein Ctcf is essential for proper control of epidermal and hair follicle development. It is expressed in all cells

of the skin including the epidermis, dermis and hair follicle. Condition ablation of *Ctcf* in developing embryos under the control of Keratin 14 promoter results in the increased keratinocyte proliferation and epidermal thickness, alterations in expression of the epidermal differentiation associated genes, and in retardation of hair follicle development.

4) Keratin 14-driven *Ctcf* ablation in adult skin also results in increase of the epidermal proliferation and thickness, alterations in expression of epidermal keratins (Krt14, Krt10), as well as in perturbation of epidermal barrier integrity accompanied by infiltration of the immune cells and development of inflammatory skin response. 3D FISH analysis of the EDC and KtyII locus showed that similarly to KtyII locus knock-out mice, *Ctcf* ablation in the epidermis results in results in relocation of the EDC locus away from the KtyII locus, thus suggesting Ctcf involvement in the control of topological associations between both loci and possible functional cross-talk between them.
5) The microarray analysis of *Ctcf*-deficient epidermis revealed that the expression of approximately 15000 genes was affected. Many of the genes, which expression is altered upon *Ctcf* ablation are involved in the control of cell proliferation, keratinocyte differentiation, immune response, as well as controlling the activities of Wnt and Ras/MAP signalling pathways. Changes in the expression profile of keratinocyte-specific genes located in the EDC locus closely match the profile of changes in expression of the EDC genes seen in the epidermis of KtyII locus published previously, which suggest a role

for Ctcf in the control of functional relationships and possibly enhancer-promoter interactions between two loci during epidermal development and keratinocyte differentiation.

Taken together, the data presented in this Thesis, demonstrate that Ctcf-mediated chromatin assembly serve as crucial mechanism which enables the coordinated gene expression and inter-chromosomal interactions between lineage-specific gene loci in epidermal keratinocytes during skin development and postnatal homeostasis, while perturbation of this mechanism result in alterations of the epidermal barrier integrity and leads to skin inflammation.

6. FUTURE DIRECTIONS OF RESEARCH

At this moment, many aspects of the biology of keratinocyte nucleus and epigenetic control of gene expression are still unclear and at least several important issues need to be resolved:

1) Because enhancer-promoter interactions play a fundamental role in the control of gene expression in differentiating cells (Bock et al., 2012), I will assess a potential impact of the functional enhancers in the KtyII locus that might be involved in coordinating the expression of lineage-specific genes in the EDC locus during keratinocyte differentiation;

2) Because *Ctcf*-deficient mice show remarkable changes in the expression of genes located in the EDC locus, I will use 3D-FISH to determine the conformational changes that occur in the different compartments of this locus and correlate these data with the data chromosome conformation capture (5C) analyses recently obtained in our laboratory.

3) The thickness of the epidermis in *Ctcf*-deficient mice is increased compared to controls. Furthermore, there was evidence that some DAPI positive cells were detected to be present above the cornified epidermal layer in *Ctcf*-deficient mice. This indicates that some keratinocytes have failed to acquire a cornified fate and might be at the initiat stages of tumour formation. Therefore, I will further investigate this phenomenon.

4) Hair follicle cycling is likely to be affected as the result of *Ctcf* ablation because Ctcf is expressed strongly in the hair follicles in WT mice. Therefore, I

will induce hair cycling to investigate further the phenotype of the hair follicles and details of their cyclic activities upon *Ctcf* deficiency.

Because advances of pharmacogenomics resulted in the development of a number of molecules that are capable of modulating distinct epigenetic regulatory mechanisms, the research in this direction will help to bridge the gap between our current knowledge of basic epigenetic mechanisms and potential applications of epigenetic modulators for treatment on many dermatological disorders including epidermal cancers and psoriasis, as well as for protection of skin against environmental stressors and aging.

Appendix A

Microarray -> Up- and Down- regulated genes located in the KtyI, KtyII and EDC loci in *Ctcf*-deficient epidermis

Location	Systematic Name	Gene Name	Fold Change (KO vs WT)
KtyI (Ch11)	NM_172946	Krt222	5.68
	NM_010660	Krt10	55.04
	NM_010661	Krt12	15.84
	NM_033373	Krt23	-28.95
	NM_001039666	Krt40	-2.11
	NM_025524	Krtap3-3	-10.56
	NM_025720	Krtap3-2	-2.92
	NM_001039502	Krtap1-4	2.88
	NM_001048196	Krtap4-1	-7.67
	NM_001126322	Gm11595	-2.32
	NM_001126322	Gm11595	7.24
	NM_001195383	2300003K06Rik	2.26
	NM_001177484	Gm11559	3.02
	NM_015741	Krtap9-1	2.71
	NM_013570	Krt33b	2.51
	chr11:99970341-99973420_R	chr11:99970341-99973420_R	-6.91
	NM_010662	Krt13	43.33
	NM_008469	Krt15	-3.03
KtyII (5' Flank)	ENSMUST00000000544	Acvr1b	38.08
	NM_019518	Grasp	14.44
	chr15:101084597-101095097_R	chr15:101084597-101095097_R	-2.15
	chr15:101084597-101095097_F	chr15:101084597-101095097_F	-9.46
	NM_010444	Nr4a1	-10.07
	NM_026566	Atg101	5.51
	NR_033803	6030408B16Rik	-3.49
KtyII (Ch15)	NM_028770	Krt80	2.24
	NM_016879	Krt85	2.13
	NR_002868	Gm5476	1,679.67

	NR_003960	Gm5478	2,439.65
	NM_010669	Krt6b	507,338.01
	NM_008476	Krt6a	5,179.94
	NM_027011	Krt5	15.69
	NR_033444	Krt74	2.96
	NM_212485	Krt73	3.79
	NM_010668	Krt2	-7.42
	NM_008473	Krt1	14.74
	NM_146063	Krt79	7,398.07
	NM_212487	Krt78	4.32
KtyII (3'Flank)	TC1699452	TC1699452	2.01
	NM_145625	Eif4b	2.96
	NM_001033277	Spryd3	-2.42
	NM_008344	Igfbp6	-6.66

EDC (5'Flank)	NM_001253738	Tpm3	4.18
	NM_206924	Jtb	2.14
	NM_145540	Ints3	31.09
	NM_133854	Snapin	44.14
	NM_026374	Ilf2	35.02
	NM_023215	Chtop	-5.63
EDC (Ch3)	NM_025393	S100a14	8.54
	NM_026416	S100a16	29.26
	NM_011310	S100a3	3.83
	NM_011311	S100a4	-2.13
	NM_011313	S100a6	5.99
	chr3:90427029-90427674_F	chr3:90427029-90427674_F	-5.71
	chr3:90425270-90435820_F	chr3:90425270-90435820_F	-2.39
	chr3:90425270-90435820_R	chr3:90425270-90435820_R	-6.52
	NM_013650	S100a8	2,223.64
	NM_001281852	S100a9	34,360.85
	XM_619923	Gm5849	-242.36
	NM_207247	Pglyrp3	8.42
	NM_008508	Lor	-48.42
	NM_175424	Prr9	32.02
	NM_001164787	Sprr2a2	44.17
	chr3:92065425-92086850_F	chr3:92065425-92086850_F	11.27
	NM_011469	Sprr2b	4.00
	NM_011470	Sprr2d	40,390.23
	NM_011471	Sprr2e	2,460.87

	NM_011472	Sprr2f	687.50
	NR_003548	Sprr2g	345.66
	NM_011474	Sprr2h	3,208.59
	NM_011475	Sprr2i	292.46
	NR_003185	Sprr2j-ps	210.57
	NM_011477	Sprr2k	157.39
	NM_009265	Sprr1b	46,799.92
	NM_009264	Sprr1a	8.04
	XM_006502579	2310046K23Rik	10.56
	NM_008412	Ivl	3.68
	AK131883	2210017I01Rik	-24.79
	NM_025984	Lce1a1	-9.22
	NM_026822	Lce1b	-113.56
	NM_028625	Lce1a2	-35.35
	NM_028622	Lce1c	-18.46
	NM_027137	Lce1d	-52.18
	NM_026811	Lce1e	-22.78
	NM_026394	Lce1f	-4.94
	NM_025413	Lce1g	-10.87
	NM_026335	Lce1h	-18.14
	NM_029667	Lce1i	-25.73
	NM_001254760	Lce1k	-2.72
	NM_028629	Kprp	-5.00
	NM_028628	Lce1l	-2,538.81
	NM_025621	2310050C09Rik	-6.89
	NM_001039594	Lce3a	4,476.79
	NM_025501	Lce3b	1,980.18
	NM_033175	Lce3c	1,947.31
	NM_001270426	Lce3d	1,836.91
	NM_001254725	Lce3e	71.06
	NM_001018079	Lce3f	38.32
	NM_028798	Crct1	-4.65
	NM_025420	Lce1m	-123.44
	NM_001177694	Gm4858	17.16
	XM_006502513	Flg	96.71
	chr3:93150619-93184368_F	chr3:93150619-93184368_F	-7.96
	chr3:93156491-93157100_R	chr3:93156491-93157100_R	2.39
	chr3:93162669-93163114_R	chr3:93162669-93163114_R	1,436.73
	NM_001163098	Tchh	10.29
	NM_027762	Tchhl1	247.22
	NM_016740	S100a11	13.94

EDC (3'Flank)	chr3:93564825-93576725_F	chr3:93564825-93576725_F	6.50
	chr3:93564825-93576725_R	chr3:93564825-93576725_R	27.59
	chr3:93582250-93592950_R	chr3:93582250-93592950_R	-3.94
	chr3:93582250-93592950_F	chr3:93582250-93592950_F	2.83
	NM_207272	Tdpoz4	3.67
	NM_025416	Them5	12.59
	NM_011281	Rorc	-82.07
	NM_030116	Mrpl9	5.04
	NM_172434	Celf3	-11.71
	NM_001082484	Snx27	8.75
	NM_011656	Tuft1	-2.78
	NR_033629	BC021767	-2.97
	NM_001037711	Cgn	-3.40
	NM_172683	Pogz	-10.13
	NM_008945	Psmb4	3.34
	NM_009150	Selenbp1	2.05
	AK080218	AK080218	8.10
	NM_175356	Pi4kb	14.37
	XR_104791	4930481B07Rik	3.29
	NM_001282017	Psmd4	4.89
	ENSMUST00000107229	Pip5k1a	13.50
	NM_027013	Scnm1	-2.17
	NM_153121	Lysmd1	-2.78
	NM_027206	Tnfaip8l2	6.94
	NM_001272024	Sema6c	-9.51
	NM_019914	Mllt11	8.41
	NM_172395	Cdc42se1	-9.75
	NM_173347	Prune	-2.16
	NM_001163641	Setdb1	6.53

Appendix B

Up- and Down- regulated genes encoding markers of inflammation in *Ctcf*-deficient epidermis

Description	Systematic Name	Gene Name	Fold change
Chemokines	NM_021274	Cxcl10	63.57293
	NM_023158	Cxcl16	10.20384
	NM_009987	Cx3cr1	43.03822
	NM_011331	Ccl12	14.17923
	NM_011332	Ccl17	8.23584
	NM_011888	Ccl19	5.285617
	NM_019577	Ccl24	10.21593
	ENSMUST00000127258	Ccl25	71.82595
	NM_013652	Ccl4	3.407974
	NM_013653	Ccl5	10.52655
	NM_009139	Ccl6	46.59656
	NM_021443	Ccl8	441.0218
	NM_011338	Ccl9	2.367918
Chemokine receptors	NM_009835	Ccr6	6.749127
	NM_009913	Ccr9	15.42049
Interleukins	NM_008355	Il13	8.009829
	NM_019508	Il17b	6.869407
	NM_145856	Il17f	8.174024
	NM_001009940	Il19	369.1288
	NM_145636	Il27	6.591907
	NM_008361	Il1b	24.48801
	NM_001164724	Il33	3.331655
	NM_153077	Il1f10	2.487037
	NM_001146087	Il1f5	3.997181
	ENSMUST00000028360	Il1f5	13.91479
	NM_019450	Il1f6	144.8322
	NM_021380	Il20	3.059243
	NM_026374	Ilf2	35.0206
	NM_001042708	Ilf3	4.866282
Interleukin receptors	NM_010555	Il1r2	26.66779
	NM_134159	Il17rc	25.99578
	NM_001034031	Il17re	70.46397
	NM_008348	Il10ra	13.14939
	NM_008349	Il10rb	2.224618
	NM_008353	Il12rb1	16.04996

	ENSMUST00000122880	Il20rb	2.586905
	NM_021887	Il21r	25.15845
	NM_178257	Il22ra1	2.501165
	NM_001008700	Il4ra	393.8084
	NM_010559	Il6ra	2.407837
	NM_008372	Il7r	7.531985
	NM_172161	Irak2	2.625167
	NM_029926	Irak4	17.3532
Interferons	NM_008390	Irf1	13.17332
	NM_001164598	Irf2bp2	6.757885
	NM_016849	Irf3	2.246504
	NM_012057	Irf5	22.88487
	NM_016851	Irf6	26.39216
	NM_016850	Irf7	4.988583
	NM_008320	Irf8	4.32837
	NM_001159417	Irf9	9.526632
	NM_008327	Ifi202b	7.068321
	NM_023065	Ifi30	5.798691
	NM_001271676	Ifi47	25.44117
	NM_027835	Ifih1	63.64412
	NM_008331	Ifit1	31.65316
	NM_010501	Ifit3	44.36186
	BC090258	Ifitm1	167.5821
	NM_001112715	Ifitm1	161.1279
	NM_030694	Ifitm2	2.042918
	NM_025378	Ifitm3	2.708868
	NM_008336	Ifnab	2.100527
	NM_010508	Ifnar1	55.14115
	NM_008338	Ifngr2	7.212033
	NM_177396	Ifnl3	2.508403
	NM_008338	Ifngr2	7.212033
Antigens	NM_027353	Cd2bp2	5.112248
	NM_013488	Cd4	6.88262
	NM_007639	Cd1d1	4.930678
	NM_013486	Cd2	6.035227
	NM_013487	Cd3d	90.69718
	NM_009858	Cd8b1	7.670959
Tumor Necrosis Factor and functionaly related proteins	NM_009395	Tnfaip1	3.51937
	NM_025566	Tnfaip8l1	3.362026
	NM_027206	Tnfaip8l2	6.94304
	NM_001033535	Tnfaip8l3	2.625648
	NM_020275	Tnfrsf10b	20.1257
	NM_009399	Tnfrsf11a	3.97871
	NM_013749	Tnfrsf12a	6.655565

	NM_021349	Tnfrsf13b	6.38663
	ENSMUST00000010286	Tnfrsf13b	3.617712
	NM_178931	Tnfrsf14	2.425671
	NM_011609	Tnfrsf1a	7.985707
	NM_011610	Tnfrsf1b	6.093975
	NM_023680	Tnfrsf22	24.20216
	NM_001291010	Tnfrsf25	13.34663
	NM_011659	Tnfrsf4	53.34445
	NM_009425	Tnfsf10	12.6998
	NM_011614	Tnfsf12	6.552348
	NM_001204129	C1qtnf1	11.87677
	NM_026161	C1qtnf4	7.003693
	NM_001135172	C1qtnf7	4.386667
	NM_013693	Tnf	-8.02892
	NM_009396	Tnfaip2	-2.90673
	NM_009396	Tnfaip2	-3.5474
	NM_009397	Tnfaip3	-3.83439
	ENSMUST00000087655	Tnfaip8	-2.99536
	NM_134131	Tnfaip8	-2.23739
	NM_178931	Tnfrsf14	-2.4443
	NM_011614	Tnfsf12	-2.88131
	NM_019418	Tnfsf14	-2.31766
	NM_177371	Tnfsf15	-3.0118
	NM_009452	Tnfsf4	-3.78697
	NM_009404	Tnfsf9	-2.20012
	NM_030888	C1qtnf3	-2.14174
	NM_001040632	C1qtnf5	-4.82601
	NM_001290413	Traf2	3.826462
	NM_009423	Traf4	38.30579

Appendix C

Microarray -> Up- and Down- regulated genes encoding the components of the Wnt, Ras/MAPK pathways and genes associated with cell proliferation in *Ctcf*-deficient epidermis

Description	Systematic Name	Gene Name	Fold change
Wnts	NM_021279	Wnt1	2.109472
	NM_009519	Wnt11	3.192289
	NM_009521	Wnt3	49.18276
	NM_009523	Wnt4	34.91845
	NM_001271757	Wnt5b	38.16997
	NM_009526	Wnt6	5.384671
	NM_139298	Wnt9a	4.290247
Frizzled	NM_021457	Fzd1	2.471462
	NM_175284	Fzd10	5.14803
	NM_020510	Fzd2	7.488425
Catenins	NM_009818	Ctnna1	12.02814
	NM_018761	Ctnnal1	24.69156
	NM_007614	Ctnnb1	2.787573
	NM_008729	Ctnnd2	933.6963
Mitogen-activated protein kinases	NM_023138	Map2k2	7.215186
	NM_008928	Map2k3	4.217574
	NM_011840	Map2k5	29.22494
	NM_022012	Map3k11	24.17372
	NM_172688	Map3k7	2.780265
	NM_009316	Map3k7	5.379415
	NM_009316	Map3k7	3.585435
	NM_001174107	Map3k9	158.3603
	NM_008279	Map4k1	3.386788
	NM_001252200	Map4k4	14.36766
	NM_011949	Mapk1	3.498964
	NM_011161	Mapk11	5.878304
	NM_011950	Mapk13	3.270181
	NM_001045483	Mapk1ip1	2.419902
	NM_178684	Mapk1ip1l	85.00155
	NM_011952	Mapk3	2.465029

	NM_027418	Mapk6	2.76048
	NM_027418	Mapk6	12.21834
	NM_001291035	Mapk7	2.069683
	NM_001163672	Mapk9	4.845601
	NM_177345	Mapkap1	14.22787
Ras oncogene family	NM_010937	Nras	41.95171
	NM_008996	Rab1	2.854228
	NM_016676	Rab10	32.20608
	NM_017382	Rab11a	20.04682
	NM_008997	Rab11b	2.06843
	NM_001162869	Rab11fip3	4.917655
	NM_011227	Rab20	2.055453
	NM_024436	Rab22a	12.15765
	NM_009000	Rab24	2.779097
	NM_016899	Rab25	47.73537
	NM_030554	Rab27b	29.86136
	NM_021518	Rab2a	3.56543
	NM_029494	Rab30	2.566998
	NM_033475	Rab34	5.028245
	NM_028238	Rab38	5.990247
	NM_001003950	Rab3ip	3.98232
	NM_139147	Rab40b	7.426587
	NM_001039394	Rab43	12.46993
	NM_025887	Rab5a	10.28514
	NM_177411	Rab5b	2.572581
	NM_024456	Rab5c	3.959347
	NM_023126	Rab8a	19.94941
	NM_023126	Rab8a	3.077203
	NM_019773	Rab9	4.682927
	NM_001042499	Rabl3	4.952166
	NM_001042499	Rabl3	3.770869
	NM_001042499	Rabl3	3.618579
	NM_001042499	Rabl3	3.550022
	NM_001042499	Rabl3	3.230798
	NM_001042499	Rabl3	3.155877
	NM_001042499	Rabl3	2.655396
	NM_001042499	Rabl3	2.368025
	NM_009391	Ran	4.025635
AP-1 transcription factor	NM_010591	Jun	6.554234
	NM_010234	Fos	4.166305
	NM_001025093	Atf2	10.33356
	NM_030693	Atf5	2.972092
	NM_030887	Jdp2	-2.97483
	NM_011045	Pcna	4.753593

Cell Proliferation	NM_007628	Ccna1	3.263863
	NM_009828	Ccna2	21.72714
	NM_172301	Ccnb1	11.53468
	NM_007630	Ccnb2	12.55595
	NM_001290422	Ccnc	3.6006
	NM_001081636	Ccnd3	2.842782
	NM_007633	Ccne1	50.0847
	NM_007634	Ccnf	6.158865
	NM_207678	Ccnl2	3.113778
	NM_026484	Ccny	2.512979
	NM_011121	Plk1	5.147278
	NM_152804	Plk2	5.142394
	NM_013807	Plk3	36.68944
	NM_008652	Mybl2	22.53564
	NM_010849	Myc	4.675824
	NM_009773	Bub1b	14.53972
	NM_009774	Bub3	3.732622
	NM_007891	E2f1	4.709477
	NM_033270	E2f6	14.82271
	NM_178609	E2f7	12.36322
	NM_001013368	E2f8	12.47226
	NM_033601	Bcl3	14.33041
	NM_001171739	Bag1	2.860185
	NM_013863	Bag3	5.820841
	NM_007527	Bax	-8.98582
	NM_016778	Bok	-5.2024
	NM_177410	Bcl2	-17.7539

7. REFERENCES

Aamodt, K., Abelev, B., Abrahantes Quintana, A., Adamova, D., Adare, A.M., Aggarwal, M.M., Aglieri Rinella, G., Agocs, A.G., Agostinelli, A., Aguilar Salazar, S.*, et al.* (2011). Higher harmonic anisotropic flow measurements of charged particles in Pb-Pb collisions at sqrt(s(NN)) = 2.76 TeV. Phys Rev Lett *107*, 032301.

Abramoff, M.D., Magelhaes, P.J., and Ram, S.J. (2004). Image Processing with ImageJ. Biophotonics International *11*, 36-42.

Agger, K., Cloos, P.A., Christensen, J., Pasini, D., Rose, S., Rappsilber, J., Issaeva, I., Canaani, E., Salcini, A.E., and Helin, K. (2007). UTX and JMJD3 are histone H3K27 demethylases involved in HOX gene regulation and development. Nature *449*, 731-734.

Albiez, H., Cremer, M., Tiberi, C., Vecchio, L., Schermelleh, L., Dittrich, S., Kupper, K., Joffe, B., Thormeyer, T., von Hase, J.*, et al.* (2006). Chromatin domains and the interchromatin compartment form structurally defined and functionally interacting nuclear networks. Chromosome Res *14*, 707-733.

Amano, T., Sagai, T., Tanabe, H., Mizushina, Y., Nakazawa, H., and Shiroishi, T. (2009). Chromosomal dynamics at the Shh locus: limb bud-specific differential regulation of competence and active transcription. Dev Cell *16*, 47-57.

Andl, T., Reddy, S.T., Gaddapara, T., and Millar, S.E. (2002). Wnt signals are required for the initiation of hair follicle development. Dev Cell *2*, 643-654.

Artavanis-Tsakonas, S., Rand, M.D., and Lake, R.J. (1999). Notch signaling: cell fate control and signal integration in development. Science *284*, 770-776.

Bantignies, F., and Cavalli, G. (2011). Polycomb group proteins: repression in 3D. Trends Genet *27*, 454-464.

Bar, J., Kumar, V., Roth, W., Schwarz, N., Richter, M., Leube, R.E., and Magin, T.M. (2014). Skin fragility and impaired desmosomal adhesion in mice lacking all keratins. J Invest Dermatol *134*, 1012-1022.

Beretta, C., Chiarelli, A., Testoni, B., Mantovani, R., and Guerrini, L. (2005). Regulation of the cyclin-dependent kinase inhibitor p57Kip2 expression by p63. Cell Cycle *4*, 1625-1631.

Berika, M., and Garrod, D. (2014). Desmosomal adhesion in vivo. Cell Commun Adhes *21*, 65-75.

Bickmore, W.A., and van Steensel, B. (2013). Genome architecture: domain organization of interphase chromosomes. Cell *152*, 1270-1284.

Bird, A. (2002). DNA methylation patterns and epigenetic memory. Genes Dev *16*, 6-21.

Black, J.C., and Whetstine, J.R. (2011). Chromatin landscape: methylation beyond transcription. Epigenetics *6*, 9-15.

Blackledge, N.P., Farcas, A.M., Kondo, T., King, H.W., McGouran, J.F., Hanssen, L.L., Ito, S., Cooper, S., Kondo, K., Koseki, Y.*, et al.* (2014). Variant PRC1 complex-dependent H2A ubiquitylation drives PRC2 recruitment and polycomb domain formation. Cell *157*, 1445-1459.

Blanpain, C., and Fuchs, E. (2009). Epidermal homeostasis: a balancing act of stem cells in the skin. Nat Rev Mol Cell Biol *10*, 207-U267.

Blanpain, C., Lowry, W.E., Pasolli, H.A., and Fuchs, E. (2006). Canonical notch signaling functions as a commitment switch in the epidermal lineage. Genes Dev *20*, 3022-3035.

Bock, C., Beerman, I., Lien, W.H., Smith, Z.D., Gu, H., Boyle, P., Gnirke, A., Fuchs, E., Rossi, D.J., and Meissner, A. (2012). DNA methylation dynamics during in vivo differentiation of blood and skin stem cells. Mol Cell *47*, 633-647.

Bognar, P., Nemeth, I., Mayer, B., Haluszka, D., Wikonkal, N., Ostorhazi, E., John, S., Paulsson, M., Smyth, N., Pasztoi, M.*, et al.* (2014). Reduced inflammatory threshold indicates skin barrier defect in transglutaminase 3 knockout mice. J Invest Dermatol *134*, 105-111.

Bolte, S., and Cordelieres, F.P. (2006). A guided tour into subcellular colocalization analysis in light microscopy. J Microsc-Oxf *224*, 213-232.

Bonora, G., Plath, K., and Denholtz, M. (2014). A mechanistic link between gene regulation and genome architecture in mammalian development. Curr Opin Genet Dev *27*, 92-101.

Botchkarev, V.A., Botchkareva, N.V., Roth, W., Nakamura, M., Chen, L.-H., Herzog, W., Lindner, G., McMahon, J.A., Peters, C., Lauster, R., *et al.* (1999). Noggin is a mesenchymally-derived stimulator of hair follicle induction. Nature Cell Biol *1*, 158-164.

Botchkarev, V.A., Gdula, M.R., Mardaryev, A.N., Sharov, A.A., and Fessing, M.Y. (2012). Epigenetic regulation of gene expression in keratinocytes. J Invest Dermatol *132*, 2505-2521.

Botchkarev, V.A., and Kishimoto, J. (2003). Molecular control of epithelial-mesenchymal interactions during hair follicle cycling. J Investig Dermatol Symp Proc *8*, 46-55.

Botchkarev, V.A., and Paus, R. (2003). Molecular biology of hair morphogenesis: development and cycling. J Exp Zool B Mol Dev Evol *298*, 164-180.

Branco, M.R., Ficz, G., and Reik, W. (2012). Uncovering the role of 5-hydroxymethylcytosine in the epigenome. Nat Rev Genet *13*, 7-13.

Byrne, C., Tainsky, M., and Fuchs, E. (1994). Programming gene expression in developing epidermis. Development *120*, 2369-2383.

Cai, S., Lee, C.C., and Kohwi-Shigematsu, T. (2006). SATB1 packages densely looped, transcriptionally active chromatin for coordinated expression of cytokine genes. Nat Genet *38*, 1278-1288. Epub 2006 Oct 1222.

Campos, E.I., and Reinberg, D. (2009). Histones: Annotating Chromatin. In Annual Review of Genetics (Palo Alto, Annual Reviews), pp. 559-599.

Candi, E., Schmidt, R., and Melino, G. (2005). The cornified envelope: a model of cell death in the skin. Nat Rev Mol Cell Biol *6*, 328-340.

Cao, R., and Zhang, Y. (2004). SUZ12 is required for both the histone methyltransferase activity and the silencing function of the EED-EZH2 complex. Mol Cell *15*, 57-67.

Carriere, L., Graziani, S., Alibert, O., Ghavi-Helm, Y., Boussouar, F., Humbertclaude, H., Jounier, S., Aude, J.C., Keime, C., Murvai, J.*, et al.* (2012). Genomic binding of Pol III transcription machinery and relationship with TFIIS transcription factor distribution in mouse embryonic stem cells. Nucleic Acids Res *40*, 270-283.

Chakalova, L., and Fraser, P. (2010). Organization of transcription. Cold Spring Harb Perspect Biol *2*, a000729.

Chavanas, S., Adoue, V., Mechin, M.C., Ying, S., Dong, S., Duplan, H., Charveron, M., Takahara, H., Serre, G., and Simon, M. (2008). Long-range enhancer associated with chromatin looping allows AP-1 regulation of the peptidylarginine deiminase 3 gene in differentiated keratinocyte. PLoS One *3*, e3408.

Chen, D., Jarrell, A., Guo, C., Lang, R., and Atit, R. (2012). Dermal beta-catenin activity in response to epidermal Wnt ligands is required for fibroblast proliferation and hair follicle initiation. Development *139*, 1522-1533.

Chuang, C.H., Carpenter, A.E., Fuchsova, B., Johnson, T., de Lanerolle, P., and Belmont, A.S. (2006). Long-range directional movement of an interphase chromosome site. Curr Biol *16*, 825-831.

Chuong, C.M., Cotsarelis, G., and Stenn, K. (2007). Defining hair follicles in the age of stem cell bioengineering. J Invest Dermatol *127*, 2098-2100.

Ciabrelli, F., and Cavalli, G. (2015). Chromatin-Driven Behavior of Topologically Associating Domains. Journal of Molecular Biology *427*, 608-625.

Clavel, C., Grisanti, L., Zemla, R., Rezza, A., Barros, R., Sennett, R., Mazloom, A.R., Chung, C.Y., Cai, X., Cai, C.L.*, et al.* (2012). Sox2 in the dermal papilla niche controls hair growth by fine-tuning BMP signaling in differentiating hair shaft progenitors. Dev Cell *23*, 981-994.

Cook, P.R. (1999). The organization of replication and transcription. Science *284*, 1790-1795.

Cooper, S., Dienstbier, M., Hassan, R., Schermelleh, L., Sharif, J., Blackledge, N.P., De Marco, V., Elderkin, S., Koseki, H., Klose, R.*, et*

al. (2014). Targeting polycomb to pericentric heterochromatin in embryonic stem cells reveals a role for H2AK119u1 in PRC2 recruitment. Cell Rep *7*, 1456-1470.

Cope, N.F., Fraser, P., and Eskiw, C.H. (2010). The yin and yang of chromatin spatial organization. Genome Biol *11*, 204.

Cremer, M., Grasser, F., Lanctot, C., Muller, S., Neusser, M., Zinner, R., Solovei, I., and Cremer, T. (2008). Multicolor 3D fluorescence in situ hybridization for imaging interphase chromosomes. Methods Mol Biol *463*, 205-239.

Cremer, T., and Cremer, M. (2010). Chromosome territories. Cold Spring Harb Perspect Biol *2*, a003889.

Cubenas-Potts, C., and Corces, V.G. (2015). Architectural proteins, transcription, and the three-dimensional organization of the genome. FEBS Lett *589*, 2923-2930.

Darido, C., Georgy, S.R., and Jane, S.M. (2016). The role of barrier genes in epidermal malignancy. Oncogene.

DasGupta, R., and Fuchs, E. (1999). Multiple roles for activated LEF/TCF transcription complexes during hair follicle development and differentiation. Development *126*, 4557-4568.

de Guzman Strong, C., Conlan, S., Deming, C.B., Cheng, J., Sears, K.E., and Segre, J.A. (2010). A milieu of regulatory elements in the epidermal differentiation complex syntenic block: implications for atopic dermatitis and psoriasis. Hum Mol Genet *19*, 1453-1460.

de Guzman Strong, C., Wertz, P.W., Wang, C., Yang, F., Meltzer, P.S., Andl, T., Millar, S.E., Ho, I.C., Pai, S.Y., and Segre, J.A. (2006). Lipid defect underlies selective skin barrier impairment of an epidermal-specific deletion of Gata-3. J Cell Biol *175*, 661-670.

Dekker, J., Marti-Renom, M.A., and Mirny, L.A. (2013). Exploring the three-dimensional organization of genomes: interpreting chromatin interaction data. Nat Rev Genet *14*, 390-403.

Di Croce, L., and Helin, K. (2013). Transcriptional regulation by Polycomb group proteins. Nat Struct Mol Biol *20*, 1147-1155.

Di Meglio, P., Perera, G.K., and Nestle, F.O. (2011). The Multitasking Organ: Recent Insights into Skin Immune Function. Immunity *35*, 857-869.

Dimitri, P., Caizzi, R., Giordano, E., Carmela Accardo, M., Lattanzi, G., and Biamonti, G. (2009). Constitutive heterochromatin: a surprising variety of expressed sequences. Chromosoma *118*, 419-435.

Djalilian, A.R., McGaughey, D., Patel, S., Seo, E.Y., Yang, C., Cheng, J., Tomic, M., Sinha, S., Ishida-Yamamoto, A., and Segre, J.A. (2006). Connexin 26 regulates epidermal barrier and wound remodeling and promotes psoriasiform response. J Clin Invest *116*, 1243-1253.

Dlugosz, A.A., and Yuspa, S.H. (1993). Coordinate changes in gene expression which mark the spinous to granular cell transition in epidermis are regulated by protein kinase C. J Cell Biol *120*, 217-225.

Driskell, I., Oda, H., Blanco, S., Nascimento, E., Humphreys, P., and Frye, M. (2012). The histone methyltransferase Setd8 acts in concert with c-Myc and is required to maintain skin. Embo J *31*, 616-629.

Dupont, C., Armant, D.R., and Brenner, C.A. (2009). Epigenetics: definition, mechanisms and clinical perspective. Semin Reprod Med *27*, 351-357.

Durmowicz, M.C., Cui, C.Y., and Schlessinger, D. (2002). The EDA gene is a target of, but does not regulate Wnt signaling. Gene *285*, 203-211.

Eckert, R.L., Broome, A.M., Ruse, M., Robinson, N., Ryan, D., and Lee, K. (2004). S100 proteins in the epidermis. J Invest Dermatol *123*, 23-33.

Egecioglu, D., and Brickner, J.H. (2011). Gene positioning and expression. Curr Opin Cell Biol *23*, 338-345.

Ellis, T., Gambardella, L., Horcher, M., Tschanz, S., Capol, J., Bertram, P., Jochum, W., Barrandon, Y., and Busslinger, M. (2001). The transcriptional repressor CDP (Cutl1) is essential for epithelial cell differentiation of the lung and the hair follicle. Genes Dev *15*, 2307-2319.

ENCODE (2012). An integrated encyclopedia of DNA elements in the human genome. Nature *489*, 57-74.

Engel, N., West, A.G., Felsenfeld, G., and Bartolomei, M.S. (2004). Antagonism between DNA hypermethylation and enhancer-blocking activity at the H19 DMD is uncovered by CpG mutations. Nat Genet *36*, 883-888.

Eskiw, C.H., Cope, N.F., Clay, I., Schoenfelder, S., Nagano, T., and Fraser, P. (2010). Transcription factories and nuclear organization of the genome. Cold Spring Harb Symp Quant Biol *75*, 501-506.

Ezhkova, E., Pasolli, H.A., Parker, J.S., Stokes, N., Su, I.H., Hannon, G., Tarakhovsky, A., and Fuchs, E. (2009). Ezh2 orchestrates gene expression for the stepwise differentiation of tissue-specific stem cells. Cell *136*, 1122-1135.

Fallon, P.G., Sasaki, T., Sandilands, A., Campbell, L.E., Saunders, S.P., Mangan, N.E., Callanan, J.J., Kawasaki, H., Shiohama, A., Kubo, A.*, et al.* (2009). A homozygous frameshift mutation in the mouse Flg gene facilitates enhanced percutaneous allergen priming. Nat Genet *41*, 602-608.

Feng, S., Cokus, S.J., Schubert, V., Zhai, J., Pellegrini, M., and Jacobsen, S.E. (2014). Genome-wide Hi-C analyses in wild-type and mutants reveal high-resolution chromatin interactions in Arabidopsis. Mol Cell *55*, 694-707.

Ferrai, C., de Castro, I.J., Lavitas, L., Chotalia, M., and Pombo, A. (2010). Gene positioning. Cold Spring Harb Perspect Biol *2*, a000588.

Fessing, M.Y. (2014). Gene regulation at a distance: higher-order chromatin folding and the coordinated control of gene transcription at the epidermal differentiation complex locus. J Invest Dermatol *134*, 2307-2310.

Fessing, M.Y., Mardaryev, A.N., Gdula, M.R., Sharov, A.A., Sharova, T.Y., Rapisarda, V., Gordon, K.B., Smorodchenko, A.D., Poterlowicz, K., Ferone, G.*, et al.* (2011). p63 regulates Satb1 to control tissue-specific chromatin remodeling during development of the epidermis. J Cell Biol *194*, 825-839.

Frauer, C., Hoffmann, T., Bultmann, S., Casa, V., Cardoso, M.C., Antes, I., and Leonhardt, H. (2011). Recognition of 5-hydroxymethylcytosine by the Uhrf1 SRA domain. PLoS ONE *6*, e21306.

Frye, M., and Benitah, S.A. (2012). Chromatin regulators in mammalian epidermis. Semin Cell Dev Biol *23*, 897-905.

Fuchs, E. (2007). Scratching the surface of skin development. Nature *445*, 834-842.

Fuchs, E., and Horsley, V. (2008). More than one way to skin. Genes Dev *22*, 976-985.

Furuse, M., Hata, M., Furuse, K., Yoshida, Y., Haratake, A., Sugitani, Y., Noda, T., Kubo, A., and Tsukita, S. (2002). Claudin-based tight junctions are crucial for the mammalian epidermal barrier: a lesson from claudin-1-deficient mice. J Cell Biol *156*, 1099-1111.

Gao, J., DeRouen, M.C., Chen, C.H., Nguyen, M., Nguyen, N.T., Ido, H., Harada, K., Sekiguchi, K., Morgan, B.A., Miner, J.H.*, et al.* (2008). Laminin-511 is an epithelial message promoting dermal papilla development and function during early hair morphogenesis. Genes Dev *22*, 2111-2124.

Gdula, M.R., Poterlowicz, K., Mardaryev, A.N., Sharov, A.A., Peng, Y., Fessing, M.Y., and Botchkarev, V.A. (2013). Remodeling of three-dimensional organization of the nucleus during terminal keratinocyte differentiation in the epidermis. J Invest Dermatol *133*, 2191-2201.

Geng, S., Mezentsev, A., Kalachikov, S., Raith, K., Roop, D.R., and Panteleyev, A.A. (2006). Targeted ablation of Arnt in mouse epidermis results in profound defects in desquamation and epidermal barrier function. J Cell Sci *119*, 4901-4912.

Gibbs, S., Fijneman, R., Wiegant, J., van Kessel, A.G., van De Putte, P., and Backendorf, C. (1993). Molecular characterization and evolution of the SPRR family of keratinocyte differentiation markers encoding small proline-rich proteins. Genomics *16*, 630-637.

Godwin, A.R., and Capecchi, M.R. (1998). Hoxc13 mutant mice lack external hair. Genes Dev *12*, 11-20.

Gopalakrishnan, S., Van Emburgh, B.O., and Robertson, K.D. (2008). DNA methylation in development and human disease. Mutat Res *647*, 30-38.

Greco, V., Chen, T., Rendl, M., Schober, M., Pasolli, H.A., Stokes, N., Dela Cruz-Racelis, J., and Fuchs, E. (2009). A two-step mechanism for stem cell activation during hair regeneration. Cell Stem Cell *4*, 155-169.

Grob, S., Schmid, M.W., and Grossniklaus, U. (2014). Hi-C analysis in Arabidopsis identifies the KNOT, a structure with similarities to the flamenco locus of Drosophila. Mol Cell *55*, 678-693.

Guastafierro, T., Cecchinelli, B., Zampieri, M., Reale, A., Riggio, G., Sthandier, O., Zupi, G., Calabrese, L., and Caiafa, P. (2008). CCCTC-binding factor activates PARP-1 affecting DNA methylation machinery. J Biol Chem *283*, 21873-21880.

Guo, Y., Xu, Q., Canzio, D., Shou, J., Li, J., Gorkin, D.U., Jung, I., Wu, H., Zhai, Y., Tang, Y.*, et al.* (2015). CRISPR Inversion of CTCF Sites Alters Genome Topology and Enhancer/Promoter Function. Cell *162*, 900-910.

Hadjur, S., Williams, L.M., Ryan, N.K., Cobb, B.S., Sexton, T., Fraser, P., Fisher, A.G., and Merkenschlager, M. (2009). Cohesins form chromosomal cis-interactions at the developmentally regulated IFNG locus. Nature *460*, 410-413.

Hattori, N., Nishino, K., Ko, Y.G., Ohgane, J., Tanaka, S., and Shiota, K. (2004). Epigenetic control of mouse Oct-4 gene expression in embryonic stem cells and trophoblast stem cells. J Biol Chem *279*, 17063-17069.

Heath, H., Ribeiro de Almeida, C., Sleutels, F., Dingjan, G., van de Nobelen, S., Jonkers, I., Ling, K.W., Gribnau, J., Renkawitz, R., Grosveld, F.*, et al.* (2008). CTCF regulates cell cycle progression of alphabeta T cells in the thymus. EMBO J *27*, 2839-2850.

Ho, L., and Crabtree, G.R. (2010). Chromatin remodelling during development. Nature *463*, 474-484.

Hou, C., Dale, R., and Dean, A. (2010). Cell type specificity of chromatin organization mediated by CTCF and cohesin. Proc Natl Acad Sci U S A *107*, 3651-3656.

Hu, Q., Kwon, Y.S., Nunez, E., Cardamone, M.D., Hutt, K.R., Ohgi, K.A., Garcia-Bassets, I., Rose, D.W., Glass, C.K., Rosenfeld, M.G.*, et al.* (2008). Enhancing nuclear receptor-induced transcription requires nuclear motor and LSD1-dependent gene networking in interchromatin granules. Proc Natl Acad Sci U S A *105*, 19199-19204.

Huh, S.H., Narhi, K., Lindfors, P.H., Haara, O., Yang, L., Ornitz, D.M., and Mikkola, M.L. (2013). Fgf20 governs formation of primary and secondary dermal condensations in developing hair follicles. Genes Dev *27*, 450-458.

Hussain, S.H., Limthongkul, B., and Humphreys, T.R. (2013). The biomechanical properties of the skin. Dermatol Surg *39*, 193-203.

Hwang, J., Mehrani, T., Millar, S.E., and Morasso, M.I. (2008). Dlx3 is a crucial regulator of hair follicle differentiation and cycling. Development *135*, 3149-3159.

Ihrie, R.A., Marques, M.R., Nguyen, B.T., Horner, J.S., Papazoglu, C., Bronson, R.T., Mills, A.A., and Attardi, L.D. (2005). Perp is a p63-regulated gene essential for epithelial integrity. Cell *120*, 843-856.

Ingraham, C.R., Kinoshita, A., Kondo, S., Yang, B., Sajan, S., Trout, K.J., Malik, M.I., Dunnwald, M., Goudy, S.L., Lovett, M.*, et al.* (2006). Abnormal skin, limb and craniofacial morphogenesis in mice deficient for interferon regulatory factor 6 (Irf6). Nat Genet *38*, 1335-1340.

Inoue, A., and Zhang, Y. (2011). Replication-dependent loss of 5-hydroxymethylcytosine in mouse preimplantation embryos. Science *334*, 194.

Ito, M., Yang, Z., Andl, T., Cui, C., Kim, N., Millar, S.E., and Cotsarelis, G. (2007). Wnt-dependent de novo hair follicle regeneration in adult mouse skin after wounding. Nature *447*, 316-320.

Ito, S., D'Alessio, A.C., Taranova, O.V., Hong, K., Sowers, L.C., and Zhang, Y. (2010). Role of Tet proteins in 5mC to 5hmC conversion,

ES-cell self-renewal and inner cell mass specification. Nature *466*, 1129-1133.

Ito, S., Shen, L., Dai, Q., Wu, S.C., Collins, L.B., Swenberg, J.A., He, C., and Zhang, Y. (2011). Tet proteins can convert 5-methylcytosine to 5-formylcytosine and 5-carboxylcytosine. Science *333*, 1300-1303.

Iyer, L.M., Tahiliani, M., Rao, A., and Aravind, L. (2009). Prediction of novel families of enzymes involved in oxidative and other complex modifications of bases in nucleic acids. Cell Cycle *8*, 1698-1710.

Jamora, C., Lee, P., Kocieniewski, P., Azhar, M., Hosokawa, R., Chai, Y., and Fuchs, E. (2005). A signaling pathway involving TGF-beta2 and snail in hair follicle morphogenesis. PLoS Biol *3*, e11.

Jaubert, J., Cheng, J., and Segre, J.A. (2003). Ectopic expression of kruppel like factor 4 (Klf4) accelerates formation of the epidermal permeability barrier. Development *130*, 2767-2777.

Jin, B., and Robertson, K.D. (2013). DNA methyltransferases, DNA damage repair, and cancer. Adv Exp Med Biol *754*, 3-29.

Joffe, B., Leonhardt, H., and Solovei, I. (2010). Differentiation and large scale spatial organization of the genome. Curr Opin Genet Dev *20*, 562-569.

Johns, S.A., Soullier, S., Rashbass, P., and Cunliffe, V.T. (2005). Foxn1 is required for tissue assembly and desmosomal cadherin expression in the hair shaft. Dev Dyn *232*, 1062-1068.

Kalb, R., Latwiel, S., Baymaz, H.I., Jansen, P.W., Muller, C.W., Vermeulen, M., and Muller, J. (2014). Histone H2A monoubiquitination promotes histone H3 methylation in Polycomb repression. Nat Struct Mol Biol *21*, 569-571.

Kareta, M.S., Botello, Z.M., Ennis, J.J., Chou, C., and Chedin, F. (2006). Reconstitution and mechanism of the stimulation of de novo methylation by human DNMT3L. J Biol Chem *281*, 25893-25902.

Kim, H., Kang, K., and Kim, J. (2009). AEBP2 as a potential targeting protein for Polycomb Repression Complex PRC2. Nucleic Acids Res *37*, 2940-2950.

Kim, L.K., Esplugues, E., Zorca, C.E., Parisi, F., Kluger, Y., Kim, T.H., Galjart, N.J., and Flavell, R.A. (2014). Oct-1 regulates IL-17 expression by directing interchromosomal associations in conjunction with CTCF in T cells. Mol Cell *54*, 56-66.

Kirkland, J.G., Raab, J.R., and Kamakaka, R.T. (2013). TFIIIC bound DNA elements in nuclear organization and insulation. Biochim Biophys Acta *1829*, 418-424.

Ko, M., Huang, Y., Jankowska, A.M., Pape, U.J., Tahiliani, M., Bandukwala, H.S., An, J., Lamperti, E.D., Koh, K.P., Ganetzky, R.*, et al.* (2010). Impaired hydroxylation of 5-methylcytosine in myeloid cancers with mutant TET2. Nature *468*, 839-843.

Kobielak, K., Pasolli, H.A., Alonso, L., Polak, L., and Fuchs, E. (2003). Defining BMP functions in the hair follicle by conditional ablation of BMP receptor IA. J Cell Biol *163*, 609-623.

Koch, P.J., de Viragh, P.A., Scharer, E., Bundman, D., Longley, M.A., Bickenbach, J., Kawachi, Y., Suga, Y., Zhou, Z., Huber, M.*, et al.* (2000). Lessons from loricrin-deficient mice: compensatory mechanisms maintaining skin barrier function in the absence of a major cornified envelope protein. J Cell Biol *151*, 389-400.

Komuves, L., Oda, Y., Tu, C.L., Chang, W.H., Ho-Pao, C.L., Mauro, T., and Bikle, D.D. (2002). Epidermal expression of the full-length extracellular calcium-sensing receptor is required for normal keratinocyte differentiation. J Cell Physiol *192*, 45-54.

Koster, M.I., Dai, D., Marinari, B., Sano, Y., Costanzo, A., Karin, M., and Roop, D.R. (2007). p63 induces key target genes required for epidermal morphogenesis. Proc Natl Acad Sci U S A *104*, 3255-3260.

Koster, M.I., Kim, S., Mills, A.A., DeMayo, F.J., and Roop, D.R. (2004). p63 is the molecular switch for initiation of an epithelial stratification program. Genes Dev *18*, 126-131.

Koster, M.I., and Roop, D.R. (2007). Mechanisms regulating epithelial stratification. In Annual Review of Cell and Developmental Biology (Palo Alto, Annual Reviews), pp. 93-113.

Kretz, M., Siprashvili, Z., Chu, C., Webster, D.E., Zehnder, A., Qu, K., Lee, C.S., Flockhart, R.J., Groff, A.F., Chow, J.*, et al.* (2013). Control of somatic tissue differentiation by the long non-coding RNA TINCR. Nature *493*, 231-235.

Kretz, M., Webster, D.E., Flockhart, R.J., Lee, C.S., Zehnder, A., Lopez-Pajares, V., Qu, K., Zheng, G.X., Chow, J., Kim, G.E.*, et al.* (2012). Suppression of progenitor differentiation requires the long noncoding RNA ANCR. Genes Dev *26*, 338-343.

Kriaucionis, S., and Heintz, N. (2009). The nuclear DNA base 5-hydroxymethylcytosine is present in Purkinje neurons and the brain. Science *324*, 929-930.

Ku, M., Koche, R.P., Rheinbay, E., Mendenhall, E.M., Endoh, M., Mikkelsen, T.S., Presser, A., Nusbaum, C., Xie, X., Chi, A.S.*, et al.* (2008). Genomewide analysis of PRC1 and PRC2 occupancy identifies two classes of bivalent domains. PLoS Genet *4*, e1000242.

Kulessa, H., Turk, G., and Hogan, B.L. (2000). Inhibition of Bmp signaling affects growth and differentiation in the anagen hair follicle. EMBO J *19*, 6664-6674.

Kumar, V., Bouameur, J.E., Bar, J., Rice, R.H., Hornig-Do, H.T., Roop, D.R., Schwarz, N., Brodesser, S., Thiering, S., Leube, R.E.*, et al.* (2015). A keratin scaffold regulates epidermal barrier formation, mitochondrial lipid composition, and activity. J Cell Biol *211*, 1057-1075.

Kumaran, R.I., Thakar, R., and Spector, D.L. (2008). Chromatin dynamics and gene positioning. Cell *132*, 929-934.

Kurek, D., Garinis, G.A., van Doorninck, J.H., van der Wees, J., and Grosveld, F.G. (2007). Transcriptome and phenotypic analysis reveals Gata3-dependent signalling pathways in murine hair follicles. Development *134*, 261-272.

Kwon, S.H., and Workman, J.L. (2011). The changing faces of HP1: From heterochromatin formation and gene silencing to euchromatic gene expression: HP1 acts as a positive regulator of transcription. BioEssays *33*, 280-289.

Lanctot, C., Cheutin, T., Cremer, M., Cavalli, G., and Cremer, T. (2007). Dynamic genome architecture in the nuclear space: regulation of gene expression in three dimensions. Nat Rev Genet *8*, 104-115.

Lanzuolo, C., Roure, V., Dekker, J., Bantignies, F., and Orlando, V. (2007). Polycomb response elements mediate the formation of chromosome higher-order structures in the bithorax complex. Nat Cell Biol *9*, 1167-1174.

Laurikkala, J., Pispa, J., Jung, H.S., Nieminen, P., Mikkola, M., Wang, X., Saarialho-Kere, U., Galceran, J., Grosschedl, R., and Thesleff, I. (2002). Regulation of hair follicle development by the TNF signal ectodysplasin and its receptor Edar. Development *129*, 2541-2553.

LeBoeuf, M., Terrell, A., Trivedi, S., Sinha, S., Epstein, J.A., Olson, E.N., Morrisey, E.E., and Millar, S.E. (2010). Hdac1 and Hdac2 act redundantly to control p63 and p53 functions in epidermal progenitor cells. Dev Cell *19*, 807-818.

Lee, E., and Yuspa, S.H. (1991). Changes in inositol phosphate metabolism are associated with terminal differentiation and neoplasia in mouse keratinocytes. Carcinogenesis *12*, 1651-1658.

Lehman, J., Laag, E., Michaud, E.J., and Yoder, B.K. (2009). An Essential Role for Dermal Primary Cilia in Hair Follicle Morphogenesis. The Journal of investigative dermatology *129*, 438-448.

Lei, H., Oh, S.P., Okano, M., Juttermann, R., Goss, K.A., Jaenisch, R., and Li, E. (1996). De novo DNA cytosine methyltransferase activities in mouse embryonic stem cells. Development *122*, 3195-3205.

Lewis, C.J., Mardaryev, A.N., Poterlowicz, K., Sharova, T.Y., Aziz, A., Sharpe, D.T., Botchkareva, N.V., and Sharov, A.A. (2014). Bone morphogenetic protein signaling suppresses wound-induced skin repair by inhibiting keratinocyte proliferation and migration. J Invest Dermatol *134*, 827-837.

Li, E., Bestor, T.H., and Jaenisch, R. (1992). Targeted mutation of the DNA methyltransferase gene results in embryonic lethality. Cell *69*, 915-926.

Li, G., Margueron, R., Ku, M., Chambon, P., Bernstein, B.E., and Reinberg, D. (2010). Jarid2 and PRC2, partners in regulating gene expression. Genes Dev *24*, 368-380.

Li, Q., Lu, Q., Estepa, G., and Verma, I.M. (2005). Identification of 14-3-3sigma mutation causing cutaneous abnormality in repeated-epilation mutant mouse. Proc Natl Acad Sci U S A *102*, 15977-15982.

Lieberman-Aiden, E., van Berkum, N.L., Williams, L., Imakaev, M., Ragoczy, T., Telling, A., Amit, I., Lajoie, B.R., Sabo, P.J., Dorschner, M.O.*, et al.* (2009). Comprehensive mapping of long-range interactions reveals folding principles of the human genome. Science *326*, 289-293.

Ling, J.Q., Li, T., Hu, J.F., Vu, T.H., Chen, H.L., Qiu, X.W., Cherry, A.M., and Hoffman, A.R. (2006). CTCF mediates interchromosomal colocalization between Igf2/H19 and Wsb1/Nf1. Science *312*, 269-272.

Luis, N.M., Morey, L., Mejetta, S., Pascual, G., Janich, P., Kuebler, B., Cozutto, L., Roma, G., Nascimento, E., Frye, M.*, et al.* (2011). Regulation of human epidermal stem cell proliferation and senescence requires polycomb- dependent and -independent functions of Cbx4. Cell Stem Cell *9*, 233-246.

Ma, L., Liu, J., Wu, T., Plikus, M., Jiang, T.X., Bi, Q., Liu, Y.H., Muller-Rover, S., Peters, H., Sundberg, J.P.*, et al.* (2003). 'Cyclic alopecia' in Msx2 mutants: defects in hair cycling and hair shaft differentiation. Development *130*, 379-389.

Magin, T.M., Vijayaraj, P., and Leube, R.E. (2007). Structural and regulatory functions of keratins. Exp Cell Res *313*, 2021-2032.

Mahy, N.L., Perry, P.E., and Bickmore, W.A. (2002a). Gene density and transcription influence the localization of chromatin outside of chromosome territories detectable by FISH. J Cell Biol *159*, 753-763.

Mahy, N.L., Perry, P.E., Gilchrist, S., Baldock, R.A., and Bickmore, W.A. (2002b). Spatial organization of active and inactive genes and noncoding DNA within chromosome territories. J Cell Biol *157*, 579-589.

Maiti, A., and Drohat, A.C. (2011). Thymine DNA glycosylase can rapidly excise 5-formylcytosine and 5-carboxylcytosine: potential implications for active demethylation of CpG sites. J Biol Chem *286*, 35334-35338.

Mardaryev, A.N., Gdula, M.R., Yarker, J.L., Emelianov, V.N., Poterlowicz, K., Sharov, A.A., Sharova, T.Y., Scarpa, J.A., Chambon, P., Botchkarev, V.A.*, et al.* (2014). p63 and Brg1 control developmentally regulated higher-order chromatin remodelling at the epidermal differentiation complex locus in epidermal progenitor cells. Development *141*, 101-111.

Mardaryev, A.N., Liu, B., Rapisarda, V., Poterlowicz, K., Malashchuk, I., Rudolf, J., Sharov, A.A., Jahoda, C.A., Fessing, M.Y., Benitah, S.A.*, et al.* (2016). Cbx4 maintains the epithelial lineage identity and cell proliferation in the developing stratified epithelium. J Cell Biol *212*, 77-89.

Margadant, C., Charafeddine, R.A., and Sonnenberg, A. (2010). Unique and redundant functions of integrins in the epidermis. The FASEB Journal *24*, 4133-4152.

Margueron, R., Li, G., Sarma, K., Blais, A., Zavadil, J., Woodcock, C.L., Dynlacht, B.D., and Reinberg, D. (2008). Ezh1 and Ezh2 maintain repressive chromatin through different mechanisms. Mol Cell *32*, 503-518.

Markova, N.G., Karaman-Jurukovska, N., Pinkas-Sarafova, A., Marekov, L.N., and Simon, M. (2007). Inhibition of histone deacetylation promotes abnormal epidermal differentiation and specifically suppresses the expression of the late differentiation marker profilaggrin. J Invest Dermatol *127*, 1126-1139.

Marshall, D., Hardman, M.J., Nield, K.M., and Byrne, C. (2001). Differentially expressed late constituents of the epidermal cornified envelope. Proc Natl Acad Sci U S A *98*, 13031-13036.

Martin, N., Patel, S., and Segre, J.A. (2004). Long-range comparison of human and mouse Sprr loci to identify conserved noncoding sequences involved in coordinate regulation. Genome Res *14*, 2430-2438.

Matsumura, H., Mohri, Y., Binh, N.T., Morinaga, H., Fukuda, M., Ito, M., Kurata, S., Hoeijmakers, J., and Nishimura, E.K. (2016). Hair follicle aging is driven by transepidermal elimination of stem cells via COL17A1 proteolysis. Science *351*.

Mecklenburg, L., Nakamura, M., Sundberg, J.P., and Paus, R. (2001). The nude mouse skin phenotype: the role of Foxn1 in hair follicle development and cycling. Exp Mol Pathol *71*, 171-178.

Meister, P., Mango, S.E., and Gasser, S.M. (2011). Locking the genome: nuclear organization and cell fate. Curr Opin Genet Dev *21*, 167-174.

Mejetta, S., Morey, L., Pascual, G., Kuebler, B., Mysliwiec, M.R., Lee, Y., Shiekhattar, R., Di Croce, L., and Benitah, S.A. (2011). Jarid2 regulates mouse epidermal stem cell activation and differentiation. EMBO J *30*, 3635-3646.

Mendenhall, E.M., Koche, R.P., Truong, T., Zhou, V.W., Issac, B., Chi, A.S., Ku, M., and Bernstein, B.E. (2010). GC-rich sequence elements recruit PRC2 in mammalian ES cells. PLoS Genet *6*, e1001244.

Merkenschlager, M. (2010). Cohesin: a global player in chromosome biology with local ties to gene regulation. Curr Opin Genet Dev *20*, 555-561.

Millar, S.E. (2002). Molecular mechanisms regulating hair follicle development. J Invest Dermatol *118*, 216-225.

Mills, A.A., Zheng, B.H., Wang, X.J., Vogel, H., Roop, D.R., and Bradley, A. (1999). p63 is a p53 homologue required for limb and epidermal morphogenesis. Nature *398*, 708-713.

Misteli, T. (2007). Beyond the sequence: cellular organization of genome function. Cell *128*, 787-800.

Moissiard, G., Cokus, S.J., Cary, J., Feng, S., Billi, A.C., Stroud, H., Husmann, D., Zhan, Y., Lajoie, B.R., McCord, R.P., *et al.* (2012). MORC family ATPases required for heterochromatin condensation and gene silencing. Science *336*, 1448-1451.

Moore, J.M., Rabaia, N.A., Smith, L.E., Fagerlie, S., Gurley, K., Loukinov, D., Disteche, C.M., Collins, S.J., Kemp, C.J., Lobanenkov, V.V., *et al.*

(2012). Loss of maternal CTCF is associated with peri-implantation lethality of Ctcf null embryos. PLoS One *7*, e34915.

Moqtaderi, Z., Wang, J., Raha, D., White, R.J., Snyder, M., Weng, Z., and Struhl, K. (2010). Genomic binding profiles of functionally distinct RNA polymerase III transcription complexes in human cells. Nat Struct Mol Biol *17*, 635-640.

Nair, M., Teng, A., Bilanchone, V., Agrawal, A., Li, B., and Dai, X. (2006). Ovol1 regulates the growth arrest of embryonic epidermal progenitor cells and represses c-myc transcription. J Cell Biol *173*, 253-264.

Nakagawa, T., Kajitani, T., Togo, S., Masuko, N., Ohdan, H., Hishikawa, Y., Koji, T., Matsuyama, T., Ikura, T., Muramatsu, M.*, et al.* (2008). Deubiquitylation of histone H2A activates transcriptional initiation via trans-histone cross-talk with H3K4 di- and trimethylation. Genes Dev *22*, 37-49.

Nakamura, M., Schneider, M.R., Schmidt-Ullrich, R., and Paus, R. (2013). Mutant laboratory mice with abnormalities in hair follicle morphogenesis, cycling, and/or structure: an update. J Dermatol Sci *69*, 6-29.

Nativio, R., Wendt, K.S., Ito, Y., Huddleston, J.E., Uribe-Lewis, S., Woodfine, K., Krueger, C., Reik, W., Peters, J.M., and Murrell, A. (2009). Cohesin is required for higher-order chromatin conformation at the imprinted IGF2-H19 locus. PLoS Genet *5*, e1000739.

Naumova, N., and Dekker, J. (2010). Integrating one-dimensional and three-dimensional maps of genomes. J Cell Sci *123*, 1979-1988.

Nguyen, B.C., Lefort, K., Mandinova, A., Antonini, D., Devgan, V., Della Gatta, G., Koster, M.I., Zhang, Z., Wang, J., Tommasi di Vignano, A.*, et al.* (2006). Cross-regulation between Notch and p63 in keratinocyte commitment to differentiation. Genes Dev *20*, 1028-1042.

Nicolas, M., Wolfer, A., Raj, K., Kummer, J.A., Mill, P., van Noort, M., Hui, C.C., Clevers, H., Dotto, G.P., and Radtke, F. (2003). Notch1 functions as a tumor suppressor in mouse skin. Nat Genet *33*, 416-421.

Noramly, S., Freeman, A., and Morgan, B.A. (1999). beta-catenin signaling can initiate feather bud development. Development *126*, 3509-3521.

Oh, W.J., Rishi, V., Orosz, A., Gerdes, M.J., and Vinson, C. (2007). Inhibition of CCAAT/enhancer binding protein family DNA binding in mouse epidermis prevents and regresses papillomas. Cancer Res *67*, 1867-1876.

Ohba, M., Ishino, K., Kashiwagi, M., Kawabe, S., Chida, K., Huh, N.H., and Kuroki, T. (1998). Induction of differentiation in normal human keratinocytes by adenovirus-mediated introduction of the eta and delta isoforms of protein kinase C. Mol Cell Biol *18*, 5199-5207.

Ohlsson, R., Bartkuhn, M., and Renkawitz, R. (2010). CTCF shapes chromatin by multiple mechanisms: the impact of 20 years of CTCF research on understanding the workings of chromatin. Chromosoma *119*, 351-360.

Okano, M., Bell, D.W., Haber, D.A., and Li, E. (1999). DNA methyltransferases Dnmt3a and Dnmt3b are essential for de novo methylation and mammalian development. Cell *99*, 247-257.

Okano, M., Xie, S., and Li, E. (1998). Cloning and characterization of a family of novel mammalian DNA (cytosine-5) methyltransferases. Nat Genet *19*, 219-220.

Oler, A.J., Alla, R.K., Roberts, D.N., Wong, A., Hollenhorst, P.C., Chandler, K.J., Cassiday, P.A., Nelson, C.A., Hagedorn, C.H., Graves, B.J.*, et al.* (2010). Human RNA polymerase III transcriptomes and relationships to Pol II promoter chromatin and enhancer-binding factors. Nat Struct Mol Biol *17*, 620-628.

Ong, C.-T., and Corces, V.G. (2014). CTCF: an architectural protein bridging genome topology and function. Nat Rev Genet *15*, 234-246.

Oshimori, N., and Fuchs, E. (2012). Paracrine TGF-beta signaling counterbalances BMP-mediated repression in hair follicle stem cell activation. Cell Stem Cell *10*, 63-75.

Park, G.T., Denning, M.F., and Morasso, M.I. (2001). Phosphorylation of murine homeodomain protein Dlx3 by protein kinase C. FEBS Lett *496*, 60-65.

Patel, S., Xi, Z.F., Seo, E.Y., McGaughey, D., and Segre, J.A. (2006). Klf4 and corticosteroids activate an overlapping set of transcriptional

targets to accelerate in utero epidermal barrier acquisition. Proc Natl Acad Sci U S A *103*, 18668-18673.

Paus, R., and Foitzik, K. (2004). In search of the "hair cycle clock": a guided tour. Differentiation *72*, 489-511.

Paus, R., Muller-Rover, S., Van Der Veen, C., Maurer, M., Eichmuller, S., Ling, G., Hofmann, U., Foitzik, K., Mecklenburg, L., and Handjiski, B. (1999). A comprehensive guide for the recognition and classification of distinct stages of hair follicle morphogenesis. J Invest Dermatol *113*, 523-532.

Perdigoto, C.N., Valdes, V.J., Bardot, E.S., and Ezhkova, E. (2014). Epigenetic regulation of epidermal differentiation. Cold Spring Harb Perspect Med *4*.

Peters, L.L., Robledo, R.F., Bult, C.J., Churchill, G.A., Paigen, B.J., and Svenson, K.L. (2007). The mouse as a model for human biology: a resource guide for complex trait analysis. Nat Rev Genet *8*, 58-69.

Petiot, A., Conti, F.J., Grose, R., Revest, J.M., Hodivala-Dilke, K.M., and Dickson, C. (2003). A crucial role for Fgfr2-IIIb signalling in epidermal development and hair follicle patterning. Development *130*, 5493-5501.

Pope, B.D., Ryba, T., Dileep, V., Yue, F., Wu, W., Denas, O., Vera, D.L., Wang, Y., Hansen, R.S., Canfield, T.K.*, et al.* (2014). Topologically associating domains are stable units of replication-timing regulation. Nature *515*, 402-405.

Probst, A.V., and Almouzni, G. (2011). Heterochromatin establishment in the context of genome-wide epigenetic reprogramming. Trends Genet *27*, 177-185.

Proweller, A., Tu, L., Lepore, J.J., Cheng, L., Lu, M.M., Seykora, J., Millar, S.E., Pear, W.S., and Parmacek, M.S. (2006). Impaired notch signaling promotes de novo squamous cell carcinoma formation. Cancer Res *66*, 7438-7444.

Pummila, M., Fliniaux, I., Jaatinen, R., James, M.J., Laurikkala, J., Schneider, P., Thesleff, I., and Mikkola, M.L. (2007). Ectodysplasin

has a dual role in ectodermal organogenesis: inhibition of Bmp activity and induction of Shh expression. Development *134*, 117-125.

Raddatz, G., Hagemann, S., Aran, D., Sohle, J., Kulkarni, P.P., Kaderali, L., Hellman, A., Winnefeld, M., and Lyko, F. (2013). Aging is associated with highly defined epigenetic changes in the human epidermis. Epigenetics Chromatin *6*, 36.

Rangarajan, A., Talora, C., Okuyama, R., Nicolas, M., Mammucari, C., Oh, H., Aster, J.C., Krishna, S., Metzger, D., Chambon, P.*, et al.* (2001). Notch signaling is a direct determinant of keratinocyte growth arrest and entry into differentiation. EMBO J *20*, 3427-3436.

Rao, S.S., Huntley, M.H., Durand, N.C., Stamenova, E.K., Bochkov, I.D., Robinson, J.T., Sanborn, A.L., Machol, I., Omer, A.D., Lander, E.S.*, et al.* (2014). A 3D map of the human genome at kilobase resolution reveals principles of chromatin looping. Cell *159*, 1665-1680.

Razin, S.V., Gavrilov, A.A., Pichugin, A., Lipinski, M., Iarovaia, O.V., and Vassetzky, Y.S. (2011). Transcription factories in the context of the nuclear and genome organization. Nucleic Acids Res *39*, 9085-9092.

Remeseiro, S., Cuadrado, A., Gómez-López, G., Pisano, D.G., and Losada, A. (2012). A unique role of cohesin-SA1 in gene regulation and development. The EMBO Journal *31*, 2090-2102.

Richardson, G.D., Bazzi, H., Fantauzzo, K.A., Waters, J.M., Crawford, H., Hynd, P., Christiano, A.M., and Jahoda, C.A. (2009). KGF and EGF signalling block hair follicle induction and promote interfollicular epidermal fate in developing mouse skin. Development *136*, 2153-2164.

Richly, H., Rocha-Viegas, L., Ribeiro, J.D., Demajo, S., Gundem, G., Lopez-Bigas, N., Nakagawa, T., Rospert, S., Ito, T., and Di Croce, L. (2010). Transcriptional activation of polycomb-repressed genes by ZRF1. Nature *468*, 1124-1128.

Rishi, V., Bhattacharya, P., Chatterjee, R., Rozenberg, J., Zhao, J., Glass, K., Fitzgerald, P., and Vinson, C. (2010). CpG methylation of half-CRE sequences creates C/EBPalpha binding sites that activate some tissue-specific genes. Proc Natl Acad Sci U S A *107*, 20311-20316.

Rishikaysh, P., Dev, K., Diaz, D., Qureshi, W.M., Filip, S., and Mokry, J. (2014). Signaling involved in hair follicle morphogenesis and development. Int J Mol Sci *15*, 1647-1670.

Robertson, E.D., Weir, L., Romanowska, M., Leigh, I.M., and Panteleyev, A.A. (2012). ARNT controls the expression of epidermal differentiation genes through HDAC- and EGFR-dependent pathways. J Cell Sci *125*, 3320-3332.

Roegiers, F., and Jan, Y.N. (2004). Asymmetric cell division. Curr Opin Cell Biol *16*, 195-205.

Romano, R.A., Birkaya, B., and Sinha, S. (2007). A functional enhancer of keratin14 is a direct transcriptional target of deltaNp63. J Invest Dermatol *127*, 1175-1186.

Saadi, I., Das, P., Zhao, M., Raj, L., Ruspita, I., Xia, Y., Papaioannou, V.E., and Bei, M. (2013). Msx1 and Tbx2 antagonistically regulate Bmp4 expression during the bud-to-cap stage transition in tooth development. Development *140*, 2697-2702.

Sandilands, A., Sutherland, C., Irvine, A.D., and McLean, W.H. (2009). Filaggrin in the frontline: role in skin barrier function and disease. J Cell Sci *122*, 1285-1294.

Sanyal, A., Bau, D., Marti-Renom, M.A., and Dekker, J. (2011). Chromatin globules: a common motif of higher order chromosome structure? Curr Opin Cell Biol *23*, 325-331.

Saunders, N., Dicker, A., Popa, C., Jones, S., and Dahler, A. (1999). Histone deacetylase inhibitors as potential anti-skin cancer agents. Cancer Res *59*, 399-404.

Schmidt-Ullrich, R., and Paus, R. (2005). Molecular principles of hair follicle induction and morphogenesis. Bioessays *27*, 247-261.

Schneider, M.R., Schmidt-Ullrich, R., and Paus, R. The Hair Follicle as a Dynamic Miniorgan. Current Biology *19*, R132-R142.

Schneider, M.R., Schmidt-Ullrich, R., and Paus, R. (2009). The hair follicle as a dynamic miniorgan. Curr Biol *19*, R132-142.

Schneider, R., and Grosschedl, R. (2007). Dynamics and interplay of nuclear architecture, genome organization, and gene expression. Genes Dev *21*, 3027-3043.

Schoenfelder, S., Clay, I., and Fraser, P. (2010a). The transcriptional interactome: gene expression in 3D. Curr Opin Genet Dev *20*, 127-133.

Schoenfelder, S., Sexton, T., Chakalova, L., Cope, N.F., Horton, A., Andrews, S., Kurukuti, S., Mitchell, J.A., Umlauf, D., Dimitrova, D.S., *et al.* (2010b). Preferential associations between co-regulated genes reveal a transcriptional interactome in erythroid cells. Nat Genet *42*, 53-61.

Schwartz, Y.B., and Pirrotta, V. (2014). Ruled by ubiquitylation: a new order for polycomb recruitment. Cell Rep *8*, 321-325.

Segre, J.A. (2006). Epidermal barrier formation and recovery in skin disorders. J Clin Invest *116*, 1150-1158.

Segre, J.A., Bauer, C., and Fuchs, E. (1999). Klf4 is a transcription factor required for establishing the barrier function of the skin. Nat Genet *22*, 356-360.

Sen, G.L., Reuter, J.A., Webster, D.E., Zhu, L., and Khavari, P.A. (2010). DNMT1 maintains progenitor function in self-renewing somatic tissue. Nature *463*, 563-567.

Sen, G.L., Webster, D.E., Barragan, D.I., Chang, H.Y., and Khavari, P.A. (2008). Control of differentiation in a self-renewing mammalian tissue by the histone demethylase JMJD3. Genes Dev *22*, 1865-1870.

Sharov, A.A., Sharova, T.Y., Mardaryev, A.N., di Vignano, A.T., Atoyan, R., Weiner, L., Yang, S., Brissette, J.L., Dotto, G.P., and Botchkarev, V.A. (2006a). Bone morphogenetic protein signaling regulates the size of hair follicles and modulates the expression of cell cycle-associated genes. Proceedings of the National Academy of Sciences *103*, 18166-18171.

Sharov, A.A., Sharova, T.Y., Mardaryev, A.N., Tommasi di Vignano, A., Atoyan, R., Weiner, L., Yang, S., Brissette, J.L., Dotto, G.P., and Botchkarev, V.A. (2006b). Bone morphogenetic protein signaling

regulates the size of hair follicles and modulates the expression of cell cycle-associated genes. Proc Natl Acad Sci U S A *103*, 18166-18171. Epub 12006 Nov 18117.

Simon, J.A., and Kingston, R.E. (2013). Occupying chromatin: Polycomb mechanisms for getting to genomic targets, stopping transcriptional traffic, and staying put. Mol Cell *49*, 808-824.

Simpson, C.L., Patel, D.M., and Green, K.J. (2011). Deconstructing the skin: cytoarchitectural determinants of epidermal morphogenesis. Nat Rev Mol Cell Biol *12*, 565-580.

Sleeman, J.E., and Trinkle-Mulcahy, L. (2014). Nuclear bodies: new insights into assembly/dynamics and disease relevance. Curr Opin Cell Biol *28C*, 76-83.

Spector, D.L., and Lamond, A.I. (2011). Nuclear speckles. Cold Spring Harb Perspect Biol *3*.

Spilianakis, C.G., Lalioti, M.D., Town, T., Lee, G.R., and Flavell, R.A. (2005). Interchromosomal associations between alternatively expressed loci. Nature *435*, 637-645.

St-Jacques, B., Dassule, H.R., Karavanova, I., Botchkarev, V.A., Li, J., Danielian, P.S., McMahon, J.A., Lewis, P.M., Paus, R., and McMahon, A.P. (1998). Sonic hedgehog signaling is essential for hair development. Curr Biol *8*, 1058-1068.

Steinert, P.M., and Marekov, L.N. (1995). The proteins elafin, filaggrin, keratin intermediate filaments, loricrin, and small proline-rich proteins 1 and 2 are isodipeptide cross-linked components of the human epidermal cornified cell envelope. J Biol Chem *270*, 17702-17711.

Stenn, K.S., and Paus, R. (2001). Controls of hair follicle cycling. Physiol Rev *81*, 449-494.

Symmons, O., and Spitz, F. (2013). From remote enhancers to gene regulation: charting the genome's regulatory landscapes. Philos Trans R Soc Lond B Biol Sci *368*, 20120358.

Tahiliani, M., Koh, K.P., Shen, Y., Pastor, W.A., Bandukwala, H., Brudno, Y., Agarwal, S., Iyer, L.M., Liu, D.R., Aravind, L.*, et al.* (2009).

Conversion of 5-methylcytosine to 5-hydroxymethylcytosine in mammalian DNA by MLL partner TET1. Science *324*, 930-935.

Tang, Z., Luo, O.J., Li, X., Zheng, M., Zhu, J.J., Szalaj, P., Trzaskoma, P., Magalska, A., Wlodarczyk, J., Ruszczycki, B.*, et al.* (2015). CTCF-Mediated Human 3D Genome Architecture Reveals Chromatin Topology for Transcription. Cell *163*, 1611-1627.

Tanizawa, H., Iwasaki, O., Tanaka, A., Capizzi, J.R., Wickramasinghe, P., Lee, M., Fu, Z., and Noma, K. (2010). Mapping of long-range associations throughout the fission yeast genome reveals global genome organization linked to transcriptional regulation. Nucleic Acids Res *38*, 8164-8177.

Testoni, B., and Mantovani, R. (2006). Mechanisms of transcriptional repression of cell-cycle G2/M promoters by p63. Nucleic Acids Res *34*, 928-938.

Tjong, H., Gong, K., Chen, L., and Alber, F. (2012). Physical tethering and volume exclusion determine higher-order genome organization in budding yeast. Genome Res *22*, 1295-1305.

Tkatchenko, A.V., Visconti, R.P., Shang, L., Papenbrock, T., Pruett, N.D., Ito, T., Ogawa, M., and Awgulewitsch, A. (2001). Overexpression of Hoxc13 in differentiating keratinocytes results in downregulation of a novel hair keratin gene cluster and alopecia. Development *128*, 1547-1558.

Truong, A.B., Kretz, M., Ridky, T.W., Kimmel, R., and Khavari, P.A. (2006). p63 regulates proliferation and differentiation of developmentally mature keratinocytes. Genes Dev *20*, 3185-3197.

Tunggal, J.A., Helfrich, I., Schmitz, A., Schwarz, H., Gunzel, D., Fromm, M., Kemler, R., Krieg, T., and Niessen, C.M. (2005). E-cadherin is essential for in vivo epidermal barrier function by regulating tight junctions. EMBO J *24*, 1146-1156.

Turksen, K., and Troy, T.C. (2003). Overexpression of the calcium sensing receptor accelerates epidermal differentiation and permeability barrier formation in vivo. Mech Dev *120*, 733-744.

Waddington, C.H. (1968). The basic ideas of biology. In: Towards a Theoretical Biology. Edinburgh, Scotland: Edinburgh University Press, p. 1-32.

Wang, H., Maurano, M.T., Qu, H., Varley, K.E., Gertz, J., Pauli, F., Lee, K., Canfield, T., Weaver, M., Sandstrom, R.*, et al.* (2012). Widespread plasticity in CTCF occupancy linked to DNA methylation. Genome Res *22*, 1680-1688.

Wang, H., Wang, L., Erdjument-Bromage, H., Vidal, M., Tempst, P., Jones, R.S., and Zhang, Y. (2004). Role of histone H2A ubiquitination in Polycomb silencing. Nature *431*, 873-878.

Wang, K.C., and Chang, H.Y. (2011). Molecular mechanisms of long noncoding RNAs. Mol Cell *43*, 904-914.

Wang, Z., Schones, D.E., and Zhao, K. (2009). Characterization of human epigenomes. Curr Opin Genet Dev *19*, 127-134.

Watanabe, D., Suetake, I., Tada, T., and Tajima, S. (2002). Stage- and cell-specific expression of Dnmt3a and Dnmt3b during embryogenesis. Mech Dev *118*, 187-190.

Watt, F.M., and Huck, W.T. (2013). Role of the extracellular matrix in regulating stem cell fate. Nat Rev Mol Cell Biol *14*, 467-473.

Wei, Z., Gao, F., Kim, S., Yang, H., Lyu, J., An, W., Wang, K., and Lu, W. (2013). Klf4 organizes long-range chromosomal interactions with the oct4 locus in reprogramming and pluripotency. Cell Stem Cell *13*, 36-47.

Weiner, L., Han, R., Scicchitano, B.M., Li, J., Hasegawa, K., Grossi, M., Lee, D., and Brissette, J.L. (2007). Dedicated epithelial recipient cells determine pigmentation patterns. Cell *130*, 932-942.

Westfall, M.D., Mays, D.J., Sniezek, J.C., and Pietenpol, J.A. (2003). The Delta Np63 alpha phosphoprotein binds the p21 and 14-3-3 sigma promoters in vivo and has transcriptional repressor activity that is reduced by Hay-Wells syndrome-derived mutations. Mol Cell Biol *23*, 2264-2276.

Williams, A., Spilianakis, C.G., and Flavell, R.A. (2010). Interchromosomal association and gene regulation in trans. Trends Genet *26*, 188-197.

Williams, R.R., Broad, S., Sheer, D., and Ragoussis, J. (2002). Subchromosomal positioning of the epidermal differentiation complex (EDC) in keratinocyte and lymphoblast interphase nuclei. Exp Cell Res *272*, 163-175.

Witcher, M., and Emerson, B.M. (2009). Epigenetic silencing of the p16(INK4a) tumor suppressor is associated with loss of CTCF binding and a chromatin boundary. Mol Cell *34*, 271-284.

Wu, C., and Morris, J.R. (2001). Genes, genetics, and epigenetics: a correspondence. Science *293*, 1103-1105.

Wu, H., D'Alessio, A.C., Ito, S., Xia, K., Wang, Z., Cui, K., Zhao, K., Sun, Y.E., and Zhang, Y. (2011). Dual functions of Tet1 in transcriptional regulation in mouse embryonic stem cells. Nature *473*, 389-393.

Wu, X., Johansen, J.V., and Helin, K. (2013). Fbxl10/Kdm2b recruits polycomb repressive complex 1 to CpG islands and regulates H2A ubiquitylation. Mol Cell *49*, 1134-1146.

Xiao, T., Wallace, J., and Felsenfeld, G. (2011). Specific sites in the C terminus of CTCF interact with the SA2 subunit of the cohesin complex and are required for cohesin-dependent insulation activity. Mol Cell Biol *31*, 2174-2183.

Xu, R.H., Ault, K.T., Kim, J., Park, M.J., Hwang, Y.S., Peng, Y., Sredni, D., and Kung, H. (1999). Opposite effects of FGF and BMP-4 on embryonic blood formation: roles of PV.1 and GATA-2. Dev Biol *208*, 352-361.

Yang, A., Kaghad, M., Wang, Y., Gillett, E., Fleming, M.D., Dotsch, V., Andrews, N.C., Caput, D., and McKeon, F. (1998). p63, a p53 homolog at 3q27-29, encodes multiple products with transactivating, death-inducing, and dominant-negative activities. Mol Cell *2*, 305-316.

Yang, L., Lin, C., Liu, W., Zhang, J., Ohgi, K.A., Grinstein, J.D., Dorrestein, P.C., and Rosenfeld, M.G. (2011). ncRNA- and Pc2 Methylation-Dependent Gene Relocation between Nuclear Structures Mediates Gene Activation Programs. Cell *147*, 773-788.

Yang, L.C., Ng, D.C., and Bikle, D.D. (2003). Role of protein kinase C alpha in calcium induced keratinocyte differentiation: defective regulation in squamous cell carcinoma. J Cell Physiol *195*, 249-259.

Yang, Y., Li, Y., Wang, Y., Wu, J., Yang, G., Yang, T., Gao, Y., and Lu, Y. (2012). Versican gene: regulation by the beta-catenin signaling pathway plays a significant role in dermal papilla cell aggregative growth. J Dermatol Sci *68*, 157-163.

Yao, H., Brick, K., Evrard, Y., Xiao, T., Camerini-Otero, R.D., and Felsenfeld, G. (2010). Mediation of CTCF transcriptional insulation by DEAD-box RNA-binding protein p68 and steroid receptor RNA activator SRA. Genes Dev *24*, 2543-2555.

Yi, R., and Fuchs, E. (2011). MicroRNAs and their roles in mammalian stem cells. J Cell Sci *124*, 1775-1783.

Yu, Z., Lin, K.K., Bhandari, A., Spencer, J.A., Xu, X., Wang, N., Lu, Z., Gill, G.N., Roop, D.R., Wertz, P.*, et al.* (2006). The Grainyhead-like epithelial transactivator Get-1/Grhl3 regulates epidermal terminal differentiation and interacts functionally with LMO4. Dev Biol *299*, 122-136.

Yuspa, S.H., Kilkenny, A.E., Steinert, P.M., and Roop, D.R. (1989). Expression of murine epidermal differentiation markers is tightly regulated by restricted extracellular calcium concentrations in vitro. J Cell Biol *109*, 1207-1217.

Zampieri, M., Guastafierro, T., Calabrese, R., Ciccarone, F., Bacalini, M.G., Reale, A., Perilli, M., Passananti, C., and Caiafa, P. (2012). ADP-ribose polymers localized on Ctcf-Parp1-Dnmt1 complex prevent methylation of Ctcf target sites. Biochem J *441*, 645-652.

ZEISS (2013). Confocal Laser Scanning Mircroscopy: Principles. Available from: http://zeiss-campus.magnet.fsu.edu/referencelibrary/pdfs/ZeissConfocalPrinciples.pdf, [Accessed: 15/07/2013].

Zhang, J., Bardot, E., and Ezhkova, E. (2012). Epigenetic regulation of skin: focus on the Polycomb complex. Cell Mol Life Sci *69*, 2161-2172.

Zhang, Y., Tomann, P., Andl, T., Gallant, N.M., Huelsken, J., Jerchow, B., Birchmeier, W., Paus, R., Piccolo, S., Mikkola, M.L.*, et al.* (2009). Reciprocal requirements for EDA/EDAR/NF-kappaB and Wnt/beta-catenin signaling pathways in hair follicle induction. Dev Cell *17*, 49-61.

Zlatanova, J., and Caiafa, P. (2009). CTCF and its protein partners: divide and rule? J Cell Sci *122*, 1275-1284.

Zuin, J., Dixon, J.R., van der Reijden, M.I., Ye, Z., Kolovos, P., Brouwer, R.W., van de Corput, M.P., van de Werken, H.J., Knoch, T.A., van, I.W.F.*, et al.* (2014). Cohesin and CTCF differentially affect chromatin architecture and gene expression in human cells. Proc Natl Acad Sci U S A *111*, 996-1001.